TRANSITION STATE AND MECHANISTIC STUDY OF *TRYPANOSOMA CRUZI* TRANS-SIALIDASE

By

JINGSONG YANG

A DISSERTATION PRESENTED TO THE GRADUATE SCHOOL
OF THE UNIVERSITY OF FLORIDA IN PARTIAL FULFILLMENT
OF THE REQUIREMENTS FOR THE DEGREE OF
DOCTOR OF PHILOSOPHY

UNIVERSITY OF FLORIDA

2001

ACKNOWLEDGMENTS

I am deeply indebted to my research advisor, Dr. Benjamin A. Horenstein. I would like to express my sincerest gratitude for his guidance and support during the course of this project and for being such a patient and helping person. My appreciation also goes to Dr. Nigel Richards, Dr. Jon Stewart, Dr. David Silverman and Dr. Weihong Tan for serving on the advisory committee and for giving their time and experience to improve my professional development in chemistry and biology.

Special thanks go to Dr. Sergio Schenkman for his generosity in providing us the plasmids for trans-sialidase overexpression, which started the entire project.

I wish to express my thanks to the past and present Horenstein group members--Mike, Eve, Kim, John, Hongbin, Mirela, Katie, Hongyi, and Erin--for their company and support. Special thanks go to Mike and Eve for their help in the laboratory. I would also like to thank Romaine for printing the dissertation and Simon for computer help. An appreciation extends to all my colleagues in the Biochemistry Division, too.

I am thankful for my friends Baocai and Wentao for their hospitality and for all the fun time we have been enjoying together. A special appreciation is also

extended to all of my friends in UF who made my stay in Gainesville a pleasant experience.

I am deeply indebted to my wife, Nianying, for her patience, friendship, support and love at all times. Without her support none of my accomplishments would have been possible. I would also like to thank my daughter, Xinyue (Sherry), for all the fun and joy we have been sharing together. My gratitude also goes to all of my family members for their constant understanding and support.

Finally, I would like to thank the National Science Foundation for funding and the University of Florida for providing the facilities and an excellent environment to complete this work.

TABLE OF CONTENTS

page

ACKNOWLEDGMENTS ii

ABSTRACT vii

CHAPTERS

1. INTRODUCTION 1

Sialic acids 2
Chagas' disease, *Trypanosoma cruzi* and Trans-sialidase 8
Glycosylhydrolases and glycosyltransferases 14
Enzymes that hydrolyse or transfer non-sialo sugars: lysozyme and β-galactosidases. 15
Enzymes that hydrolyse or transfer sialo sugars: sialidases and sialyltransferases. 22
Mechanistic background of *Trypanosoma cruzi* trans-sialidase 34

2. RECOMBINANT TRANS-SIALIDASE OVEREXPRESSION AND SUBSTRATE SYNTHESIS 37

Introduction. 37
Results 38
Discussion. 43
Overexpression and purification of recombinant trans-sialidase. 43
Synthesis of ([6-^{3}H] Glc) Lactose. 46
Synthesis of sialyl-lactose isotopomers. 47
Synthesis of sialyl-galactose isotopomers 53
Characterization of sialyl-lactose and sialyl-galactose isotopomers. 54
Purification of α-2,3-sialyl-lactose from bovine colostrum. 55
Synthesis of [3,3'-dideuterio, ^{3}H-N-acetyl]sialyl-α-D-octyl-galactose. 58
Synthetic route for the preparation of ([3-^{3}H, 3-^{18}O)] Gal) sialyl-galactose. 61
Experimental 81

3. KINETIC ISOTOPE EFFECT STUDIES ON TRANS-SIALIDASE 81

Introduction 81
Kinetic isotope effect background 82
Isotope effect theory 82
Primary isotope effect 89
Secondary isotope effect 90
KIE in enzymatic reactions: commitment to catalysis (C_f) 94
KIE measurement 95
The competitive method 96
The non-competitive method 99
KIE methodology for trans-sialidase 99
Results 100
Discussion 106
KIE methodology 106
Kinetic parameters for sialyl-galactose 108
Kinetic isotope effect studies 108
Conclusions 120
Experimental 121

4. MECHANISTIC STUDIES ON TRANS-SIALIDASE 127

Introduction 127
Chemical trapping experiment 127
Initial velocity studies 128
Site-directed mutagenesis and chemical rescue studies 132
Inhibition tests of sialidase transition state analogs on trans-sialidase 133
Results 135
Discussion 143
Chemical trapping experiments 143
Initial velocity studies 147
Site-directed mutagenesis and chemical rescue studies 151
Inhibition tests of sialidase transition state analogs on trans-sialidase 154
Conclusions 154
Experimental 155

5. CONCLUSIONS AND FUTURE WORK 164

Conclusions 164
Future work 165

APPENDICES 167

A ^{1}H NMR OF SIALYL-LACTOSE SYNTHESIZED ENZYMATICALLY 167

B ^{1}H NMR OF SIALYL-GALACTOSE SYNTHESIZED ENZYMATICALLY. ... 168

C ^{1}H NMR OF 4,6-BENZYLIDENE-A-D-METHYL GALACTOSIDE. 169

D ^{1}H NMR OF 2-BENZOYL-4,6-BENZYLIDENE-A-D-METHYL GALACTOSIDE. 170

E ^{1}H NMR OF 2-BENZOYL-3-KETP-4,6-BENZYLIDENE-A-D-METHYL GALACTOSIDE. 171

REFERENCES 172

BIOGRAPHICAL SKETCH 183

Abstract of Dissertation Presented to the Graduate School
of the University of Florida in Partial Fulfillment of the
Requirements for the Degree of Doctor of Philosophy

TRANSITION STATE AND MECHANISTIC STUDY OF *TRYPANOSOMA CRUZI* TRANS-SIALIDASE

By

Jingsong Yang

May, 2001

Chair: Dr. Benjamin A. Horenstein
Major Department: Chemistry

Trypanosoma cruzi trans-sialidase transfers the sialic acid group from host cell surface glycoconjugates to parasite surface glycoconjugates or to water, a function believed to be involved in the pathogenic process of *T. cruzi*, the causative agent of Chagas' disease. Trans-sialidase belongs to a family of glycosyltransferases whose mechanisms of action have not been well characterized. This dissertation describes the transition state analysis and mechanistic study on trans-sialidase with the long term goal of providing mechanistic information for the design of specific trans-sialidase inhibitors that may have clinical application.

The first part of this work describes the overexpression and purification of recombinant trans-sialidase, and the synthesis of a series of substrates necessary for the kinetic experiments. Two substrates, sialyl-lactose and sialyl-

galactose, with a wide variety of isotopic labels in specific positions have been synthesized. The synthetic approach, purity, yield and characterization of these molecules is presented.

The kinetic isotope effect studies with the above mentioned substrates are discussed next. These include the measurements of ^{13}C primary isotope effects and β-dideuterio secondary isotope effects. Both non-enzymatic solvolysis and enzymatic transfer reactions have been investigated. The solvolysis reactions serve as a point of comparison for the enzyme catalyzed reactions. Kinetic isotope effects have been measured with both the natural substrate, sialyl-lactose, and the slow substrate, sialyl-galactose. The results from these experiments are compared and the transition state structure for trans-sialidase is proposed.

The dissertation concludes with the discussion of a series of kinetic experiments on trans-sialidase. These include initial velocity kinetics, a chemical trapping experiment, site-directed mutagenesis experiments and inhibition studies. The results of these experiments are discussed and a reaction mechanism for trans-sialidase is proposed.

CHAPTER 1
INTRODUCTION

Trypanosoma cruzi is the causative agent of human Chagas' disease, an epidemic illness prevalent in Central and South America. *T. cruzi* expresses on its surface the trans-sialidase activity that transfers the sialic acid group from host cell surface glycoconjugates to its own surface glycoconjugates (transferase activity) or, less efficiently, to water (hydrolase activity). It is the only enzyme that creats glycosidic bonds to sialic acid without using cytidine-5'-monophosphate-N-acetyl-neuraminic acid (CMP-NeuAc) as the donor substrate. A better understanding of the mechanism and function of trans-sialidase may contribute to the control of Chagas' disease and also may allow us to have insight into why this homolog of the sialidases prefers transferase activity rather than hydrolase activity. The work presented in this dissertation represents a study of the transition state structure and mechanism of trans-sialidase, with the long term goal of providing mechanistic information for the design of specific trans-sialidase inhibitors with possible extension to the neuraminidases and sialidases which are structurally homologous.

Sialic Acids

Trans-sialidase is involved in the transfer of sialic acid between glycoconjugates. It functions by altering the distributions of sialic acids on both the host cell and the parasite's own cell surface. Therefore, the biological roles of trans-sialidase are closely related to the functions of sialic acids. A brief review of the biological functions of sialic acids is given below for the purpose of helping readers better understand how trans-sialidase activity might be involved in the pathogenic process of *Trypanosoma cruzi*.

Sialic acids (figure 1-1) are composed of a family of derivatives of neuraminic acid (5-amino-3,5-dideoxy-D-*glycero*-D-*galacto*-nonulosonic acid). Up to now, 36 different sialic acid molecules have been found in various organisms. They are usually linked to the carbohydrate chain of glycoproteins and glycolipids via α-glycosidic bonds (1,2). Sialic acids and sialic acid conjugates exhibit a variety of structural features. Sialic acids can be linked to the polysaccharide chain via either α-2,3, α-2,6, or α-2,8 glycosidic bonds (1,2). Terminal sialic acids usually form α-glycosidic bonds between C-2 hydroxyl of the sialic acid molecule and C-3, -4 and -6 of the penultimate non-sialic acid moiety, such as galactose (Gal), N-acetylglucosamine (GlcNAc) and N-acetylgalactosamine (GalNAc), with the most common linkages being α-2,3 to Gal and α-2,6 to Gal and GalNAc. These can be found in both N- and O-linked glycoproteins. Sialic acids also attach to other sialic acid molecules via α-2,8 linkage in oligosialylglycoconjugate and sialylpolysaccharide structures. These structures are found in bacterial saccharides and glycoproteins as well as in

gangliosides. Besides the usual terminal positions, sialic acids are also found to link to internal GalNAc or Gal via α-2,3 or α-2,6 bonds. Modifications on the parent neuraminic acid structure add more structural diversity. There are two parent molecules in the sialic acid family, N-acetylneuraminic acid (NeuAc) and N-glycolylneuraminic acid (NeuGc), that differ in N-acylation (figure 1-1). Additional modifications are found on these two parent structures, including the substitution of the hydroxyl group on C-4, -7, -8, and -9 by acetyl, lactoyl, methyl, sulphate and phosphate moieties as well as the introduction of a double bond between C-2 and C-3 in free sialic acids (1,2).

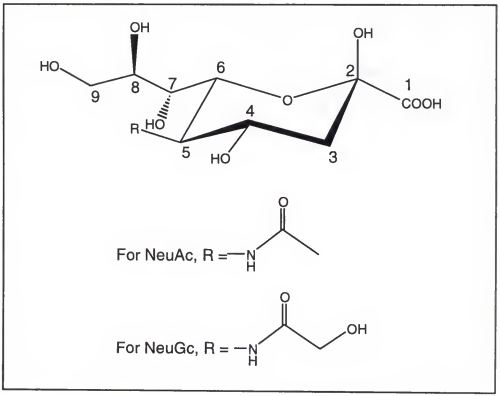

Figure 1-1. Parent structures of sialic acids: N-acetylneuraminic acid (NeuAc) and N-glycolylneuraminic acid (NeuGc).

Since the first observation and isolation by Ernest Klenk in 1935 (3), sialic acids have been found in many organisms, including all mammals, some microorganisms such as bacteria and protozoa, and viruses. This widespread pattern and various structural features of sialic acids suggest diverse functions of this family of molecules. One function of sialic acids is believed to be related to their hydrophilicity, acidity and negative molecular charge. These properties affect the glycoconjugates to which they are part of as well as the surrounding environment (4,5). The attachment of sialic acids influences and stabilizes the conformations of both the saccharide chain and the protein part of the glycoconjugates, conferring them higher thermal and proteolytic stability (2). The high viscosity of mucin is believed to be due to the negative charge of sialic acids lining the mucin surface. Mucin is known for its protective and lubricating functions (6). Cell surface sialic acids form a surrounding shell of negative charge on the cell membrane. This causes cell repulsion and prevents cell aggregation, contributing to the spreading of cells along the mucin surface. This same effect is thought important to prevent erythrocyte aggregation.

Sialic acids are also involved in biological recognition processes. Sialic acids usually occupy the outermost positions of polysaccharide chains. As a result, they are frequently found to be involved in biological recognition events. However, they play dual roles in these processes. They can either serve as the recognition sites, as in the case of sialic acid/hemagglutinin interaction during the influenza virus infection, or mask other recognition sites, such as the masking of the penultimate galactose residue which serves as the receptor molecule in

many recognition processes. Many sialic acid binding proteins have been found in microorganisms, plants and animals. In pathogenic processes, there is evidence that host cell sialo-glycoconjugates are factors in the primary adhesion event. A number of microbial pathogens were found to adhere to host cell surface sialic acids. This interaction helps mediate cell invasion processes (7,8,9). One example is the sialic acid/hemagglutinin interaction in the internalization of influenza virus. The function of sialic acid binding proteins in plants might be involved in the defensive mechanism against the invasion of sialic acid-containing microorganisms (10). A number of sialic acid receptors were also found in mammals that mediate the adhesion of mammalian cells. The most studied of these proteins are selectins, sialoadhesin and CD22. Selectins function in the rolling process initiated by the adhesion of white blood cells to specific endothelia, mediated by the interaction between selectin and sialic acids in the sialyl Lewis $(Le)^x$ and sialyl Le^a structures on the surface of leukocytes (11). Selectins are also found on certain tumor cells and the selectin-sialic acid interaction is implicated in the metastasis of tumor cells (12). Sialoadhesin is a receptor found on specific macrophage subpopulations in murine bone marrow, spleen, and lymph nodes (13). It has been suggested that sialoadhesin functions in the development of myeloid cells in bone marrow and also in the trafficking of leukocytes in lymphatic organs (14). CD22 is a receptor found on B-cells. It is an immunoglobulin-like transmembrane protein with a C-terminal cytosolic domain (15). The CD22-sialic acid interactions mediate the binding of B cells to B and T cells, as well as to neutrophils, monocytes or erythrocytes (16). The

ligands of CD22 are α-2,6 linked sialic acid glycoconjugates. Evidence suggested that these interactions may be involved in the early B-cell activation and in modulating certain signal transduction processes (17).

From the above discussion, it is clear that via the sialic acid-sialic acid receptor interactions, various biological processes are mediated. Besides the recognition function, sialic acid also serves to mask the cell surface recognition sites. Desialylation causes rapid removal of erythrocytes from the circulating blood (18). The galactose residue unmasked by desialylation binds to a lectin-like receptor on Kupffer cells and eventually leads to the degradation of erythrocytes (19). Desialylation of platelets (20), lymphocytes (21) and serum glycoconjugates (22) also leads to their rapid removal from circulation. Again, there is evidence indicating that galactose-cell receptor interactions are functioning in these cases (23,24).

Another function of sialic acids is their effects on the immune system. Sialic acids are themselves antigenic in some cell lines (25). However, they can also either directly mask an antigenic carbohydrate to which they attach, or indirectly mask the antigenicity of a neighboring antigen of various natures. The hydration shell of sialic acids makes them very effective in antigenic masking. Terminal sialic acids of IgG have virus-neutralizing properties, since IgG prevents virus adhesion to the sialo-glycoconjugates of the cell membrane (26). Deglycosylation of IgG leads to a decreased capacity of binding complement (C1q), which is required for the immunologically directed cytolysis of foreign cells to occur (27). Cell surface sialic acids also affect the alternative complement

activation pathway (figure 1-2). In this pathway, the binding of complement C3 and factor B exposes a proteolytic site on factor B, which is then cleaved by factor D, leading to the formation of C3Bb. C3Bb cleaves C3 and forms C3b. C3b is then combined with B and converted to C3bBb, or C3 convertase, which cleaves C3 and forms more C3b. This initial event then triggers a cascade of events that follow and eventually leads to the lysis of the cell membrane (28). The positive feedback of C3b formation by C3bBb is under tight control. In solution, factor β1H has a much higher affinity for C3b than factor B does. Hence C3bBb is readily displaced by β1H to form C3bβ1H. Once this complex is formed, it is subject to the attack by factor I, causing its decomposition (figure 1-2). However, a number of microorganisms bind C3bBb on its cell surface. This binding greatly stabilizes the C3bBb complex and reduces its affinity for β1H. Membranes that stabilize C3bBb were found to be generally sialic acid deficient. Experimental evidence showed a positive correlation between the increased amount of cell surface sialic acids and the increased affinity of bound C3bBb for β1H, indicating that cell surface sialic acids destabilize the bound C3bBb and inactivate the alternative complement activation pathway (29).

Besides the above-discussed functions, sialic acids also participate in biological processes such as blood coagulation, fibrinolysis, and the signal transmission of nerve cells (1, 2). Given the important biological functions of sialic acids, enzymes that are involved in their metabolism and chemistry are under intense investigation. These studies have yielded important information

which may eventually lead to the control of various sialic acid related biological processes.

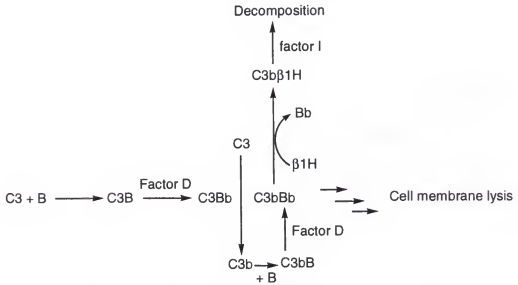

Figure 1-2. Control of the alternative complement activation pathway by β1H.

Chagas' Disease, *Trypanosoma cruzi* and Trans-sialidase

Chagas' disease is an epidemic disease commonly found in Central and South American areas. It is a severe illness that affects 18-20 million people among the Latin American population. There are currently more than 550,000 new cases and 50,000 deaths associated with this disease each year (30). The causative agent of Chagas' disease is the parasite *Trypanosoma cruzi*. During the early infection stage, there is an acute inflammatory phase that causes tissue necrosis in various locations (31). This acute phase is mainly the result of the rapid reproduction of the parasite inside the host organism due to the lack of the immune response from the host. The infection of the parasites leads to cell lysis that releases parasites into blood and tissue. In the later stage of infection, with

the development of the immune response, the number of parasites in blood and tissue drops. Nevertheless, they still exist inside the host organism and gradually develop the chronic phase of Chagas' disease. The major symptoms in this phase include the development of cardiomyopathy in the cardiac forms as well as the mega-syndrome in the gastrointestinal forms (32). Because of the severity and prevalence of Chagas' disease, extensive efforts have been made on the discovery of new drugs that could lead to the control of this disease. However, no drug so far has been found that can cure this disease. Proper hygenic protocol is currently the major way to control the disease. In spite of that, people are still contracting the disease and Chagas' disease remains a major threat to public health in the endemic areas.

Trypanosoma cruzi is a protozoan hemoflagellate with a complex life cycle (figure 1-3). It undergoes a number of biochemically and morphologically distinct stages during its life cycle (33). *T. cruzi* can reside in both mammalian and insect hosts. The metacyclic trypomastigote form infects mammalian hosts. This form of the parasite enters the mammalian host through feces contamination or via the bite of the blood-sucking reduviid bug. Metacyclic trypomastigotes can not multiply and must enter the host cells in order to divide. Once inside the cytoplasm, metacyclic trypomastigotes differentiate into nonflagellated amastigotes that are able to multiply extensively and subsequently differentiate into the flagellated trypomastigote form of parasites. Following cell burst, trypomastigotes are released into blood and tissue, causing acute parasitemia. Again, through feces contamination or insect bite, trypomastigotes can re-enter

the insect hosts and differentiate into the dividing epimastigote form. During the later stage of insect infection, epimastigotes gradually re-differentiate into the metacyclic trypomastigote form in the midgut of insects, which can once more infect mammalian hosts.

T. cruzi surface glycoproteins and glycolipids have been the subjects of intense scrutiny for decades. The finding of the surface sialidase/trans-sialidase activity (34) and the resulting assembly of Ssp-3 (stage specific) epitope (35) was a major advance in this area. Later it was found that these two enzymatic activities reside on the same enzyme form, *T. cruzi* trans-sialidase (TCTS) (36). The studies on this enzyme have led to the proposal about its functions in the *T. cruzi* life cycle.

Trypanosoma cruzi trans-sialidase is a unique enzyme that transfers a sialic acid group from host and serum glycoconjugates to parasite surface glycoconjugates or to water and leads to the formation of α-2,3 linked product. Its function has been suggested to be important in the invasive process of *Trypanosoma cruzi*, the causative agent of Chagas' disease. TCTS can utilize a wide range of glycoproteins and glycolipids as substrates. It strongly prefers that the donor substrates have the presence of α-2,3-sialic acid units linked to a terminal galactosyl residue and that the acceptor substrates have the presence of α-linked galactosyl residues (37). TCTS is believed to play several important roles in the life cycle of parasite *T. cruzi*. These include the following: (a) TCTS facilitates the internalization of *T.cruzi* by host nonphagocytes and phagocytes (38, 39). *T.cruzi* is not capable of synthesizing its own sialic acids. It instead

transfers sialic acids from the serum and host cell surface glycoconjugates to its own surface glycoconjugates and forms the Ssp-3 epitope (35). Several lines of evidence suggested that this epitope is implicated in the attachment and invasion of host cells by *T.cruzi* (40, 41). (b) It is known that parasite surface sialic acids inhibit complement C3bBb assembly of the host immune system. This is one of the strategies adopted by parasites to evade the host immune system. This strategy is most likely effective in the pathogenic process of *T. cruzi* through the action of TCTS (34, 42, 43). (c) *T. cruzi* enters the host cell through endophagocytosis. The vacuole thus formed can fuse with lysosomes as shown by the experimental findings that lysosomal membrane proteins can be found on the surface of the vacuole (44). Therefore, it is to the advantage of the parasites to escape from the vacuole and to replicate in the cytosol. Experimental evidence suggests that the reduction of lumen face sialic acids of the phagosome activates a pore-forming protein (Tc-tox) which inserts into and disintegrates the vacuole membrane and helps the parasite to escape from the vacuole after internalization (45, 46). The trans-sialidase activity facilitates the removal of sialic acids from the lumen face of the phagosome, which results in the activation of Tc-tox and the release of the parasite inside the cytosol.

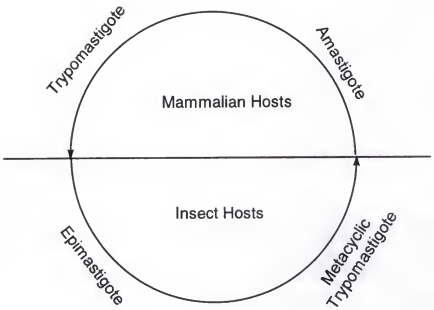

Figure 1-3. Schematic illustration of the life cycle of *Trypanosoma cruzi*.

T.cruzi trans-sialidase from the trypomastigote stage is a natural chimeric protein with two functionally-independent domains, an N-terminal catalytic domain and a C-terminal repetitive domain (47). The C-terminus is composed of tandems of 12 amino acid repeats and is thought to be immunodominant (47). Deletion of C-terminus does not affect the enzymatic activity (48, 49). Recent findings suggest that C-terminus may function in modulating trans-sialidase activity. It stabilizes the trans-sialidase activity during the early stage of infection, yet facilitates the formation of antibody against the N-terminal catalytic domain during the later infection stage (50, 51). The N-terminus of TCTS contains full catalytic activity. It can be further divided into two domains, the catalytic domain (AA 1-372), which has 30% sequence similarity with *Salmonella typhimurium* sialidase, and a lectin-like FnIII domain (47). TCTS is linked to the cell membrane through a glycosyl phosphatidylinositol (GPI) anchor and has been

found to shed into the medium (52). The schematic illustration of TCTS structure is shown in figure 1-4.

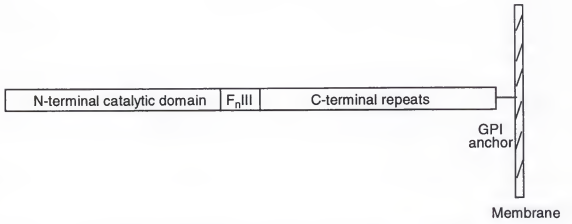

Figure 1-4. Schematic illustration of the primary structure of trypomastigote trans-sialidase.

Trans-sialidase was found to be encoded by a gene family whose expression is developmentally regulated (53, 54). Trans-sialidase activity is absent in the dividing amastigote form, but reaches the peak level in the highly infective bloodstream/tissue culture trypomastigotes. Trans-sialidase in this form of the parasite is capable of forming polymers by interactions of the C termini (55). Its molecular weight ranges from 100-220 kDa, depending on the length of the C-terminal repeats (47). Trans-sialidase activity in the epimastigote stage is 7- to 15-fold lower than that in the trypomastigote stage. Structurally, epimastigote trans-sialidase does not contain the C-terminal repeats and therefore does not polymerize. It is also smaller with a molecular weight of about 90 kDa (55). Trans-sialidase activity in the metacyclic trypomastigote stage varies, which may depend on the parasite strains or culture conditions (54, 56).

The developmentally regulated trans-sialidase plays important roles in several aspects in the parasite's life cycle. Trans-sialidase is not found in mammalian organisms. Therefore, it serves as a promising target for drug design. Antibodies against trans-sialidase have been shown to reduce the infectivity of *T. cruzi* (57). The design of specific inhibitors of trans-sialidase may lead to drugs helpful in treatment of Chagas' disease. This dissertation provides information regarding the transition state structure and mechanism of trans-sialidase catalysis that can find application toward the rational design of enzyme specific inhibitors.

Glycosylhydrolases and Glycosyltransferases

Trans-sialidase belongs to the glycosylhydrolases and glycosyltransferases family that display diverse and important biological functions. This family of enzymes has been found in various organisms, ranging from virus, bacteria and parasites to higher plants and animals. Because of their ubiquitous existence and important functions, they have been the subjects of extensive research over decades. The research on hen egg white (HEW) lysozyme resulted in the resolution of its crystal structure (58), leading to the proposal of the reaction mechanism that serves as the paradigm model for glycosidases (59). With the ever-increasing sequence and crystallographic data, this large group of enzymes is now classified into different families that share sequence similarities (60,61). This Henrissat classification has revealed valuable information on a number of enzymes even before their crystal structures are available (62). In the present discussion, glycosylhydrolases and

glycosyltransferases will be divided into two major categories: those that hydrolyse or transfer non-sialo sugars (the first category) and those that hydrolyse or transfer sialo sugars (the second category). These two groups of enzymes are functionally and mechanistically related, yet different in various respects. Knowledge obtained from the studies on these enzymes provides the basis for the mechanistic study on trans-sialidase.

Many enzymes in the first category have been studied extensively and the information obtained from these studies has greatly enriched our knowledge about their mechanistic enzymology. Studies on the enzymes in the second category are relatively recent. However, many exciting results have been generated and this area remains one of the most fascinating areas in enzymology.

Enzymes that Hydrolyse or Transfer Non-sialo Sugars: Lysozyme and β-Galactosidase

Enzymes in this category can be further divided into two groups based on their stereochemical outcome of the catalyzed reactions, namely, retaining and inverting enzymes. In 1953, Koshland proposed a general mechanistic scheme for these two groups of enzymes (63). The inverting enzymes were proposed to undergo a single displacement mechanism, whereas the retaining enzymes undergo a double displacement mechanism. After more than forty years of research, this statement has survived experimental tests and proven to be generally applicable for this category of enzymes, although exceptions do exist. Glycosidases are the most extensively studied enzymes in this category and will be discussed in more detail in this section. With the aid of powerful techniques

such as site-directed mutagenesis, kinetic experiments, intermediate trapping, chemical rescue and affinity labeling, two acidic amino acid residues, Asp and/or Glu, were found in most glycosidases that play crucial catalytic roles. The pH profiles of this family of enzymes are usually bell-shaped, indicating that optimal activities are achieved in the presence of one protonated and one deprotonated group in the active site. These results, when combined, suggest the following mechanistic scenario. For the inverting enzymes, the mechanistic scheme requires a general acid catalyst that donates a proton to the leaving group, and a general base catalyst that deprotonates the attacking nucleophilic substrate, typically water. Reactions proceed through an oxocarbenium ion-like transition state. For the retaining enzymes, again two acidic amino acid residues are involved. One of them acts as a nucleophile, leading to the formation of a glycosyl-enzyme covalent intermediate, while the other acts first as a general acid catalyst to facilitate the departure of the leaving group, then as a general base catalyst to deprotonate the incoming nucleophilic substrate in the deglycosylation portion of the reaction. Both glycosylation and deglycosylation reactions again proceed through oxocarbenium ion-like transition states.

These two groups of enzymes therefore display two different reaction mechanisms, with single and double displacement mechanisms for inverting and retaining enzymes, respectively. This difference reflects differences in reaction pathways and stereochemical outcomes. The transition state structures may also vary among different glycosidases. Despite the proposal that oxocarbenium-like transition states are experienced in both retaining and

inverting mechanisms, they may differ in the degree of nucleophilic participation which is not present in the limiting S_N1 transition state, but must take part in the S_N2-like transition state.

The most studied glycosidases are retaining glycosidases. Two examples of this group of enzymes will be given below. They serve as a good starting point for the study of other glycosylhydrolases and glycosyltransferases. Hen egg white lysozyme (EC 3.2.1.17) is among the earlier enzymes whose crystal structures were revealed (58). It catalyzes the cleavage of the glycosidic bond linking 2-acetamido-2-deoxy-D-muramic acid (NAM) residue and 2-acetamido-2-deoxy-D-glucose (NAG) residue in a sugar substrate that is a natural component of cell wall peptidoglycan of gram negative bacteria (64, 65).

The proposed mechanism for HEW lysozyme is S_N1-like (59). Two active site acidic residues, Asp52 and Glu35, were found to be essential for enzymatic activity (66). Glu35 was proposed to be the general acid/base catalyst that facilitates the departure of the leaving group by donating a proton to the exocyclic oxygen, and later in the catalytic cycle deprotonates the attacking water molecule and enhances its nucleophilicity. The reaction proceeds through an oxocarbenium ion-like transition state, as suggested by α-^{2}H-secondary isotope effects (67) and leaving group ^{18}O isotope effects (68). The formation of an oxocarbenium ion intermediate was proposed based on the crystal structure. This intermediate is thought to be stabilized by Asp52 in the active site. The important features of the proposed mechanism for HEW lysozyme, therefore, include the participation of a general acid/base catalyst, the formation of an

oxocarbenium ion intermediate, and the stabilization of such an intermediate by an acidic amino acid residue in the active site. Note that this mechanism is different than the one suggested by Koshland for the retaining glycosidases in that an S_N1, rather than an S_N2 mechanism, was proposed for lysozyme. The mechanism is illustrated in figure 1-5.

E.coli β-galactosidase (EC 3.2.1.23) is also a retaining glycosidase that belongs to glycosidase family 2 of Henrissat classification. Research on β-galactosidase has led to the assignment of the roles of two important active site amino acid residues, Glu537 and Glu461. J. C. Gebler et al. identified Glu537 as the nucleophile by using a fluorinated sugar substrate which allowed the accumulation and trapping of a covalent intermediate (69). The same approach has been employed for the trapping of the covalent intermediates in a number of other retaining glycosidases (70-76) and, along with other lines of evidence, has led to the proposal that covalent intermediates are formed in most retaining glycosidase reactions. Glu461 is in the active site of β-galactosidase and its essential role in catalysis was demonstrated by site-directed mutagenesis studies (77, 78). Mutations of Glu 461 decrease both k_2 (galactosylation) and k_3 (degalactosylation), implying the role of this residue as the general acid-base catalyst (77). More support for this came from the study of the E461G mutant based on the change of its substrate specificity and from the rescue of its activity by small organic nucleophiles (79, 80). It was found that when using 4-nitrophenyl-β-D-galactopyranoside as the substrate, E461G galactosidase showed high reactivity toward the anionic nucleophile azide, but no detectable

activity toward the neutral nucleophile trifluoroethanol. However, the wild type enzyme takes trifluoroethanol, but not azide as the acceptor substrate. This change in substrate specificity was rationalized by assigning Glu461 as the general acid-base catalyst. In the wild type enzyme, there exists a repulsive interaction between the negatively charged Glu461 side chain and azide ion. This interaction prevents azide from entering the acceptor site. In the case of trifluoroethanol, however, Glu461 acts as the general base catalyst, deprotonating trifluoroethanol and making it a better nucleophile. It was also shown that when formate reacted with the galactosylated E461G enzyme, galactose product was formed. Formate ion therefore diffuses and fills in the cavity of the excised propionate side chain of glutamate, and chemically rescues the general base function of Glu461. These results provided convincing evidence for the role of Glu461 as the general acid-base catalyst in β-galactosidase reaction. The β-galactosidase reaction follows an S_N-2 like double displacement mechanism with the formation of an enzyme-bound covalent intermediate. The mechanism also features general acid-base catalysis. Both galactosylation and degalactosylation steps proceed through an oxocarbenium-ion like transition state. The mechanism is shown in figure 1-6.

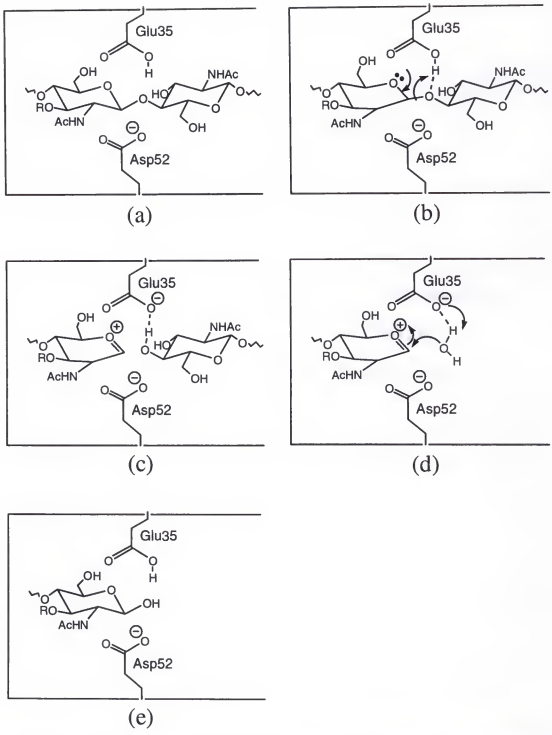

Figure 1-5. The proposed mechanism for HEW lysozyme. In this mechanism, Glu35 acts as the general acid/base catalyst. The oxocarbenium ion intermediate is stabilized by Asp52.

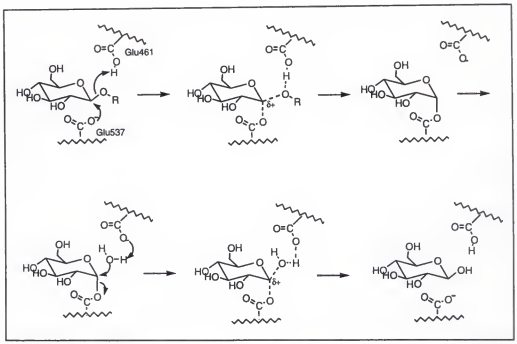

Figure 1-6. Proposed mechanism for β-galactosidase. In this mechanism, Glu537 is the nucleophile leading to the formation of the covalent intermediate. Glu461 is the general acid/base catalyst.

Although two acidic amino acid residues were found to be crucial in both lysozyme and β-galactosidase reactions, their roles are not exactly the same. The major difference lies in the nature of the reaction intermediate. In the case of lysozyme, an oxocarbenium ion intermediate was proposed which is stabilized by the active site Asp52. However, for β-galactosidase, a covalent intermediate was observed. The formation of a covalent intermediate seems to be followed by most of the retaining glycosylhydrolases. The difference in the nature of the intermediate follows the difference in the transition states. While an S_N2-like transition state results in the formation of a covalent intermediate (although short-lived in some cases), an S_N1 transition state could lead to either an ion pair intermediate or a covalent intermediate if the ion pair collapses to form a covalent

bond. This area is where the major debate resides for this group of enzymes, which will be discussed in more detail later in this chapter.

Enzymes that Hydrolyse or Transfer Sialo Sugars: Sialidases and Sialyltransferases

Sialidases, sialyltransferases and trans-sialidase constitute the second category of glycosylhydrolases and glycosyltransferases. They are directly involved in sialic acid metabolism and chemistry. The reactions catalyzed by these three groups of enzymes are illustrated in figure 1-7. Sialidases are found in bacteria, virus, parasite and mammalian cells with different biological functions. Sialyltransferases also exist in various organisms, with the main function being in the synthesis of sialic acid containing glycoconjugates. Research on these two groups of enzymes provides the basis for the mechanistic study on trans-sialidase.

Although the major function of sialidases in bacteria is thought to be nutritional (81), virus sialidases may be directly involved in pathogenic processes. Influenza neuraminidase activity was implied in two processes during invasion. By removing sialic acid residues on the cell surface, it helps virus pass through mucin and later facilitates the release of virus progeny from the host cells (82, 83). Because of its role in pathogenesis, influenza neuraminidases have been studied extensively. There are different families of influenza neuraminidases from different virus strains. Neuraminidase A/Tokyo/3/67 from virus N2 strain (hereafter abbreviated neuraminidase A) will be discussed here because of the available structural and mechanistic information on this enzyme.

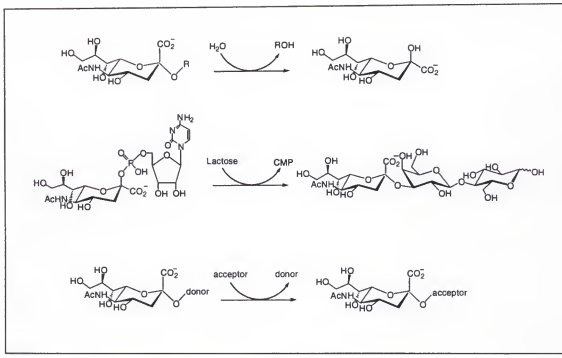

Figure 1-7. Reactions catalyzed by sialidases (above), α-2,3-sialyltransferases (middle) and trans-sialidase (bottom).

Influenza neuraminidase A acts with net retention of configuration (84). The crystal structure of influenza A neuraminidase/sialic acid complex has been determined and the product sialic acid was found to be bound in a $_2B_5$ boat conformation (85). In the active site, three Arg residues (Arg triad) are in close proximity to the C-1 carboxylate group of NeuAc and are presumably involved in the binding and electrostatic stabilization of this group in the transition state. There is also a hydrophobic pocket in the active site that accommodates the N-acetyl group of sialic acid. Other residues found in the active site that merit investigation are Tyr406, Glu276, Glu277 and Asp151. All these residues are found to be essential for enzymatic activity. A mutagenesis study on influenza A neuraminidase led to a proposed mechanism analogous to the one for lysozyme

which involves general acid catalysis and the formation of a stabilized oxocarbenium ion intermediate (86). The later kinetic isotope effect studies on this enzyme with the substrate 4-methylumbelliferyl-N-acetyl-α-D-neuraminic acid (MuNANA) provided strong evidence for the existence of such an oxocarbenium ion intermediate (84). β-dideuterio secondary isotope effects on V were found to be normal and inverse for the glycosylation and deglycosylation step, respectively. This result was interpreted to indicate that the reaction proceeds through an oxocarbenium ion intermediate. Again, both glycosylation and deglycosylation steps proceed through an oxocarbenium ion-like transition state. Asp151 was proposed to stabilize the positive transition states. It is also thought to facilitate the donation of one proton from the solvent to the leaving group and later in the reaction to deprotonate the incoming water nucleophile. The enzyme was shown to bind the α-anomer of substrate exclusively. The ES complex thus formed undergoes a conformational change to achieve the $_2B_5$ conformation of NeuAc that was observed in the crystal structure. Arg371 was suggested to facilitate this conformational change by positioning the C-2 carboxylate group of NeuAc in the active site. The ring distortion of the substrate is believed to contribute to catalysis. In a further study on this enzyme with a different substrate, *p*-nitrophenyl-α-D-N-acetyl-neuraminic acid (PNPNeuAc), the $^2C_5$ to $_2B_5$ conformational change of NeuAc was confirmed. β-dideuterio secondary and ^{18}O leaving group isotope effects also suggested an oxocarbenium ion-like transition state with a large degree of bond cleavage between C-2 of NeuAc and the leaving group oxygen. General acid catalysis was indicated by the leaving

group isotope effects. However, the inverse β-dideuterio isotope effect with MuNANA in the above experiment, on which the proposal of an oxocarbenium ion intermediate solely stands, was not observed. The possibility of nucleophilic participation in the transition state was hence raised based on the observed normal β-dideuterio isotope effects of both glycosylation and deglycosylation portions of the reaction. Without the presence of an appropriately positioned active site carboxylate residue, this led to the suggestion of the involvement of the carboxylate group of NeuAc in the transition state, forming an α-lactone intermediate (87). The presence of such an intermediate was suggested in the studies of the acid hydrolysis reaction of PNPNeuAc (88). There was, however, argument about whether the difference in the KIE results were due to a different reaction mechanism, or simply due to the use of two different leaving group aglycons (89). Further experiments need to be carried out to determine the degree of the nucleophilic participation in the transition state of the glycosylation reaction, which will lead to a definitive conclusion about the nature of the reaction intermediate.

In general, the proposed mechanism for influenza A neuraminidase includes the binding of the α-anomer substrate, the conformational change to achieve the catalytically competent $_2B_5$ conformation, the departure of the leaving group leading to the oxocarbenium ion-like transition state that is stabilized by acidic residue(s) in the active site, the formation of an enzyme oxocarbenium ion intermediate or an α-lactone intermediate and finally, the attack of water to give the product. This mechanism is shown in figure 1-8.

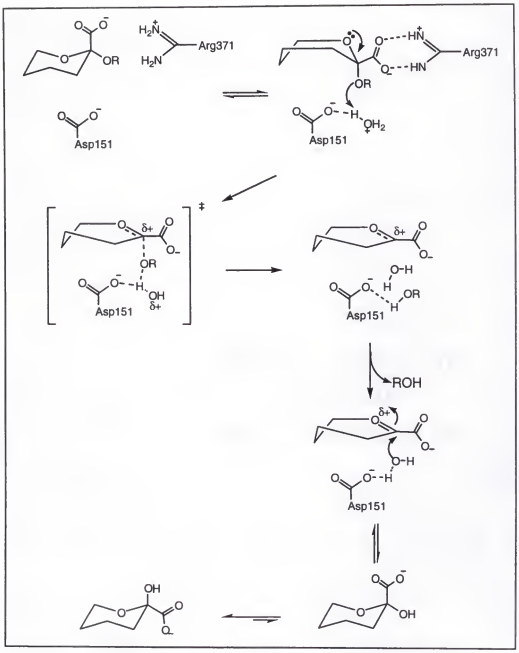

Figure 1-8. Proposed mechanism for influenza A neuraminidase. This figure is taken from reference (84).

Among various bacterial sialidases, *Salmonella typhimurium* sialidase will be discussed here because this enzyme exhibits sequence similarity with trans-sialidase (47, 90). The crystal structures of *Salmonella* sialidase and its

complexes with product and inhibitors are available (91). The overall structure was found to be very similar to that of the influenza neuraminidases, in spite of the lack of apparent sequence similarities between bacterial and viral sialidases. Furthermore, most of the active site residues found in the influenza neuraminidase active site are conserved in *Salmonella* sialidase. These include the Arg triad, the hydrophobic pocket, Tyr342 and Glu231 (92).

β-dideuterio secondary and ^{18}O leaving group isotope effects of *Salmonella* sialidase suggest an oxocarbenium ion-like transition state with a large degree of glycosidic bond cleavage in the transition state (87). Tyr342 is in close distance (~ 3 Å) to C-2 of NeuAc-2en (DANA or 2,3-dehydro-3-deoxy neuraminic acid) in the crystal structure and was proposed to stabilize the oxocarbenium ion-like transition state (93). The large β leaving group values on both V and V/K, as well as the large ^{18}O leaving group isotope effect indicated little protonation to the leaving group aglycon. The catalytically competent sugar conformation was suggested to be $^{2}C_{5}$ (87).

In general, both influenza nueraminidase and *Salmonella* sialidase proceed through an oxocarbenium ion-like transition state. However, they differ in the conformation of the bound substrate as well as in the requirement for general acid catalysis. The catalytically competent NeuAc conformations in *Salmonella* sialidase and influenza neuraminidase were also obtained by QM/MM simulations (94).

Sialyltransferases represent another group of enzymes involved in sialic acid glycosyltransfer. Unlike sialidases which use various glycoconjugates as

substrates, sialyltransferases take a universal sugar nucleotide, cytidine 5'-monophosphate N-acetyl-neuraminic acid (CMP-NeuAc), as the donor substrate and transfer the NeuAc group to various glycoconjugates (95). Sialyltransferases are inverting enzymes (96) that follow a sequential mechanism (97). Due to the weaker C-N glycosidic bond in CMP-NeuAc than the C-O bond found in glycoconjugates, it is expected that sialyltransferases will behave differently than sialidases. Multiple kinetic isotope effects on the acid solvolysis of CMP-NeuAc (β-dideuterio 1.276, 2-^{14}C 1.030) revealed a nearly complete departure of the leaving group CMP and virtually no nucleophilic participation in the transition state (98). The same features were found for the transition states of rat liver α-2,3- and rat liver α-2,6-sialyltransferase reactions, as revealed by multiple kinetic isotope effect studies with a slow substrate UMP-NeuAc (99, 100). The low ^{14}C primary isotope effect (1.028) of enzymatic reactions undoubtedly supports a dissociative transition state with little nucleophilic participation. A conformational change prior to catalysis was also revealed by comparing the KIE results of CMP-NeuAc and UMP-NeuAc. KIEs obtained for CMP-NeuAc were much smaller than those for UMP-NeuAc, even after the correction for the external commitment. Hence, an internal commitment must exist that masks the intrinsic isotope effects. This is best explained by a conformational change of ES complex before catalysis (99).

The discussion so far has outlined the general mechanistic schemes for glycosylhydrolases and glycosyltransferases, including what is known about the enzymes acting on the sialic acids. The transition states of this family of

enzymes generally possess oxocarbenium ion character. In spite of the considerable amount of research on this family of enzymes, controversies still exist in the detailed mechanisms of individual enzyme, especially in the nature of the reaction intermediate. The oxocarbenium ion intermediate of HEW lysozyme was proposed based on its crystal structure. The presence of such an intermediate was challenged by the mutagenesis study on T4 lysozyme which suggested that this intermediate was covalent in nature (101), and by the observation of the formation of a covalent intermediate in a mutated T4 lysozyme (70). The formation of a covalent intermediate was also supported by the increasing number of trapped covalent intermediate of retaining glycosidases (70-76). This same controversy also exists for influenza A neuraminidase as discussed above. This controversy arises partly from the realization that the oxycarbenium ion has a very short life time. Jencks et al. estimated the life time of the glucosyl oxocarbenium ion to be approximately $1X10^{-12}$ s (102), which is on the borderline of a real existence in aqueous solution. In the presence of anionic nucleophiles, a glucosyl cation could not be detected as an intermediate. Compared to a glycosyl oxocarbenium ion, the sialyl oxocarbenium ion has an increased life time because of two structural features that are absent in common glycosides (98). First, sialic acids bear on its anomeric carbon a carboxylate group which is responsible for the highly acidic nature of these molecules. This group, in principle, could stabilize the sialyl oxocarbenium ion via electrostatic interactions. Second, unlike the common glycosides, sialic acids are 2-deoxy sugars. The lack of the induction effect by a hydroxyl group on this position

further contributes to the stability of the sialyl oxocarbenium ion. It was estimated that the life time is increased by roughly 4 fold, as compared with glycosyl oxocarbenium ion, as the result of the lack of this induction effect (102). Azide trapping experiments have provided evidence for the increased life time of the sialyl oxocarbenium ion by showing that it has a real existence in the presence of the anionic nucleophile (103). It was estimated that the life time of the sialyl oxocarbenium ion is about two order of magnitude greater than that of a glycosyl oxocarbenium ion (98, 103). Therefore, the sialyl oxocarbenium ion, although unstable, may have a real existence as an intermediate in the enzyme active site.

In solution reactions, the lifetime of the intermediate could affect the reaction pathway as suggested by Jencks et al.. They provided evidence for different mechanistic pathways with leaving groups of different ionic properties. In the presence of a neutral methoxy leaving group, the hydrolysis of α-D-glucopyranoside follows essentially an S_N1 pathway with the formation of a glycosyl oxocarbenium ion intermediate, which is subsequently trapped by water. However, when the leaving group is anionic in nature, as in the case of a fluoride ion, the reaction follows an enforced S_N2 mechanism (104). The glycosyl oxocarbenium ion is too unstable to have a real existence in the face of an anionic leaving group. Therefore, the intimate ion pair between the oxocarbenium ion and fluoride ion can not form and must collapse to regenerate the reactant. This result was later confirmed by kinetic isotope effect studies performed on the hydrolyses of α-glucopyranosides (105). ^{13}C primary isotope effect of methyl α-glycoside hydrolysis was 1.007, right in the range for an S_N1

reaction mechanism. In contrast, ^{13}C primary isotope effect of α-glucosyl fluoride was 1.032, which was interpreted as the reaction going through an associative (S_N2 like) transition state (105).

Because of their short life times in solution, oxocarbenium ions need to be stabilized by an active site machinery provided by enzyme catalysis. Different strategies can be employed by enzymes to reach this goal which result in different reaction pathways. Two general strategies are: 1) to stabilize the oxocarbenium ion intermediate via electrostatic interactions provided by the enzyme active site; and 2) to form an enzyme covalent intermediate. The differentiation of these two strategies provides great challenges in mechanistic studies. As mentioned above, even in the case of HEW lysozyme whose mechanism was proposed some thirty years ago, there is still debate about whether it forms an oxocarbenium ion intermediate or a covalent intermediate. This controversy is a direct result of the lack of information concerning the amount of nucleophilic participation in the transition state. Mutagenesis studies may not necessarily reveal the nucleophilic nature of the amino acid residue. The trapped reaction covalent intermediate could simply be a result of the collapse of an oxocarbenium ion intermediate with a nearby acidic amino acid residue. Fluorinated sugar substrates have been used to demonstrate the formation of covalent intermediates in many glycosidase reactions. However, the much stronger electronegativity of fluorine, compared to that of hydrogen, could in principle change the nature of the transition state. A fluoro-oxocarbenium ion intermediate should have intrinsically lowered stability relative to the one derived

from the "natural' substrate, so the observation of covalent adducts using fluorosugars could represent a tipping of the reaction coordinate away from an oxocarbenium ion intermediate and towards a covalent intermediate. Kinetic studies, especially kinetic isotope effect studies, are crucial in providing such information regarding the transition state structures. KIE studies employ isotopic substrates that have essentially no perturbation on the electronic and steric properties of the substrate, hence providing direct information on the transition state structures of reactions with natural substrates. However, even within the scope of kinetic isotope effect studies, care must be taken in data interpretation because different isotope effects provide information regarding different aspects of the transition state structure. For example, an α-secondary isotope effect depicts the change in the hybridization state of the reaction center atom along the reaction coordinate. The magnitude of this type of KIE is not indicative of the amount of nucleophilic participation in the transition state. Therefore, it is of little value in differentiating between S_N1 and S_N2 transition states (106). Primary carbon isotope effect provides information regarding the nucleophilic participation in the transition state and thus can be used to distinguish S_N1 and S_N2 mechanisms. The lack of the primary isotope effect information is one of the major reasons for the above-mentioned controversy on lysozyme and many other glycosidases. Although α-secondary and leaving group isotope effects were measured on lysozyme, none of them are suitable in distinguishing a dissociative and an associative transition state. As a result, the presence of nucleophilic participation in the transition state and the nature of the intermediate remain

unknown. One example of the application of carbon primary KIE studies on glycosidases is found in sugar beet seed α-glucosidase and *Rhizopus niveus* glucoamylase where ^{14}C primary isotope effects were measured using the substrate α-D-glucopyranosyl fluoride (107). These two enzymes catalyze reactions with different stereochemical outcomes, yet they possess a similar oxocarbenium ion-like transition state as revealed by ^{14}C primary isotope effects and α-secondary ^{3}H isotope effects. The small ^{14}C primary isotope effects (1.022 and 1.033 for sugar beet seed α-glucosidase and *Rhizopus niveus* glucoamylase, respectively) and large α-secondary ^{3}H isotope effects provide strong evidence for such an S_N1-like transition state for both enzymes. It is interesting to note that although hydrolysis of α-D-glucopyranosyl fluoride in aqueous solution involves a transition state with a significant amount of nucleophilic participation (105) as indicated by a 1.032 ^{13}C primary isotope effect, enzymatic hydrolysis of the same molecule can proceed through an entirely different transition state. These results, therefore, challenge the idea that solution and enzyme reactions must follow the same path. Carbon primary isotope effects were the key data in the above studies that provided crucial information on the nature of the transition state. Unfortunately, carbon primary isotope effects have rarely been applied in the study of sialidases. The isotope effect study on trans-sialidase as presented in this dissertation, therefore, provided this needed information and allowed the direct observation of nucleophilic participation in the transition state, which provided the first evidence for a covalent intermediate.

Mechanistic Background of *Trypanosoma cruzi* Trans-sialidase

Mechanistically, little was known about *T. cruzi* trans-sialidase except for the following points. Unlike sialyltransferases, trans-sialidase catalyzes the retention of configuration of the anomeric carbon and does not use CMP-NeuAc as the sialic acid donor (108). It is a dual-function enzyme catalyzing both a glycosyltransfer and a glycosylhydrolysis reaction. The hydrolytic reaction is suppressed in the presence of sugar acceptors and becomes increasingly significant as the sugar acceptor concentration decreases (36). Previous steady state kinetic studies suggested a bisubstrate sequential mechanism for trans-sialidase (108, 109). However, its mechanism was reinvestigated in this project and will be presented later in this dissertation. The rates of the glycosyltransfer reaction vary significantly with different donor substrates, implying that a long-lived sialosyl-enzyme intermediate may not be formed (109). Different acceptor concentrations have no effect on the release of the leaving group of the donor substrate, suggesting that the rate limiting step could be the initial breakage of the sialic acid bond and that in trans-sialidase, the donor and acceptor substrates may coexist in the active site of the enzyme (109). Sequence alignment among trans-sialidase and bacterial neuraminidases revealed some conserved sequence motifs. Both TCTS and *Salmonella* sialidase belong to subfamily 33 of the Henrissat classification. There are three Asp boxes (SXDXGXTW) in the N-terminal domain of TCTS which are conserved in bacterial sialidases (47). Besides, 14 out of 16 of the active site amino acids of *salmonella* sialidase as deduced from its crystal structure are conserved in the same or similar positions

in TCTS, strongly implying a similar active site structure in both enzymes (90). Among these residues, a highly conserved Tyr342 was proposed to stabilize the oxocarbenium ion formed in the *Salmonella typhimurium* neuraminidase catalyzed reactions (93). In the crystal structure of *Salmonella* sialidase/DANA complex, the hydroxyl oxygen of Tyr342 is ~3 Å from C-2 of DANA bound in the active site (92). This tyrosine is also conserved in the active site of *T. rangeli* sialidase, of which the crystal structure was recently reported to be very similar to that of *Salmonella* sialidase (110). Given the high sequence similarity (~70%) between TCTS and *T. rangeli* sialidase (111, 112), it is very likely that Tyr342 is in a similar location in the active site of TCTS. The essential role of Tyr342 was shown by site-directed mutagenesis study in which Y342P mutation totally abolished the catalytic activity of TCTS (113). The importance of Tyr342 was also suggested by the studies on the TCTS gene family. Some members in this family encode active TCTS while others encode inactive enzyme forms. The function of the inactive enzymes is not clear. Nevertheless, study has shown that Tyr342 is conserved in all active TCTS while a histidine replaces Tyr342 in all inactive enzyme forms (90).

Although Try342 was implicated in the catalysis of both *Salmonella* sialidase and TCTS, it was not clear whether or not it plays the same role in these two enzymes. In spite of the sequence similarities, TCTS and *Salmonella* sialidase must differ mechanistically as the former is a glycohydrolase with little transferase activity while the latter is mainly a transferase. It is of interest,

therefore, to compare the mechanisms of these two enzymes that are structurally similar but functionally different.

CHAPTER 2
RECOMBINANT TRANS-SIALIDASE OVEREXPRESSION AND SUBSTRATE SYNTHESIS

Introduction

Trypanasoma cruzi trans-sialidase transfers an α-2,3-linked sialic acid group from glycoconjugates to acceptor molecules. Trypomastigote trans-sialidase contains two functionally separate domains, an N-terminal domain with full catalytic activity and a C-terminal domain consisting of tandems of 12-amino acid repeats which is thought to be immunodominant (47). The cloning and expression of the N-terminal catalytic domain of trans-sialidase has been accomplished (109), which greatly facilitates kinetic study of this enzyme.

In order to carry out the kinetic isotope effect study on trans-sialidase, a series of isotope-labeled substrates needed to be synthesized. We utilized two sialic acid-containing sugars, sialyl-lactose and sialyl-galactose, as the donor substrate and designed and synthesized a series of substrate molecules with different isotopic labels. We used these two saccharides as model compounds to study the trans-sialidase catalyzed reactions. The availability of enzymes in all steps leading to the desired substrates enabled the application of enzymatic synthesis which has been extensively applied in carbohydrate synthesis due to its strict substrate specificity and stereochemistry. Chemical synthesis was also applied where enzymatic synthesis could not be carried out.

Results

Overexpression and Purification of Recombinant Trans-sialidase

Trans-sialidase purified from parasites of the trypomastigote stage is a heterogeneous mixture of enzymes with varied lengths of C-terminus. Kinetic experiments are advantageously performed with the use of a homogenous enzyme preparation. This was achieved by the successful overexpression of the N-terminal catalytic domain of TCTS in *E.coli* expression system. In this project, two recombinant trans-sialidase constructs, kindly provided by our collaborator Sergio Schenkman, were used to overexpress trans-sialidase which was purified to homogeneity (109).

For the purification of trans-sialidase from plasmid TCTS/pQE60, ammonium sulfate precipitation, Ni^{2+} affinity chromatography and anion-exchange chromatography were employed. An activity assay and a protein assay were performed in each step and the results are given in table 2-1. SDS-PAGE electrophoresis of the purified trans-sialidase is shown in figure 2-1 (left panel).

For the purification of trans-sialidase from plasmid TCTS/pET14b, Ni^{2+} affinity chromatography and anion-exchange chromatography were employed. Purified recombinant trans-sialidase gave a single band in the SDS-PAGE gel (figure 2-1, right panel). The activity assay was conducted with an assay mixture containing 1 mM ([1-^{14}C]Glc) sialyl-lactose (30,000 cpm, 54.3 mCi/mmol), 1.15 mM lactose in pH 7.3, 60 mM HEPES buffer with 2 mg/ml BSA. The specific

activity of the purified trans-sialidase was 6.8 μmol/min/mg. The specific activity of the first construct under the same condition was 13.8 μmol/min/mg.

Table 2-1. Trans-sialidase (from TCTS/pQE60) purification table

sample[a]	Total activity (Unit)	Total Protein (mg)	S. A.[b,c] (units/mg)	Yield (%)	Purification
1	1.58	260	0.0061		
2	4.22	240	0.018		2.89
3	1.55	150	0.010	98	1.69
4	1.34	6	0.22	85	36.55
5	0.80	0.1	8.01	51	1315.27

a. sample 1 through 5 represents those taken from cell lysate, supernatant of 30% ammonium sulfate precipitation, pellet of 60% ammonium sulfate precipitation, Ni^{2+} affinity column fractions, and MonoQ anion-exchange column fractions, respectively. b. S. A.--specific activity. c. Activity assay mixture contains: 0.4 mM sialyl-lactose, 7.4 mM ([1-^{14}C] Glc) lactose with 0.16 mM cold lactose in pH 7.0, 20 mM HEPES buffer with 0.2% ultrapure BSA.

Substrate Synthesis

The work presented in this dissertation is focused on the resolution of the transition state structure of the trans-sialidase catalyzed reaction. The major methodology employed in this project is dual-label competitive kinetic isotope effect studies which necessitate the synthesis of a series of molecules with different isotopic labels. These molecules include those with radioactive trace labels, those with stable isotope labels, and those with both radioactive and stable isotope labels. Both enzymatic and chemical synthesis methods were employed to synthesize the desired substrates. To study the transition state of trans-sialidase catalysis, it was necessary to synthesize a slow donor substrate

that could eliminate the commitment to catalysis or be used to show that one did not exist. In this project, both sialyl-lactose (a good substrate) and sialyl-galactose (a slow substrate) were synthesized. The positions of isotopic labels on these two substrates are given in figure 2-2. The isolated yields for the substrates synthesized enzymatically are given in table 2-2. The yields for the chemical synthesis is given in table 2-3.

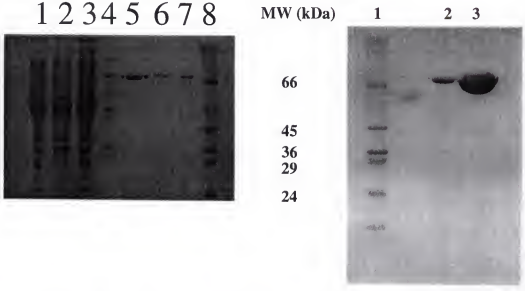

Figure 2-1. SDS-PAGE analysis of trans-sialidase from TCTS/pQE60 (left panel) and TCTS/pET14b (right panel). Left panel: lane 1, cell lysate; lane 2, after ammonium sulfate precipitation; lane 3, Ni^{2+} column flow-through; lane 4, after Ni^{2+} column; lane 5, TCTS fractions after HPLC MonoQ column; lane 6 and 7, other fractions after MonoQ column; lane 8, MW standard. Right panel: lane 1, MW standard; lane 2 and 3, purified trans-sialidase.

Purification of α-2,3-Sialyl-lactose from Bovine Colostrum

Previous kinetic experiments (108, 109) indicated a millimolar K_m for the donor substrate, sialyl-lactose. Therefore, for a full range initial velocity experiment with trans-sialidase, milligram quantity of pure sialyl-lactose was required. This was achieved by the purification of α-2,3-sialyl-lactose from

bovine colostrum (114). The entire purification procedure consists of three steps: MeOH/$CHCl_3$ extraction, Sephadex G-25 chromatography and anion exchange chromatography. The average yield is 30 mg α-2,3-sialyl-lactose from 200 ml of colostrum. The purified α-2,3-sialyl-lactose was characterized by ^{1}H-NMR (figure 2-4) and estimated to be greater than 95% pure.

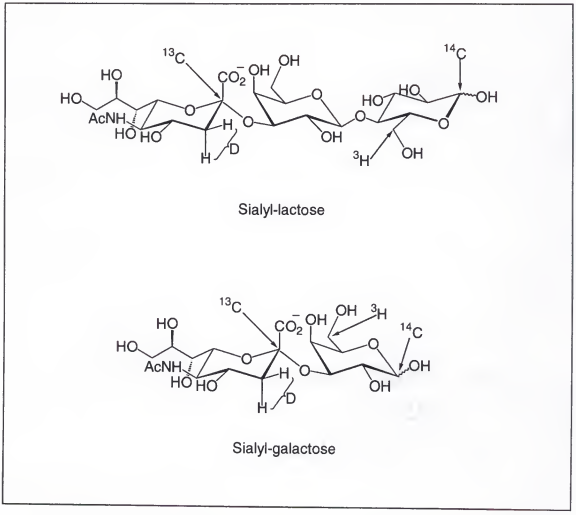

Figure 2-2. Positions of isotope labels in sialyl-lactose and sialyl-galactose.

Table 2-2. Yields of substrate synthesis for KIE experiments

Compound	Isotope & Position	Yield (%)
Sialyl-lactose	[3,3'-^{2}H] NeuAc, [1-^{14}C] Glc	67
Sialyl-lactose	[2-^{13}C] NeuAc, [1-^{14}C] Glc	76
Sialyl-lactose	[1-^{14}C] Glc	74
Sialyl-lactose	[6-^{3}H] Glc	52
Sialyl-galactose	[3,3'-^{2}H] NeuAc, [6-^{3}H] Gal	75
Sialyl-galactose	[1-^{14}C] Gal	80
Sialyl-galactose	[2-^{13}C] NeuAc, [6-^{3}H] Gal	82
Sialyl-galactose	[6-^{3}H] Gal	75

Table 2-3. Yields of chemical synthesis for the preparation of [3-^{18}O] galactose

Product	Yield (%)
4,6-benzylidene methyl galactoside	50
2-benzoyl-4,6-benzylidene methyl galactoside	30
2-benzoyl-3-keto-4,6-benzylidene methyl galactoside	70
4,6-benzylidene methyl galactoside	50
Methyl-a-D-galactoside	> 95
Galactose	> 60

Discussion

Overexpression and Purification of *Trypanosoma cruzi* Trans-sialidase

Trans-sialidases are encoded by a family of genes. The structure and function of trans-sialidase vary in different stages of the parasite's life cycle. Because the trypomastigote form of the parasite has the highest trans-sialidase activity, and also because the trans-sialidase activity of this form of the parasite is directly implicated in the invasion of mammalian hosts, trans-sialidase expressed in the trypomastigote stage was studied in this project. As noted earlier, trans-sialidase from the trypomastigote stage of *Trypanosoma cruzi* contains an N-terminal catalytic domain and a C-terminal domain with tandems of amino acid repeats. The lengths of the C-terminus vary, causing the heterogeneous migration pattern of the enzyme on SDS-PAGE gel (47). Therefore, early work on trans-sialidase purified from parasites were actually done with a mixture of trans-sialidases of different lengths of C-terminus. In order to obtain kinetic data on trans-sialidase with a uniform molecular weight and conformation, cloning and expression of this enzyme is necessary. The N-terminus of trans-sialidase has been successfully cloned and expressed in *E.coli* cells in Dr. Sergio Schenkman's lab (109). Two plasmids containing trans-sialidase gene were sent to us as gifts from Dr. Schenkman. In the first construct, trans-silaidase gene was cloned into pQE60 vector and overexpressed in *E.coli* TG-1 cells. In the second construct, trans-sialidase gene with slight modifications was cloned into pET14b vector and expressed in *E.coli* BL21 (DE3) cells. The C-terminal amino acid sequence is slightly different in these two

constructs, with GSRS and GSGC in the first and second construct, respectively. In both constructs, a His tag was linked to the C-terminus of the enzyme to facilitate the purification by Ni^{2+} affinity column. The overexpression and purification of trans-sialidase from these two constructs followed generally the same procedure (109), with a few modifications which will be mentioned below. It was found that inclusion bodies formed during the expression when the normal growth condition (37 °C, 250rpm) was used. To minimize inclusion body formation, all expressions were carried out at 30 °C and 150 rpm. IPTG was the inducer for the expression of the first construct (TCTS/pQE60), but it was not required for the expression of the second construct (TCTS/pET14b), probably because the high amount of trans-sialidase expressed by this plasmid exposes galactose on the polysaccharide molecules that can serve as the activator for gene expression. PMSF was present in the purification process of the first construct expressed in TG-1 cells, but not in the second construct expressed in BL21 cells. Ammonium sulfate precipitation was performed for the first construct, but not for the second construct. Trans-sialidase was further purified by Ni^{2+} affinity chromatography and anion-exchange chromatography. Chromatograms for these two steps are shown in figure 2-3 and 2-4, respectively. The purity of final purified trans-sialidase was assessed by SDS-PAGE. An average of 0.1 and 10 mg/liter trans-sialidase can be purified from the expression of the plasmid TCTS/pQE60 and TCTS/pET14b, respectively. TCTS from TCTS/pQE60 was used in all KIE and steady-state kinetic experiments. TCTS from TCTS/pET14b was used in the trapping experiment.

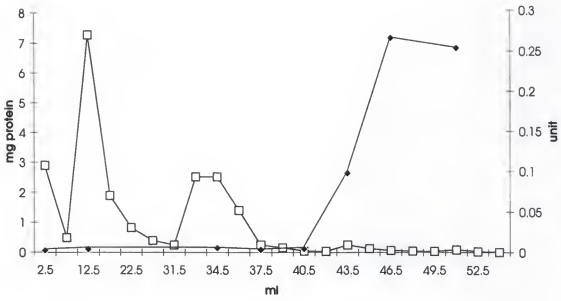

Figure 2-3. The chromatogram of Ni^{2+} affinity column purification of recombinant trans-sialidase from TCTS/pQE60. Open squares: protein amount; Solid diamonds: TCTS activity.

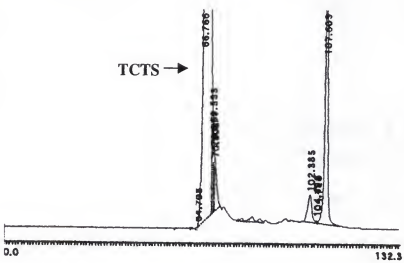

Figure 2-4. The chromatogram of HPLC MonoQ anion-exchange column purification of recombinant trans-sialidase from TCTS/pET14b.

Synthesis of ([6-^{3}H]Glc) Lactose

Due to the limited source of commercially available ([6-^{3}H]Glc) lactose, an enzymatic synthesis of this compound was designed, as shown in figure 2-5, to synthesize ([6-^{3}H]Glc) lactose from a readily available reactant, [6-^{3}H] Glucose. Two reactions were combined in a one-pot process. UDP-Glucose was first converted to UDP-galactose by UDP-Gal-4' epimerase. The equilibrium was driven forward by the removal of UDP-Gal in the next reaction where it reacted with [6-^{3}H] glucose to give ([6-^{3}H]Glc) lactose, a reaction catalyzed by galactosyltransferase. α-lactalbumin is a crucial component for galactosyltransferase activity and was included in the reaction mixture.

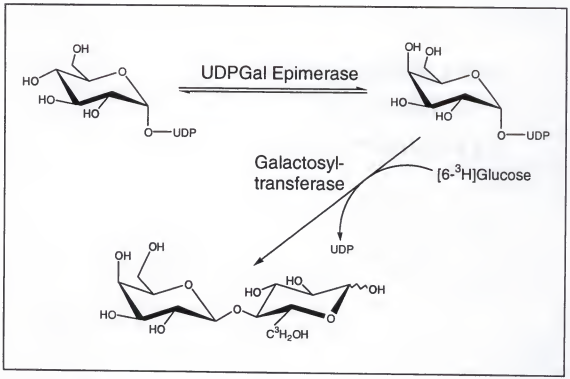

Figure 2-5. Enzymatic synthesis of ([6-^{3}H]Glc) lactose.

The reaction progress was monitored by two methods. In the first method, a reaction aliquot was added to an ATP/hexokinase reaction mixture which converted unreacted [6-^{3}H] glucose into [6-^{3}H] glucose 6-phosphate. The separation of [6-^{3}H] glucose 6-phosphate from product [6-^{3}H] lactose on Dowex-1 (formate) columns allowed estimation of the fractional conversion. The second method to monitor the reaction conversion was by thin-layer chromatography. Glucose and lactose can be separated on silica TLC system $CHCl_3$/i-PrOH/H_2O, 2:7:1. The presence of product lactose in the reaction mixture was confirmed by its co-elution with an authentic standard. A conversion of ca. 90% was estimated by both methods.

Synthesis of Sialyl-lactose Isotopomers

Isotopomers of sialyl-lactose were synthesized enzymatically and chemically as shown in figure 2-6. NeuAc was synthesized from N-acetyl-mannosamine (ManNAc) and pyruvate, catalyzed by NANA aldolase (115). [2-^{13}C] NeuAc was synthesized from [2-^{13}C] pyruvate. [9-^{3}H] NeuAc and [1-^{14}C] NeuAc were synthesized from [6-^{3}H] ManNAc and [1-^{14}C] pyruvate, respectively. The reaction equilibrium was shifted to the product NeuAc side by using an excess amount of pyruvate for unlabeled NeuAc and [9-^{3}H] NeuAc syntheses, or an excess amount of ManNAc for [2-^{13}C] NeuAc and [1-^{14}C] NeuAc syntheses. The progress of the NeuAc synthesis reaction was monitored by ^{1}H-NMR. The characteristic ^{1}H-NMR peaks of NeuAc include the triplet at 1.8 ppm (C-3 axial proton) and the doublet of doublets at 2.2 ppm (C-3 equatorial proton) (116) as shown in figure 2-7. The integration of these peaks with respect to those of the

starting ManNAc peaks allows the calculation of the reaction fractional conversion. When radioactive NeuAc was synthesized, the fractional conversion was monitored by HPLC. The product and remaining substrate were separated by HPLC and quantified by liquid scintillation counting. Generally, yields of 85 ~ 95% were obtained for these reactions.

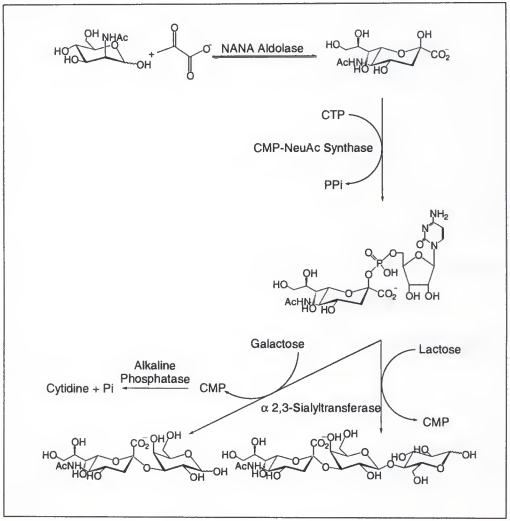

Figure 2-6. Enzymatic synthesis of sialyl-lactose and sialyl-galactose.

NeuAc thus synthesized was purified on Dowex (formate) anion-exchange column and assayed and quantified by the thiobarbituric acid (TBA) method

(117). At this stage, the introduction of the 3,3'-dideuterio substitution into the NeuAc molecule can be carried out. NeuAc performs a ring-opening reaction at basic pH (pH>12) as shown in figure 2-8. The 3,3'-protons in the ring-opened product undergo exchange in alkaline D_2O (118, 119). The complete exchange was confirmed by the disappearance of the 1.8 ppm triplet and the 2.2 ppm doublet of doublets (figure 2-9). The incorporation of [2-^{13}C] label into NeuAc can also be confirmed by ^{1}H-NMR. A small split of both 1.8 and 2.2 ppm peaks can be observed in [2-^{13}C] NeuAc ^{1}H-NMR due to the coupling between 2-^{13}C and 3,3'-protons (figure 2-10).

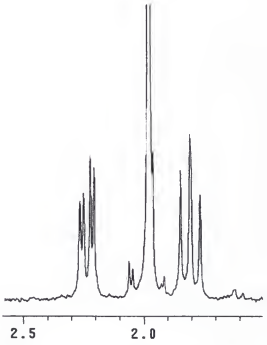

Figure 2-7. ^{1}H-NMR peaks of NeuAc 3,3'-protons.

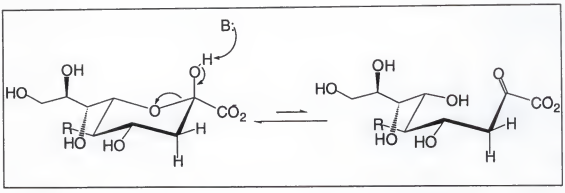

Figure 2-8. The ring opening reaction of NeuAc.

Figure 2-9. ^{1}H-NMR of [3,3'-^{2}H] NeuAc, showing the complete exchange with D_2O of NeuAc 3,3'-protons.

At this stage, NeuAc with different stable isotope labels can be used to synthesize cytidine 5'-monophosphate N-acetylneuraminic acid (CMP-NeuAc) with the corresponding stable isotope labels. This was carried out by CMP-NeuAc synthase (98, 120, 121). Cytidine-triphosphate (CTP) was the other

substrate in this reaction. The reactions proceeded at 37 °C and were monitored by HPLC. Control of pH is important in this reaction because the reaction releases protons which need to be neutralized in order to prevent the acid hydrolysis of CMP-NeuAc. For the synthesis of [3,3'-dideuterio] CMP-NeuAc, all the reagents used were pre-exchanged in D_2O and the reaction was run in D_2O solution. Again, pH was kept at ~7 to prevent the hydrolysis of CMP-NeuAc at acidic condition as well as the back exchange of 3,3'-dideuterio with solvent when the pH is too high. The lack of back exchange was confirmed by the lack of 3,3'-proton peaks in the ^{1}H-NMR spectrum (figure 2-11). The reaction conversion can be calculated by the integration of CTP and CMP-NeuAc peaks in the HPLC chromatogram. The reactions under the above described conditions generally gave a yield greater than 90%. CMP-NeuAc thus synthesized was purified by HPLC and was subsequently desalted with Amberlite IR120-H^+ resin as described in the experimental section.

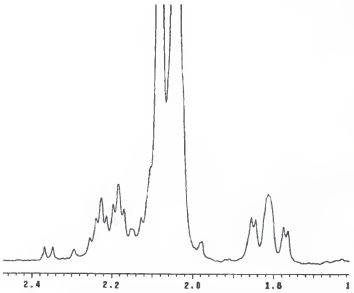

Figure 2-10. ^{1}H-NMR of the crude reaction mixture for [2-^{13}C] NeuAc synthesis.

Figure 2-11. ^{1}H-NMR of [3,3'-dideuterio] CMP-NeuAc. The disappearance of 3,3'-proton peaks indicates their total exchange with D_2O.

With CMP-NeuAc isotopomers in hand, the last step in the substrate synthesis was to synthesize sialyl-lactose isotopomers. This step was catalyzed by rat liver recombinant α-2,3-sialyltransferase that transfers the sialic acid group from CMP-NeuAc to the acceptor molecule and mediates regiospecific formation of an alpha glycosidic bond between carbon 2 of NeuAc and the 3-OH group of a galactose residue (122). Two acceptor lactose molecules were used: the commercially available ([1-^{14}C] Glc) lactose and the synthesized ([6-^{3}H] Glc) lactose. The desired isotopic substitution patterns were obtained by combination of the appropriate CMP-NeuAc and lactose isotopomers. CMP is the other reaction product and is also a potent inhibitor of α-2,3-sialyltransferase with a K_i of 50 μM (123). Alkaline phosphatase cleaves CMP (124) and eliminates its inhibitory effect. The inclusion of alkaline phosphatase in this reaction, therefore,

shortened the reaction time and increased the yields to ~98%. Two chromatographic steps were used to purify the final sialyl-lactose isotopomers. Anion-exchange chromatographic step removed lactose, CMP-NeuAc and most of NeuAc. However, the complete separation of sialyl-lactose from NeuAc could not be achieved by this step alone. The remaining NeuAc was removed by HPLC chromatography. The final radioactive purity of all sialyl-lactose isotopomers was greater than 99.9%.

Synthesis of Sialyl-galactose Isotopomers

The same synthetic route as described above was adopted for the synthesis of sialyl-galactose isotopomers. The only difference was in the last step catalyzed by rat liver recombinant α-2,3-sialyltransferase. In this step, galactose, instead of lactose, was used as the acceptor substrate in the reactions. Both [1-^{14}C] galactose and [6-^{3}H] galactose are commercially available. Again, by combination of the appropriate CMP-NeuAc and galactose isotopomers, the desired isotopic substitution patterns were obtained. Galactose is a poor substrate for α-2,3-sialyltransferase with a K_m of 268 mM (125). The use of radioactive galactose limited the galactose concentration in the reaction mixture. As a result, the reaction proceeded very slowly and the accumulation of CMP, both by the action of the enzyme and by the hydrolysis of CMP-NeuAc, caused inhibition of α-2,3-sialyltransferase. This problem was circumvented by the addition of alkaline phosphatase in the reaction mixture. Other modifications of conditions included using lower temperature (30 °C) and slightly basic pH (7.5) to minimize CMP-NeuAc decomposition, as well as using more α-2,3-

sialyltransferase and small reaction volumes to increase the substrate concentrations. Yields higher than 90% were obtained for these reactions. The purification of sialyl-galactose isotopomers followed the same procedure as described above for the purification of sialyl-lactose isotopomers.

Characterization of Sialyl-lactose and Sialyl-galactose Isotopomers

Kinetic isotope effect studies require high purity substrates with correct structures. Therefore, it is crucial to characterize and verify the synthesized compounds before proceeding to KIE experiments. ^{1}H-NMR, mass spectroscopy and TLC were used to identify the substrates synthesized by the above described methods. Unlabeled sialyl-lactose and sialyl-galactose were synthesized and purified by the same method and subjected to ^{1}H-NMR and MS analyses. Sialyl-lactose prepared in this way co-migrated with an authentic standard by silica TLC (EtOH:n-BuOH:pyridine:H_2O:HOAc, 100:10:10:30:3, v/v; visualized by heating a plate dipped in H_2SO_4/MeOH). The sialyl-lactose so obtained consisted of the two anomers at the Glc C-1. The ^{1}H-NMR (300 MHz, pH 7, room temperature) spectrum of sialyl-lactose prepared by this method (see Appendix A) agreed with reported data (126, 127) and also with standard sialyl-lactose purified from colostrum in this lab: δ=1.8 (apparent t, J=12.1, H3a); 2.02 (s, H of N-acetyl); 2.75(d-d, J=4.7, 12.4, H3e); 3.28 (t, J=8.6, 0.6 H); 4.11 (d-d, J=3.3, 10, 1H); 4.54 (d, J=7.9, 1.5H); 5.28 (d, J=3.4, 0.3H). The negative-ion FAB-MS (glycerol) of sialyl-lactose prepared by this method gave a molecular ion of 632.2039 (calculated 632.2038). The sialyl-galactose so obtained consisted of the two anomers at the Gal C-1. The ^{1}H-NMR (300 MHz, pH 7, room

temperature) of sialyl-galactose synthesized by this method (see Appendix B) agreed with reported data (126). δ=1.79 (apparent t, J=12.1, H3a); 1.81 (apparent t, J=12.1, H3a); 2.02 (s, Me of N-acetyl); 2.73, 2.75 (apparent overlapping d-d, J=4.66, 12.34; J=4.4, 12.2); 3.52 (d-d, J=7.8, 9.7, 0.6H); 4.07 (d-d, J=3.3, 9.8, 1H); 4.32 (d-d, J=3.1, 10.3, 0.3H); 4.64 (d, J=7.9, 0.6H); 5.28 (d, J=4.0, 0.25H). The negative-ion FAB-MS (glycerol) of sialyl-galactose prepared by this method gave a molecular ion of 470.1508 (calculated 470.1510).

Purification of α-2,3-Sialyl-lactose from Bovine Colostrum

In order to carry out an initial velocity kinetic study of trans-sialidase, milligram quantities of unlabeled sialyl-lactose are needed. For large scale synthesis, enzymatic synthesis is not generally applicable, mainly due to the enzyme inactivation by prolonged reaction time and by product inhibition, and also due to the expense associated with the need for large amount of pure enzymes. Bovine colostrum is a rich source of the disaccharide sialyl-lactose. In this experiment, sialyl-lactose was purified from colostrum based on the published method (114) with some modifications. After methanol/chloroform extraction, carbohydrate components of colostrum were purified by size exclusion chromatography to separate the low molecular weight component (mono- and di-saccharides) from the high molecular weight component (glycopeptides and glycolipids). The chromatogram of this step is shown in figure 2-12. The NeuAc concentration in each fraction was quantified by the thiobarbituric acid (TBA) assay (117). Absorbance at 280 nm was also measured, which indicated the amount of peptides in each fraction. Fractions

with high NeuAc content and low 280 nm absorbance were pooled and further purified by anion-exchange chromatography. The chromatogram is shown in figure 2-13. Neutral monosaccharides were separated from sialyl-lactose in this step. One challenge in this purification was to separate α-2,3-sialyl-lactose from its α-2,6 isomer that was also present in a lesser amount in colostrum. Both isomers possess the same molecular charge. Therefore on an anion-exchange column they coelute under one peak. Fractions under the peak were analyzed by ^{1}H-NMR and it was found that although the first half of the peak contained both α-2,3- and α-2,6-sialyl-lactose, the second half of the peak was virtually free of α-2,6-sialyl-lactose (figure 2-14). The C-3 equatorial protons on the NeuAc portion of α-2,3- and α-2,6-sialyl-lactose have a slight but distinguishable difference in chemical shift (127). This serves to differentiate α-2,3-sialyl-lactose from its 2,6 isomer. Thus, the second half of the peak was collected and concentrated. The pH was adjusted to alkalinity with ammonia in order to allow removal of pyridine by rotary evaporation. The ammonium acetate salt was then desalted by treatment with Amberlite IR120-H^{+} resin. An average of 30 mg of α-2,3-sialyl-lactose can be obtained from 200 ml of colostrum with an estimated purity of ~95%.

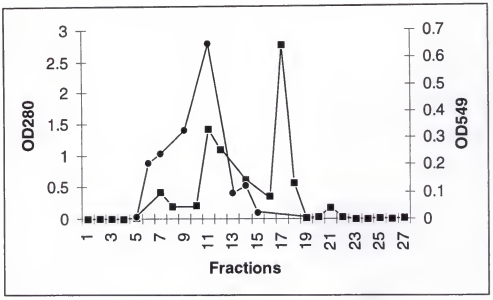

Figure 2-12. The chromatogram of Sephadex G-25 column purification of α-2,3-sialyl-lactose from bovine colostrum. Solid circles: OD549 (total NeuAc content); Solid squares: OD280 (peptide content).

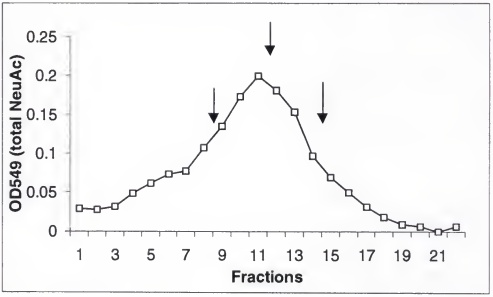

Figure 2-13. The chromatogram of Dowex (acetate) anion exchange column purification of α-2,3-sialyl-lactose from bovine colostrum. Arrows indicate fractions analyzed by NMR (see figure 2-14).

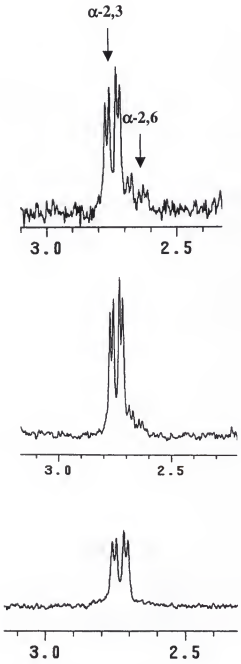

Figure 2-14. ^{1}H-NMR of fractions (shown by arrows in figure 2-13) taken after anion exchange chromatography. Different chemical shifts of C-3 equatorial proton of α-2,3- and 2,6-sialyl-lactose around 2.7 ppm can be used to differentiate these two isomers. From top to bottom: first half, middle and last half of sialyl-lactose peak as shown in figure 2-13.

Synthesis of [3,3'-dideuterio, ^{3}H-N-acetyl] Sialyl-α-D-octyl-galactoside

This compound was synthesized for the future kinetic isotope effect study of trans-sialidase catalyzed hydrolysis reactions. There are two obstacles in the study of the hydrolysis reaction that must be overcome. First, an appropriate leaving group aglycon must be used that can not act as an acceptor substrate. This ensures that no transfer reaction will take place at any time during the reaction. Second, due to the difficulty in separating sialyl-lactose (and sialyl-galactose) from the hydrolysis product NeuAc, an appropriate donor substrate need to be employed that can be readily separated from NeuAc.

Sialyl-α-D-octyl-galactoside is such a compound that can meet both requirements. First, control experiment showed that α-D-octyl-galactose is not a substrate for trans-sialidase. Second, due to the long hydrophobic carbon chain on this molecule, it is easily separated from product NeuAc by HPLC on a C18 column. The synthesis of sialyl-α-D-octyl-galactoside from CMP-NeuAc and α-D-octyl-galactoside was attempted. [3,3'-dideuterio, ^{3}H-N-acetyl] CMP-NeuAc (synthesized and purified by Michael Bruner) was allowed to react with α-D-octyl-galactoside catalyzed by α-2,3-sialyltransferase. The product was readily purified on HPLC C18 column because of the much longer retention time of [3,3'-dideuterio, ^{3}H-N-acetyl] sialyl-α-D-octyl-galactoside than that of CMP-NeuAc. A yield of 80% was obtained in this synthesis.

Synthetic Route for the Preparation of ([3-^{3}H, 3-^{18}O] Gal) Sialyl-galactose

The synthetic route shown in figure 2-15 can lead to the synthesis of [3-^{3}H, 3-^{18}O] Galactose. This compound can then be used to synthesize ([3-^{3}H, 3-

^{18}O]Gal) sialyl-galactose which can be used to measure the leaving group isotope effect of trans-sialidase catalysis. The synthesis involves the protection of all sugar hydroxyl groups except C-3 hydroxyl (128, 129). This group is then oxidized to the corresponding ketone in order to perform the exchange reaction in $H_2{}^{18}O$ (130). After the exchange, the ^{18}O-labeled ketone is reduced by NaB^3H_4 to incorporate the tritium label. The final product is obtained after the deprotection of the hydroxyl groups. This synthetic route was tested by using nonisotopic labeled reagents. In the first step, the C-4 and -5 hydroxyl groups of methyl-α-D-galactoside (**1**) were reacted with benzaldehyde dimethyl acetal to form 4,6-benzylidene methyl galactoside (**2**) (128) with a yield of 50%. The side product of this reaction is 3,4-benzyldiene methyl galactoside which can be separated from compound **2** by column chromatography. Compound **2** was further protected by reaction with benzoyl chloride to give 2-benzoyl-4,6-benzylidene methyl galactoside (**3**) (129) with a yield of 30%. The side product 3-benzoyl-4,6-benzylidene methyl galactoside can be separated from compound **3** by crystallization. The 3-hydroxyl group of compound **3** was oxidized by PCC to form 2-benzoyl-3-keto-4,6-benzylidene methyl galactoside (**4**) with a yield of 70%. At this point, compound **4** can be exchanged in $H_2{}^{18}O$ to incorporate ^{18}O label at C-3 (130). Sodium borohydride reduction of compound **4** reduced both the C-3 keto and C-2 ester groups to give compound **2** with a combined yield of 50%. The deprotection of compound **2** by hydrogenation was nearly quantitative (>95% yield). The final step involves the hydrolysis of compound **1** by α-galactosidase to give galactose with a yield greater than 60%. The ^{1}H-NMR

spectra for compound **2**, **3** and **4** are shown in the Appendix C, D and E, respectively.

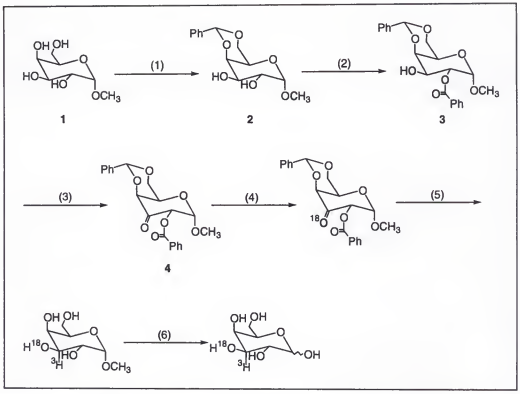

Figure 2-15. Synthetic route for the preparation of [3-^{3}H, 3-^{18}O] Galactose. (1) Benzaldehyde dimethyl acetal, pyridinium *p*-toluenesulfonate, DMF,100 °C, argon; (2) Tetrabutyl ammonium chloride, benzoyl chloride, CH_2Cl_2/40% NaOH, ice/H_2O bath; (3) Pyridinium chlorochromate, benzene, reflux; (4) [^{18}O] H_2O, THF, R. T.; (5) $NaB^{3}H_4$, 2-methoxyethyl ether, R. T.; (6) α-galactosidase, pH 4.1, 50 mM citrate buffer.

Experimental

Materials

Common reagents and buffers were purchased from Sigma and Fisher. His-resin was purchased from Novagen. UDPGal-4'-epimerase, galactosyltransferase, α-D-methyl-galactoside, pyridinium chlorochromate, [^{18}O] H_2O, *Aspergillus niger* α-galactosidase, octyl-α-D-galactoside, alkaline

phosphatase, Dowex resin, Amberlite resin and ([1-^{14}C] Glc) lactose with specific activities of 54.3 and 60 mCi/mmol were purchased from Sigma-Aldrich Chemical Co.. [6-^{3}H] glucose (27 Ci/mmol) was purchased from ICN Pharmaceuticals, Inc.. [1-^{14}C]sodium pyruvate, [1-^{14}C] galactose (52 mCi/mmol) and [6-^{3}H (N)] galactose (29.5 Ci/mmol) were purchased from Moravek Biochemicals. 6-^{3}H ManNac was purchased from American Radiolabeled Chemicals, Inc.. Recombinant rat liver α-2,3-sialyltransferase was purchased from Calbiochem-Novabiochem Corp. [2-^{13}C] pyruvate was purchased from Isotec. NeuAc aldolase was purchased from Toyobo Co., Ltd.. BL21(DE3) competent cells were purchased from Novagen. Deuterium hydroxide was purchased from Cambridge Isotope Laboratories, Inc.. Plasmid pWV200B containing the gene for CMP-NeuAc synthase was a gift from Dr. W. Vann of the NIH. Two recombinant trans-sialidase plasmids TCTS/pQE60 and TCTS/pET14b were gifts from Dr. Sergio Schenkman of the Universidade Federal de São Paulo. Bovine colostrum was given to us as a gift from the Dairy Research Unit, Department of Animal Sciences, University of Florida. Liquid scintillation fluid (ScintiSafe 30%) was purchased from Fisher. Corp..

Instrumental

HPLC was performed on a Rainin HPXL gradient unit with a Rainin Dynamax UV-1 detector interfaced to a Macintosh personal computer. A MonoQ HR 10/10 anion exchange column was employed for the enzyme and substrate purifications. A Retriever 500 fraction collector from ISCO, Inc. was used for the collection of fractions after column chromatography. A pH meter (Accumet

model 15) from FisherScientific with a Accumet gel-filled polymer body combination electrode was employed for all pH adjustments. Centrifugation was performed on a Sorvall RC 5B centrifuge and a Sorvall MC12V microcentrifuge. Liquid scintillation counting was performed using a Packard 1600 TR instrument which dumped data to a floppy disk for subsequent analysis on a personal computer. ^{1}H-NMR was performed on a Gemini 300 MHz spectrometer and data was subsequently processed on a Unix Sun station. Mass spectrometry analysis was carried out on a Finnigan MAT95Q hybrid-sector mass spectrometer (Finnigan MAT, San Jose, CA). Cells were lysed using a French pressure cell with a Carver hydraulic press.

Overexpression of Recombinant Trans-sialidase

E.coli TG-1 competent cell preparation. The calcium chloride method was used to make the competent TG-1 cells (131). The experiment followed the standard procedures (131).

Transformation. Transformation of TCTS/pQE60 into *E.coli* TG-1 cells (made competent by the above method) and TCTS/pET14b into BL21(DE3) competent cells follows the standard procedures (132), except that a 90 seconds heat shock was applied on TG-1 competent cells.

Expression and purification. Two constructs of recombinant trans-sialidase were overexpressed with near identical procedures as described below (109). *E.coli* cells were picked from transformant cell stock (stored at -80°C) and inoculated 5 ml LB with 100 μg/ml ampicillin. Cells were grown at 37°C, 200 rpm for 7 hours and used to inoculate 1 L LB medium with 100 μg/ml ampicillin. Cells

continued to grow at 37°C, 200 rpm for 3 hours (OD600=0.6) and the expression was initiated by addition of IPTG to a final concentration of 0.1 mM. (The overexpression of TCTS/pET14b does not require IPTG induction). After another 16 hours of growth at 30 °C, 150 rpm, cells were collected by centrifugation at 6000 rpm for 10 minutes. The pellet was resuspended in 10 ml pH 8.0, 20 mM Tris-HCl buffer which was centrifuged again to re-collect cells. The pellet was then resuspended in 20 ml purification buffer 1 (50 mM sodium phosphate, 0.3 M NaCl, 2 mM $MgCl_2$ at pH 8.0) and cells were lysed by pre-chilled French pressure cell and Carver hydraulic press. Phenylmethylsulfonyl fluoride (PMSF, 1 mM) was maintained in TG-1 cell lysate and also in all solutions throughout the purification process, whereas no PMSF was used for the purification from BL21 cells. The cell lysate was centrifuged at 19,000 rpm, 4°C for 1 hour and the supernatant was transferred into a beaker pre-chilled on ice. Ammonium sulfate precipitation was performed in the expression of TCTS/pQE60, but not in the expression of TCTS/pET14b. An appropriate amount of ammonium sulfate was added to achieve 30% ammonium sulfate saturation. The solution was centrifuged at 4 °C, 7000 rpm for 25 minutes. The supernatant was adjusted to 60% ammonium sulfate saturation and the solution was centrifuged as above. The pellet was collected and resuspended in 40 ml buffer 1 and mixed with Ni^{2+} resin pretreated as follows: Ni^{2+} resin in the storage bottle was gently resuspended. An appropriate amount of resin (depends on the scale of expression) was cast into a column. The resin was first washed with 3 volumes of sterile water, followed with 5 volumes of charge buffer (50 mM N_iSO_4) and 3

volumes of purification buffer 1. The resin was then stored in the cold room until use. The mixture of the sample and Ni^{2+} resin was stirred at 4 °C for 1 hour and then loaded into a column. The column was first washed with purification buffer 1 until no protein content was detected in the eluate, then washed with purification buffer 2 (50 mM sodium phosphate, 0.3 M NaCl, 10% glycerol at pH 6.0) extensively until no protein was detected in the eluate. After this step, the column was washed with a step gradient of imidazole solution (150 mM, 300 mM, and 500 mM) in buffer 2. All fractions were assayed for protein concentration by Bradford assay (133) and for trans-sialidase activity by trans-sialidase activity assay (the assay mixture contained 0.4 mM sialyl-lactose, 7.4 μM ([1-^{14}C] Glc) lactose with 0.16 mM cold lactose in pH 7.0, 20 mM HEPES buffer with 0.2% ultrapure BSA). Fractions containing trans-sialidase activity were pooled and dialyzed against 1 liter of pH 8.0, 20 mM Tris-HCl buffer at 4 °C for 16 hours. The dialyzing buffer was changed once after 8 hours of dialysis. The dialyzed solution was centrifuged at 4 °C, 19,000 rpm for 1 hour and the supernatant was concentrated by centricon to a final volume of ~ 5ml. The sample was further purified on HPLC MonoQ HR 10/10 anion exchange column. The column was first equilibrated in pH 8.0, 20 mM Tris-HCl buffer. After sample loading, the column was first washed with the same buffer for 20 minutes at 1 ml/min, then washed with a gradient of 0 to 0.33 M NaCl in Tris-HCl buffer for 40 minutes. The column was finally washed with a gradient of 0.33 to 1 M NaCl in Tris buffer for 10 minutes followed with 1 M NaCl until all peaks were eluted off the column. Protein fractions were monitored by the absorbance at 280 nm. Fractions

containing trans-sialidase activity as detected by activity assay were pooled and concentrated with an Amicon centricon unit (YM-10) at 4 °C. Concentrated trans-sialidase solution was mixed with equal volume of glycerol and stored at -20 °C. Trans-sialidase concentrations were determined by Bradford protein assay. The purity of trans-sialidase was analyzed by SDS-PAGE electrophoresis.

Overexpression of CMP-NeuAc Synthase

The plasmid pWV200B containing CMP-NeuAc synthase gene was a generous gift from Dr. W. F. Vann (134). The expression and purification of CMP-NeuAc synthase followed the published method (135). Twenty mg of CMP-NeuAc synthase was obtained from 2 liters of culture. The purity of CMP-NeuAc synthase was determined by SDS-PAGE.

Synthesis of ([6-^{3}H] Glc) Lactose

The ([6-^{3}H] Glc) lactose synthesis reaction was run in pH 8.6, 100 mM glycine buffer. The reaction mixture contained 20 μCi [6-^{3}H] glucose (27 Ci/mmol), 7.2 mM UDP-glucose, 5 mM Mn^{2+}, 50 mM KCl, 34 μl 0.6 % (w/v) α-lactalbumin solution (dissolved in pH 8, 50 mM gly-gly buffer), 0.1 U UDP-Gal-4'-epimerase (dissolved in pH 7, 100 mM citric acid buffer) and 50 mU galactosyltransferase (dissolved in 20 mM Tris-HCl buffer, pH 7.5 with 2 mM EDTA and 2 mM 2-mercaptoethanol). The total volume was 1.0 ml. The reaction was run at 37 °C for 6 hours and was monitored by the reaction of aliquots with ATP/hexokinase which converted unreacted [6-^{3}H] glucose into [6-^{3}H] glucose 6-phosphate. The separation of [6-^{3}H] glucose 6-phosphate from

product [6-^{3}H] lactose on Dowex-1X8-200 (formate) columns (4 cm height in a Pasteur pipet) allowed estimation of the fractional conversion. After the fractional conversion had been determined to be 93%, the crude lactose product was chromatographed on a Dowex 1X8-200 (chloride) column in a Pasteur pipet which was eluted with deionized water. The silica TLC system $CHCl_3$/i-PrOH/H_2O, 2:7:1 was able to cleanly separate glucose and lactose (R_f=0.32 and 0.1 for glucose and lactose, respectively), and was used to confirm the presence of lactose by its co-elution with an authentic standard. Isolation of the glucose and lactose components confirmed the earlier estimate of ca. 90% conversion. The crude ([6-^{3}H]Glc) lactose was used in the next step without further purification.

Synthesis of NeuAc

N-acetyl mannosamine (752 mg, 3.40 mmol), sodium pyruvate (2.5 g, 22.5 mmol) and 5 U NANA aldolase were mixed in pH 7.5, 50 mM sodium phosphate buffer containing 30 mg sodium azide and 80 mg BSA. The total reaction volume was 40 ml. The reaction mixture was contained in a plastic bottle. The reaction was carried out at room temperature and stopped when it reached the equilibrium as monitored by ^{1}H-NMR. NeuAc was purified on Dowex 1X8-200 (formate form) anion exchange column (4.5cm x 30 cm). The column was first eluted by 250 ml deionized water, followed by a gradient wash from 0 to 2N formic acid in a total volume of 500 ml. NeuAc was detected by TBA assay (117). Fractions containing NeuAc were pooled and concentrated by rotary evaporation to dryness. Deionized water (50 ml) was added and the solution

was concentrated on a rotovap again to dryness to remove residual formic acid. Purified NeuAc was obtained as a white solid. The yield was around 85%.

Synthesis of [3,3'-dideuterio] NeuAc

NeuAc obtained from above synthesis can be used directly to synthesize [3,3'-dideuterio] NeuAc. NeuAc (50 mg) was dissolved in 500 µl D_2O. The pH of the solution was adjusted to ~12 by addition of NaOD. The solution was then kept at room temperature for 12 hours. The complete exchange of 3,3'-protium by solvent deuterium was confirmed by the disappearance of the corresponding peaks in the ^{1}H-NMR spectrum.

Synthesis of [2-^{13}C] NeuAc

The reaction mixture for the synthesis of [2-^{13}C] NeuAc contained N-acetyl mannosamine (1 g, 4.5 mmol), [2-^{13}C] sodium pyruvate (100 mg, 0.9 mmol), 1 mg/ml sodium azide, 2 mg/ml BSA and 2 U NANA aldolase in pH 7.5, 50 mM sodium phosphate buffer. The total reaction volume was 4.2 ml. The reaction was allowed to proceed at room temperature for 4 days. A yield greater than 90% was shown by ^{1}H-NMR. [2-^{13}C] NeuAc thus synthesized was used to synthesize [2-^{13}C] CMP-NeuAc without further purification.

Synthesis of [1-^{14}C] NeuAc

[1-^{14}C] NeuAc was synthesized in a reaction mixture containing 10 µCi [1-^{14}C] pyruvate (8 µCi/µmol), 20 mg ManNAc (0.09 mmol), 1 mg/ml BSA, 1 mg/ml sodium azide and 2 U NANA aldolase in pH 7.6, 50 mM Tris-HCl buffer. The total reaction volume was 300 µl. The reaction was carried out at room

temperature and monitored by MonoQ anion-exchange chromatography. The column was eluted with pH 7.5, 25 mM ammonium bicarbonate buffer with 15% MeOH. [1-^{14}C] NeuAc and [1-^{14}C] pyruvate were separated completely under this condition. [1-^{14}C] NeuAc and [1-^{14}C] pyruvate fractions were collected and quantified by liquid scintillation counting for the estimation of the percent conversion. The typical yield for [1-^{14}C] NeuAc synthesis was greater than 85%.

Synthesis of [9-^{3}H] NeuAc

[6-^{3}H] N-acetyl-mannosamine and pyruvate were used to synthesize [9-^{3}H] NeuAc by NANA aldolase. Typical reaction mixture contained 50 µmol pyruvate, 100 µCi [6-^{3}H] ManNAc (10 Ci/mmol), 1 mg/ml BSA, 1 mg/ml sodium azide and 1 U NANA aldolase in pH 7.6, 50 mM Tris-HCl buffer. The reaction volume was 100 µl. The reaction was monitored by MonoQ anion-exchange column as described above. The typical yield for the synthesis of [9-^{3}H] NeuAc was greater than 85%.

CMP-NeuAc Synthesis and Purification

The NeuAc isotopomers synthesized in the previous section were used to synthesize CMP-NeuAc isotopomers. The reaction mixtures for the synthesis of different CMP-NeuAc isotopomers were similar. Typically, the reaction mixture contained NeuAc (10 mg, 0.03 mmol), CTP (20 mg, 0.038 mmol), $MnCl_2$ (100 mM) and CMP-NeuAc synthase (1 U) in pH 7.5, 50 mM Tris-HCl buffer. The reactions were run at 37°C for 2.5 hours and the fractional conversion was monitored by HPLC MonoQ chromatography. The pH of the reaction mixture

was kept neutral by periodically adding small amount of NaOH solution. CMP-NeuAc was purified by HPLC on a MonoQ column with the following condition: 0% B (B = pH 7.5, 500mM ammonium bicarbonate buffer with 15% methanol; 0% B= 15% methanol) from 0 to10 minutes; 0 - 5% B from 10 to 20 minutes; 5% B from 20 to 30 minutes; 5 - 10% B from 30 to 40 minutes and then the column was eluted with 10% B for the remainder of the purification. The flow rate was 2ml/min. The CMP-NeuAc peak was detected by the absorbance at 260 nm and collected in a polyethylene tube placed on ice. The eluent was desalted by Amberlite IR120-H^+ cation-exchange resin. The resin was previously prepared by washing first with ethanol, then with 3 batches of 4 N HCl (~150 ml each batch), and finally with deionized water until the pH of the resin reached neutral. The prepared resin was stored at 4°C until future use. The eluate containing CMP-NeuAc fractions was first concentrated to about 30 ml, and then transferred to a 50 ml polyethylene tube on ice. All reagent and devices were pre-cooled on ice. Approximately 3 g of Amberlite resin was first washed with 1 L deionized water, and then with 20 ml of pre-cooled deionized water. The resin was then added into the CMP-NeuAc eluate. The tube was tightly capped and vortexed for 1 minute. The solution was then filtered directly into a round-bottom flask on ice through a glass Pasteur pipette containing a glass wool plug. The resin was rinsed twice with cold deionized water (2 ml each time) which was also filtered through the pipette into the round-bottom flask. The solution was then concentrated by rotary evaporation to dryness. Cold deionized water (1 ml) was immediately added into the round bottom flask and the pH of the solution was

adjusted to neutral by the addition of 1 M ammonium hydroxide solution. The solution was again concentrated to dryness and redissolved in an appropriate amount of deionized water and stored at -20°C. The purity of CMP-NeuAc was checked by HPLC on a MonoQ column.

Synthesis of Sialyl-lactose Isotopomers

Sialyl-lactose isotopomers include ([6-^{3}H] Glc) sialyl-lactose, ([1-^{14}C]Glc) sialyl-lactose, ([2-^{13}C] NeuAc, [1-^{14}C]Glc) sialyl-lactose and ([3,3'-^{2}H] NeuAc, [1-^{14}C] Glc) sialyl-lactose. The general procedure for sialyl-lactose synthetic reactions involved reaction of the appropriate CMP-NeuAc isotopomer and 10 μCi of ^{3}H or ^{14}C radiolabeled lactose (27 Ci/mmol and 60 mCi/mmol, respectively) in 40 mM cacodylate buffer with 0.2 mg/mL BSA, 0.2% Triton CF-54, at pH 6.8, catalyzed by 10 mU of recombinant rat liver α-2,3-sialyltransferase and 5 U alkaline phosphatase. The following concentrations of CMP-NeuAc and final reaction mixture volumes were employed.

([6-^{3}H] Glc) sialyl-lactose

CMP-NeuAc (1.8 mM) was used in a reaction volume of 250 μL.

([1-^{14}C]Glc) sialyl-lactose

CMP-NeuAc (1.8 mM) was used in a reaction volume of 100 μL.

([2-^{13}C] NeuAc, [1-^{14}C] Glc) sialyl-lactose

[2-^{13}C] CMP-NeuAc (5 mM) was used in a reaction volume of 120 μL.

([3,3'-^{2}H] NeuAc, [1-^{14}C] Glc) sialyl-lactose

[3,3'-^{2}H] CMP-NeuAc (3.7 mM) was used in a reaction volume of 135 μL.

All reactions were run at 37 °C for 3 days. Reaction progress was followed by fractionation of reaction mixture aliquots on Dowex 1X8 (formate) mini-columns (4 cm height in Pasteur pipets). Initial washing with deionized water eluted unreacted lactose. The product sialyl-lactose was eluted with pH 6.6, 200 mM ammonium formate buffer and then quantified by liquid scintillation counting. After the reactions had ceased to progress, the product was isolated by chromatography on a Dowex 1x8 (formate form) column (0.7 x 8 cm). The column was first washed with water, followed by pH 7.5, 5 mM ammonium bicarbonate buffer. The fractions containing sialyl-lactose were concentrated and desalted with Amberlite IR120 H^+ resin, and then further purified by HPLC on a MonoQ HR10/10 anion exchange column. The column was eluted first with 15% $MeOH/H_2O$, followed by a gradient of 0-5 mM NH_4HCO_3 with 15% MeOH. Sialyl-lactose fractions were detected by liquid scintillation counting, collected and desalted as described above. The final sialyl-lactose isotopomers were greater than 99.9% free of radioactive lactose, with yields ranging from 52-76 %.

Synthesis of Sialyl-galactose Isotopomers

The sialyl-galactose isotopomers ([1-^{14}C] Gal) sialyl-galactose, ([6-^{3}H] Gal) sialyl-galactose, ([2-^{13}C] NeuAc, [6-^{3}H] Gal) sialyl-galactose and ([3,3'-^{2}H] NeuAc, [6-^{3}H] Gal) sialyl-galactose were synthesized enzymatically. The specific activities of galactose radioisotopomers were adjusted to the desired level by addition of nonradioactive galactose, which was recrystallized in 80% EtOH before use. Recombinant rat liver α-2,3-sialyltransferase was first concentrated with an Amicon microcon (YM-10) at 4 °C. An α-2,3-sialyltransferase stock

solution (100 mU in 100 µl) was diluted by 5 fold in pH 7.5, 50 mM Tris-HCl buffer with 0.2 mg/ml BSA and 0.2% Triton CF-54. The mixture was transferred in an Amicon microcon (YM-10) and centrifuged at 4 °C until the volume inside the tube was less than 50 µl. 400 µl of the dilution buffer was then added and the mixture was centrifuged again at 4 °C. The centrifugation was stopped when the volume inside the tube was ~20 µl, which was transferred to the reaction mixture. Typically, reaction mixtures (~50 µL) contained 70-100 mU of recombinant rat liver α-2,3-sialyltransferase and 5 U of alkaline phosphatase in 50 mM Tris-HCl, pH 7.5 containing 0.2 mg/ml BSA and 0.2% Triton CF-54. The reactions were typically conducted for 4 days at 30 °C. The same purification method used for sialyl-lactose was used to purify sialyl-galactose. The final sialyl-galactose isotopomers were greater than 99.9% free of radioactive galactose. The yields ranged from 75-82%. Given below are the reaction mixtures and conditions for the synthesis of different sialyl-galactose isotopomers.

([1-^{14}C] Gal) sialyl-galactose

CMP-NeuAc (1.8 µmol) and [1-^{14}C] Gal (20 µCi, s.a. 52 mCi/mmol) were reacted with 100 mU of sialyltransferase to afford the title compound in 80% yield after HPLC purification.

([6-^{3}H] Gal) sialyl-galactose

CMP-NeuAc (1.8 µmol) and [6-^{3}H] Gal (30 µCi, s.a. 60 mCi/mmol) were reacted with 70 mU of sialyltransferase to afford the title compound in 75% yield after HPLC purification.

([2-^{13}C] NeuAc, [6-^{3}H] Gal) sialyl-galactose

[2-^{13}C]-CMP-NeuAc (3.0 μmol) and [6-^{3}H] Gal (30 μCi, s.a. 20 mCi/mmol) were reacted with 70 mU of sialyltransferase to afford the title compound in 82% yield after HPLC purification.

([3,3'-^{2}H] NeuAc, [6-^{3}H] Gal) sialyl-galactose

[3,3'-^{2}H]-CMP-NeuAc (3.0 μmol) and [6-^{3}H] Gal (20 μCi, s.a. 20 mCi/mmol) were reacted with 100 mU of sialyltransferase to afford the title compound in 75% yield after HPLC purification.

Synthetic Route for the Preparation of ([3-^{18}O] Gal) Sialyl-galactose

4,6-benzylidene-α-D-methyl galactoside (128). α-D-methyl galactoside (2.147g, 11 mmol) and 80 mg of pyridinium *p*-toluenesulfonate were added into a dry round-bottom flask under argon. Into the same flask 15 ml of distilled DMF was added. The reaction mixture was heated to 100 °C under a stream of argon. Benzaldehyde dimethyl acetal (3g, 20 mmol) was dissolved in 15 ml of distilled DMF and added dropwise into the reaction mixture. The reaction was carried out at 100 °C for 2.5 hours. The product was purified by flash chromatography (silica, ethyl acetate/petroleum ether: 4:1). The typical yield was 50%. ^{1}H-NMR (300 MHz, $CDCl_3$, room temperature): δ =3.48 (s, 3H, C-1 methyl); 3.72 (m, 1H, H-5); 3.92 (m, 2H, H-2 and H-3); 4.10 (d-d, J=1.8, 12.7, 1H, H-6); 4.31 (d-d, J=1.4, 12.7, 2H, H-6' and H-4); 4.95 (d, J=2.7, 1H, H-1); 5.57 (s, 1H, H-7); from 7.25 to 7.6 (m, 5H, Ph-H).

2-benzoyl-4,6-benzylidene-α-D-methyl galactoside (129). 4,6-benzylidene-α-D-methyl galactoside (452 mg, 1.53 mmol) was dissolved in 7.5

ml of CH_2Cl_2 and cooled on ice to 5 °C. Tetrabutyl ammonium chloride (70 mg) was added into the flask, followed by addition of 1.5 ml of 40% NaOH. Benzoyl chloride (210 µl, 1.8 mmol) was added dropwise into the flask. The reaction mixture was kept on ice and stirred vigorously for 10 minutes. The CH_2Cl_2 phase was separated from the aqueous phase and washed with water until the pH of the washes was neutral. The CH_2Cl_2 phase was further dried over anhydrous Na_2SO_4 and concentrated by rotary evaporation. The product was crystallized in hexane/ethyl acetate. The remaining product in the mother liquor can be purified by flash chromatography (silica, CH_2Cl_2 /ethyl ether: 25:1). The yield was 30%. ^{1}H-NMR (300 MHz, $CDCl_3$, room temperature): δ =3.45 (s, 3H, C-1 methyl); 3.80 (m, 1H, H-5); 4.13 (d-d, J= 1.8, 12.6, 1H, H-6); 4.27 (d-d, J=3.9, 10.4, 1H, H-6'); 4.35 (m, 2H, H-3 and H-4); 5.13 (d, J=3.5, 1H, H-1); 5.39 (d-d, J=3.6, 10.3, 1H, H-2); 5.6 (s, 1H, H-7); from 7.3 to 8.2 (m, 10H, Ph-H).

3-keto-2-benzoyl-4,6-benzylidene-α-D-methyl galactoside. 2-benzoyl-4,6-benzylidene-α-D-methyl galactoside (134 mg, 0.348 mmol) was dissolved in 5 ml of benzene. Pyridinium chlorochromate (113 mg, 0.52 mmol) was added and the reaction mixture was refluxed for 1.5 hr. The product was separated by flash chromatography (silica, CH_2Cl_2/petroleum ether: 4:1). The yield was 70%. ^{1}H-NMR (300 MHz, $CDCl_3$, room temperature): δ=3.51 (s, 3H, C-1 methyl); 4.00 (m, 1H, H-5); 4.23 (d-d, J=1.7, 12.8, 1H, H-6); 4.47 (d-d, J=1.4, 13.1, 1H, H-6'); 4.59 (d, J=1.2, 1H, H-4); 5.42 (d, J=3.9, 1H, H-1); 5.65 (s, 1H, H-7); 6.16 (d, J=4.0, 1H, H-2); from 7.3 to 8.2 (m, 10H, Ph-H).

4,6-benzylidene-α-D-methyl galactoside. 3-keto-2-benzoyl-4,6-benzylidene-α-D-methyl galactoside (6 mg, 0.0155 mmol) was dissolved in 170 µl of distilled 2-methoxyethyl ether. $NaBH_4$ (1.6 mg, 0.04 mmol) dissolved in 30 µl of 2-methoxyethyl ether was then added. The reaction was run at room temperature for 6 hr. The reaction mixture was concentrated by rotary evaporation and extracted with CH_2Cl_2 three times. The product was purified by flash column (CH_2Cl_2 /ethyl ether: 25:1). The yield was 50%.

α-D-methyl galactoside. 10 mg 4,6-benzylidene-α-D-methyl galactoside was dissolved in 2 ml of glacial acetic acid. A catalytic amount of Pd-C (1 mg) was then added. The reaction was run under H_2 at room temperature. After rotary evaporation, the reaction mixture was dissolved in MeOH and the product was purified by flash chromatography (silica, ethyl acetate/petroleum ether: 4:1). The yield was near quantitative (>95%).

D-galactose. The reaction mixture contained 18 mM α-D-methyl galactoside and 80 mU α-galactosidase in pH 4.1, 50 mM citrate buffer. The reaction was run at 37 °C for 1 week and a yield of greater than 60% was obtained.

Synthesis of [3,3'-dideuterio, ^{3}H-N-acetyl] Sialyl-octyl-α-D-galactoside

[3,3'-dideuterio, ^{3}H-N-acetyl] CMP-NeuAc (35 µCi, 60 µCi/µmol, synthesized by Michael Bruner) and 3.75 µmol of octyl-α-D-galactoside were added to pH 7.6, 50 mM Tris-HCl buffer containing 0.2 mg/ml BSA and 0.2% Triton CF-54. The reaction was initiated by addition of 10 U alkaline

phosphatase and 80 mU rat liver recombinant α-2,3-sialyltransferase which was pre-concentrated with an Amicon microcon (YM-10) as described above. The reaction was run at 30 °C and monitored by HPLC on a C18 (10 x 250 mm) column. The product was purified on the same column with a gradient of 0-50% MeOH. The product [3,3'-dideuterio, ^{3}H-N-acetyl] sialyl-octyl-α-D-galactoside was detected and quantified by liquid scintillation counting. The yield was 80%.

Purification of α-2,3-Sialyl-lactose from Bovine Colostrum (114)

Colostrum (200 ml) was mixed with 330ml methanol and 660ml chloroform and stirred vigorously at 4°C for 20 minutes. After centrifugation at 4°C for 10 minutes, the upper layer was transferred into a round-bottom flask and the organic solvents were removed by rotory evaporation. The final volume after rotovaping was ~10ml. This sample was then loaded onto a Sephadex G-25 column (4.5 cm x 30 cm) with deionized water as the mobile phase. Fractions (10 ml) were collected and both free sialic acid and total sialic acid concentrations were measured by TBA assay. For the assay of total sialic acids, the samples were mixed with equal volume of 0.1N HCl and incubated at 80°C for 30 minutes. The samples thus treated were then analyzed by TBA assay for sialic acid concentrations. The OD280 was also measured for each fraction to determine the glycoprotein elution pattern. Fractions containing sialyl-lactose were pooled and loaded onto Dowex 1X8-200 (acetate form, 4.5 cm X 30 cm) anion exchange column. The column was first washed with a gradient from deionized water to pH 5.0, 20 mM pyridinium acetate buffer in a total volume of 1 liter, and then washed with 800 ml of pH 5.0, 20 mM pyridinium acetate buffer.

Fractions (9 ml) were collected and assayed for the total sialic acid content as described above. A broad peak was detected and the second half of the peak was determined by ^{1}H-NMR to contain >95% of α-2,3-sialyl-lactose. The corresponding fractions were then pooled and concentrated down to ~ 30 ml. Ammonium hydroxide solution (1 M) was added to adjust the pH to ~ 8. The solution was concentrated to dryness to remove pyridine, and was then desalted three times by Amberlite IR120-H^+ resin with the above-described procedure. The final desalted α-2,3-sialyl-lactose was assigned by ^{1}H-NMR to be >95% pure and quantified by the reducing sugar assay method (136).

CHAPTER 3
KINETIC ISOTOPE EFFECT STUDIES ON TRANS-SIALIDASE

Introduction

Knowledge about the transition state structures of both organic and enzymatic reactions is important in that it provides valuable information about the reaction mechanisms and that it is needed in the case of enzymatic reactions for the rational design of specific inhibitors. Therefore, both theoretical and practical applications pertain. A transition state is a hypothetical transient state. Few methods are available that allow the direct observation and interpretation of the transition state structures for enzyme catalyzed reactions. Kinetic isotope effects (KIEs) are one of the major tools utilized so far in the determination of the transition state structures of both organic and enzymatic reactions. There are different types of kinetic isotope effects, depending on the position of isotopic substitutions. They reflect various aspects of the transition state structure. Therefore, multiple isotope effects on a certain reaction are generally desired in order for the experimenter to draw a more definitive description of the transition state structure. One experimental approach for the KIE study of enzymatic reactions is to study the KIEs of both the enzymatic reaction and its counterpart reaction in solution. This approach has been applied in the study of sialyltransferases (98, 99). Study on the solution reaction provides the

information on the intrinsic reactivity of the substrate under a given condition. When compared with the results of the enzymatic reaction, one gains insight into how an enzyme might manipulate the reactivity of the substrate by providing unique catalytic machinery.

Kinetic Isotope Effect (KIE) Background

Isotope Effect Theory

Isotope effects can be described as the perturbation of the reaction equilibrium constant (equilibrium isotope effect, EIE), or of the reaction rate (kinetic isotope effect, KIE) due to isotopic substitutions. Theories have been developed for the origin and prediction of the magnitude of an EIE. The link between EIEs and KIEs is the transition state theory, in which the fundamental assumption is the existing equilibrium between the reactant in the ground state and the reactive species in the transition state. As a result, all theories about equilibrium isotope effect can be directly applied to kinetic isotope effect when the transition state is considered to be in equilibrium with the ground state.

An equilibrium constant can be expressed as the ratio of the partition functions (Q in the following equations) for products and reactants (equation 3-1). EIEs can then be expressed as ratios of partition function ratios for the two reactions with different isotopic substitutions (equation 3-2):

$$K_{eq}=Q_{product}/Q_{reactant} \quad (3\text{-}1)$$

$$EIE=(Q_{product}/Q_{reactant})_D/(Q_{product}/Q_{reactant})_H \quad (3\text{-}2)$$

The partition function is the sum over the entire energy levels that follow a Boltzmann distribution. Energy in each level is related to the molecular mass, the principal rotational moments of inertia, the vibrational frequencies and the electronic energies. An EIE is therefore directly related to the molecular properties through the partition function. Among all those contributors, the electronic energy is not affected by the isotopic substitution, as dictated by the Born-Oppenheimer approximation. Namely, the nuclei are far heavier than the electrons. Therefore they can be considered as essentially stationary. As a result, their inertia and mass can have no effect on the electronic energy. Based on thermodynamic statistics, Bigeleisen and Mayer (137) developed the Bigeleisen equation (equation 3-3) for the calculation of the equilibrium isotope effect:

$$\text{Isotope effect} = \text{MMI} * \text{ZPE} * \text{EXC} \qquad (3\text{-}3)$$

where MMI represents mass-moment of inertia, reflecting isotope effects on the translational and rotational energies (138). ZPE is the isotope effect on the zero point energy of the 3N-6 normal vibrations. And EXC includes the isotope effect on the molecules in excited vibrational states.

Molecules of biological interest are generally large. The isotope effect on the translational and rotational energies is therefore often insignificant. The contribution to isotope effects by the excited vibrational states is also usually small. As a result, zero-point energy, in many cases, becomes the main source of the isotope effect. The relation between zero-point energy and the isotope effect will be discussed in more detail later in this chapter.

As noted above, equilibrium isotope effects arise from the changes in translational, rotational, and most of all, ZPE of two molecules with different isotopic substitutions. Therefore, isotope effects can provide important information regarding structural changes of the molecule between two different states. As structural information is closely related to reaction mechanism (e.g. a question about a bond formation between two atoms in a reaction mechanism is equivalent to a question of the bond distance between these two atoms.), isotope effects have now become a powerful tool for mechanistic enzymologists to probe the mechanisms of enzymatic reactions (139). However, in this area, it is not the equilibrium isotope effect, but the kinetic isotope effect that plays a major role. To understand the kinetic isotope effect, we need to first review one of the most important theories about reaction kinetics, and certainly the one that is most often used by mechanistic enzymologists, transition state theory.

The basis for the transition state theory is the assumption of an equilibrium between the reactant in the ground state and a reactive species in the transition state. The transition state is a hypothetical state that occupies the highest energy point on the reaction coordinate diagram. Therefore, it is a highly unstable state and will collapse to either reactant or product rapidly and equally. The reaction rate constant can be derived from the transition state theory (equation 3-4):

$$k = (\mathbf{k}T/h)\exp(-\Delta G^{\ddagger}/RT) \qquad (3\text{-}4)$$

where **k** is Boltzmann's constant, h is Planck's constant, T is the temperature in Kelvin, $\Delta G^{\ddagger}$ is the activation energy and R is the gas constant. Because of the equilibrium between the ground state and the transition state, the theory about equilibrium isotope effect discussed above can be directly applied to kinetic isotope effect. The expanded terms of the Bigeleisen equation for KIE are shown in figure 3-1. As in the case of equilibrium isotope effects, kinetic isotope effects will also be largely determined by the zero-point energy difference between the ground state and the transition state.

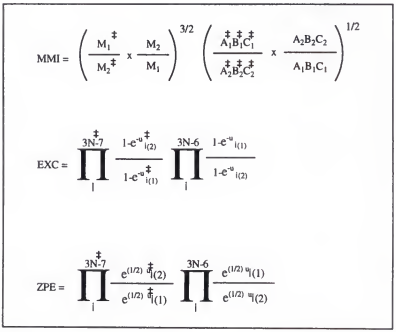
MMI = (M1‡/M2‡ x M2/M1)^3/2 (A1B1C1‡/A2B2C2‡ x A2B2C2/A1B1C1)^1/2
EXC = ∏ 3N-7 (1-e^-u‡i(2))/(1-e^-u‡i(1)) ∏ 3N-6 (1-e^-ui(1))/(1-e^-ui(2))
ZPE = ∏ 3N-7 e^(1/2) ν‡i(2)/e^(1/2) ν‡i(1) ∏ 3N-6 e^(1/2) νi(1)/e^(1/2) νi(2)

Figure 3-1. Expanded terms of the Bigeleisen equation for KIE.

For a molecule with N atoms in the ground state, there are 3N-6 vibrational modes. In the transition state, however, one normal mode becomes the reaction coordinate motion with an imaginary frequency. Therefore, transition states have 3N-7 frequencies with one imaginary frequency (137). Each

vibrational mode can be represented by two or more atoms linked by chemical bonds. The vibrations can be simulated by a harmonic oscillator with parabolic potential energy function. The vibrational potential energy of a chemical bond is quantized and there exits the lowest potential energy level called the zero-point energy. The potential energy well along the reaction coordinate changes its shape as the reaction proceeds from the reactants to products. If the bonding environment of a bond to which the isotopic atom attaches becomes looser in the transition state, the force constant of this particular bond will diminish in the transition state and the vibrational frequency decreases, so does the zero-point energy. This is reflected in the opening up of the potential energy well in the transition state as depicted in figure 3-2. This is called a loose potential energy well in which the difference between the zero-point energies of two isotopic substituted bonds is narrowed. The difference of the zero-point energy differences between the ground state and the transition state gives rise to different activation energies and therefore, different reaction rates of the two isotopic substituted molecules. For a looser potential energy well in the transition state, a normal (>1) KIE will be observed. Conversely, an inverse isotope effect (<1) will be observed if the potential energy well is tighter in the transition state (figure 3-3). It can be summarized by the following rule that the light isotopic molecule prefers a looser state in which the restrictions to vibration are lower (139).

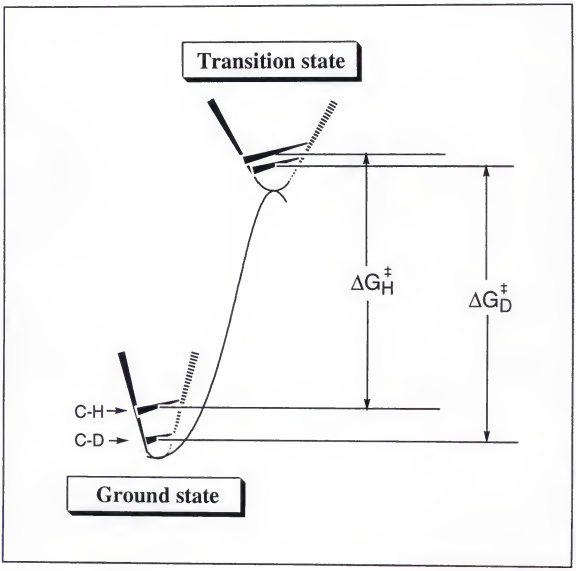

Figure 3-2. Change in ZPE that gives rise to a normal isotope effect.

An isotope effect is a local effect, which means that the effect of isotopic substitution extend only one or two bond distances. As a result, isotopic substitutions that give rise to an isotope effect can assume the position either on the reaction center, or on the α and β positions relative to the reaction center.

These substitutions give primary, α-secondary and β-secondary isotope effects, respectively.

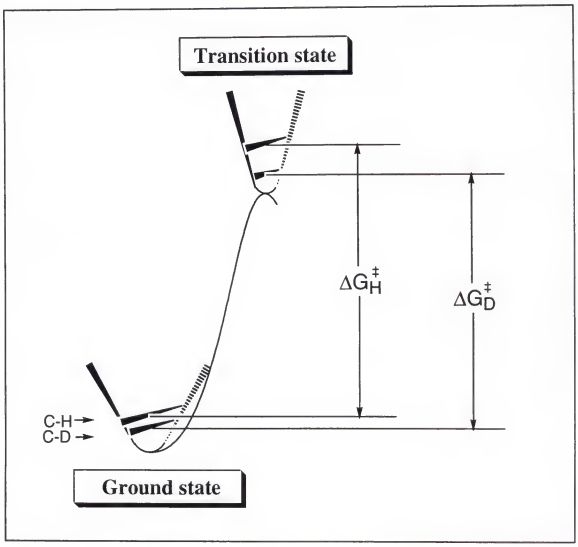

Figure 3-3. Change in ZPE that gives rise to an inverse isotope effect.

Primary Isotope Effects

A primary isotope effect is observed when the isotopically substituted bond undergoes bond cleavage or formation in the transition state. Primary isotope effects are generally larger than secondary isotope effects. Therefore it

is possible to measure heavy atom primary isotope effects. Among them, carbon isotope effects (both ^{14}C and ^{13}C) are widely used in kinetic isotope effect studies. The magnitude of the primary isotope effect is dictated by the symmetry around the reaction center atom in the transition state. In a model depicted in figure 3-4, atom C is being transferred from A to B. The vibrational modes in the reactant include both stretching and bending vibrations. In the transition state, however, the stretching vibration has become the reaction coordinate. Two other vibrational modes in the transition state are the bending vibration and the symmetric stretching vibration. The bending frequencies are lower than the stretching frequencies and are usually considered to cancel each other between the ground state and the transition state. Therefore, they contribute less to the primary isotope effect. The symmetric stretching vibration in the transition state then becomes the major contributor to the primary isotope effect (140). If the transition state is symmetrical, which means the bond order between A and C equals the one between C and B, the symmetric stretching vibration will involve only A and B with atom C being motionless. Hence, there will be no zero-point energy difference by the isotopic substitutions on C. As a result, all the zero-point energy difference between two isotopomers in the ground state contributes to the difference in the activation energy and this gives the largest primary isotope effect. This symmetrical transition state in nucleophilic substitution reactions indicates a limiting S_N2 transition state, which is associative in nature. Conversely, in an asymmetrical transition state, atom C still retains some symmetric stretching vibrational frequency, which partly cancels the zero-point

energy difference in the ground state and as a result, the isotope effect decreases (140). This corresponds to a diminished S_N2 character in the transition state. A pure S_N1 reaction have a highly asymmetrical transition state (a dissociative transition state). Therefore, primary isotope effects in S_N1 reactions are small. For a classic S_N2 reaction, ^{13}C primary isotope effects typically fall in the range between 1.04 to 1.08. In contrast, for a classic S_N1 reaction, the typical values for ^{13}C primary isotope effects are in the range of 1.00 to 1.02 (141). From the above discussion, it is clear that carbon primary isotope effects describe directly the degree of nucleophilic participation in the transition state and can be used to distinguish between an associative and a dissociative transition state.

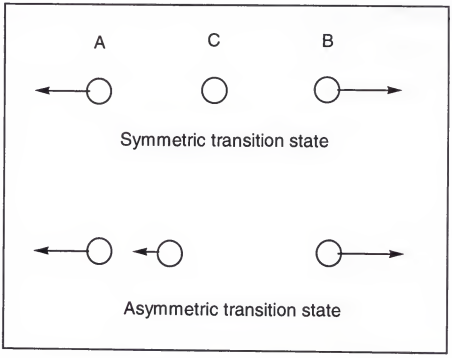

Figure 3-4. The symmetric stretching vibration mode in the transition state of transfer reactions. C is the atom being transferred between A and B (140).

Secondary Isotope Effects

Secondary isotope effects arise when the force field around the isotopic substituted atoms changes along the reaction coordinate without direct bond formation or cleavage. They are generally smaller and thus are rarely measured for heavy atom substitutions. There are two common types of secondary isotope effects, α- and β-secondary isotope effects, with the isotopic substitutions on or adjacent to the reaction center atom, respectively.

α-secondary isotope effects usually result from the change of the hybridization state of the reaction center atom when the reaction proceeds from the ground state to the transition state. There are three vibrational modes that may change along the reaction coordinate: the stretching vibration, the in-plane vibration and the out-of-plane vibration. For the α-secondary isotope effects, the out-of-plane bending motion changes the most when the hybridization state around the isotopic substituted atom shuffles between sp2 and sp3. This bending motion is therefore the major contributor to the α-secondary isotope effects (140). If the hybridization state follows a sp3 to sp2 change, the potential energy well in the transition state becomes looser and a normal isotope effect is observed as depicted in figure 3-2. Similarly, an inverse isotope effect is obtained if the change is from sp2 to sp3 (refer to figure 3-3). Although α-secondary isotope effects can be used to detect the change in the hybridization state of the reaction center atom, it is not suitable in distinguishing S_N1 and S_N2 mechanisms. By studying the second order reactions between N-(methoxymethyl)-N, N-dimethylanilinium ion and different nucleophilic reagents,

Knier and Jencks showed that α-secondary isotope effects ranging from 0.99 (fluoride ion as the nucleophile) to 1.18 (iodide ion as the nucleophile) were observed (106). Polarizable nucleophiles, such as iodide ion, can provide electrons to stabilize the electron-deficient reaction center from a greater distance. This results in an "exploded" transition state with a considerable amount of positive charge build-up on the reaction center, leading to a large α-secondary isotope effect even though the reaction follows an S_N2 mechanism.

β-deuterium secondary isotope effects are an important type of secondary isotope effects. It largely arises from the hyperconjugation between the isotopically substituted atom (H or D) and the positive charge formed on the reaction center in the transition state (142). This effect is almost always normal. The equation for the calculation of β-deuterium secondary isotope effect is given below:

$$\ln (k_H/k_D) = \cos^2\theta \ln (k_H/k_D)_{max} + \ln (k_H/k_D)_i \qquad (3\text{-}5)$$

Its magnitude depends on the amount of positive charge formation and the dihedral angle (θ) between the C-H(D) bond and the vacant *p* orbital on the reaction center (105). The other contributor of β-secondary isotope effects is the inductive effect from deuterium substitution ($(k_H/k_D)_i$), which gives a small and inverse isotope effect (143). This inductive effect is rarely considered in the interpretation of β-secondary isotope effects because of its small magnitude. Therefore, a β-secondary isotope effect is the indication of the positive charge formation on the reaction center and can also provide information about transition

state geometry around the reaction center atom due to the angular dependence of the isotope effect. For a classic S_N2 reaction, β-dideuterio isotope effects are in the range of 1.00 to 1.02. In contrast, for a classic S_N1 reaction, the typical values for β-dideuterio isotope effects are in the range of 1.08 to 1.15 per deuterium (141).

Isotope effects of different origins thus provide different information regarding the transition state structure. The magnitude of the primary KIE is indicative of the symmetry around the reaction center atom in the transition state. Therefore, in nucleophilic substitution reactions, primary isotope effects can be used to determine the degree of nucleophilic participation in the transition state. α-secondary KIEs provide information on the change of the hybridization state of the reaction center atom along the reaction coordinate. A β-secondary KIE is a good indication of the positive charge formation on the reaction center. When multiple kinetic isotope effect results are available, a clear transition state structure can usually be proposed.

KIE in Enzymatic Reactions: Commitment to Catalysis (C_f)

It has long been realized that the interpretation of the KIE results of enzymatic reactions was often complicated by the so-called commitment to catalysis (commitment factor, commitment, C_f) associated with the enzymatic reactions (144). A commitment is defined as the ratio of the rate constant for the isotope sensitive step to the net rate constant for release of the reactant from enzyme (145). When a commitment factor exists, the observed KIEs tend to be smaller than the real (intrinsic) KIEs. Their relationship is given in equation 3-6:

$$KIE_{obsd} = (KIE_{intrinsic} + C_f)/(1 + C_f) \qquad (3\text{-}6)$$

The simplest enzymatic reaction scheme includes two steps, the binding of free substrate and free enzyme to form the metastable ES complex, and the chemistry step that follows. This is shown in figure 3-5.

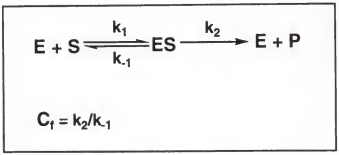

Figure 3-5. An enzymatic reaction scheme and the commitment factor.

In this scheme, $C_f = k_2/k_{-1}$. If the binding step is in rapid equilibrium (the substrate is therefore called non-sticky) and the chemistry step is rate-limiting, C_f is eliminated and the intrinsic kinetic isotope effect is revealed on step k_2. However, when the binding is rate limiting and the chemistry step is rapid, any ES complex formed will then be committed to catalysis. Therefore, no difference in the *kinetic* rate can be detected and the KIE is masked. In applying KIE studies to enzymatic systems, it is thus crucial to choose a method that allows the control over the commitment factor. The commitment factor can either be eliminated by altering the reaction conditions, or be measured by kinetic methods, such as the pulse-chase experiment.

KIE Measurement

Except for primary isotope effects of hydrogen, such as those in the hydride transfer reactions, isotope effects are generally small. This is especially true for secondary isotope effects and heavy-atom isotope effects that are becoming more and more important in the study of enzymatic reactions. Therefore, the establishment of methodologies for KIE measurement with high accuracy and precision is required. Two general methods have been applied to KIE measurement in different reaction systems. These are the competitive method and the non-competitive or direct measurement method. Both methods have advantages and disadvantages, which will be discussed below.

The Competitive Method

In the competitive method, two isotopomers are included in the same reaction mixture and the reaction rates of both isotopomers are measured simultaneously. Therefore, only isotope effects on V/K can be obtained by this method (146). The major advantage of competitive methods is the high precision of data obtained. The errors associated with this method are generally below 1%. The presence of inhibitor in the reaction mixture does not affect the result because both reaction rates are equally suppressed. However, for the application of this method, techniques need to be developed in order to differentiate between the two isotopomers. This is done either by gas-ratio mass spectroscopy method or by the dual-label method.

Gas-ratio mass spectroscopy can be used when a gaseous product is available (147). The precision of this method is high. The dual-label method

takes advantage of two sets of isotope labels (67), one set of isotopic substitution on the isotopic sensitive position and another set of radiolabels on the remote position that is away from the reaction center. The radiolabels are usually a pair of $^{3}H/^{14}C$ labels, with one label on each of the two isotopomers. They are easily quantified by liquid scintillation counting and serve to differentiate between the two isotopomers. Hence they are called the reporter labels. This method is highly sensitive and easily quantifiable. Furthermore, the specific activity of the reporter labels can vary without affecting the KIE results. This method can also tolerate a small amount of non-radioactive contaminants (147). However, it does require a high purity of radioactive substrates. The impure radioactive material could seriously affect the KIE result, especially when it coelutes with either product or substrate that is being quantified for KIE measurement. The other disadvantage of the dual-label method is the requirement of substrates with dual isotope labels in the desired positions. The synthesis is the major "rate limiting step" in most KIE measurements with this method. Substrates can be synthesized either enzymatically or chemically. Enzymatic synthesis has gained more and more attention because of its high substrate specificity, high stereospecificity, high yields, lack of side reactions, and the ability to perform multiple reactions in one-pot reaction mixture. However, it is limited by the available enzymatic reactions that could lead to the target compound synthesis, as well as by the availability of high purity enzymes. When required, chemical synthesis can be employed to synthesize the desired compounds. Once a set of isotopic substrates are synthesized with the position of isotopic labels

characterized, they can be used in the KIE measurement. There are a couple of important considerations in the development of KIE methodology of using the dual-label competitive method (147).

A method must be established to separate the reaction product from the remaining substrate in a clean and complete fashion. This is usually done by column chromatography. One control experiment must be performed to test any isotopic fractionation by chromatography, which will cause an additional isotope effect other than the desired kinetic isotope effect. This is tested by measuring the $^{3}H/^{14}C$ ratios of a substrate (or product) mixture before and after chromatography. The identical ratios serve to exclude any column isotopic fractionation.

Fractions after chromatography should be collected directly in liquid scintillation vials to avoid errors associated with aliquoting. Care must be taken to ensure the identical composition in all liquid scintillation vials. This is required to eliminate the quenching effects of liquid scintillation counting in which different sample compositions may cause different sample quenching and thus different counting results even if both samples have the same amount of radioactivity. The vials are then counted for 10 minutes each for a minimum of 6 cycles to reduce the standard deviation of data. The multi-channel liquid scintillation counting method and data analysis will be described in the "experimental" section.

The errors associated with this method can be reduced by the appropriate design of the experiment. It was found that the least amount of error was

experienced when the reactions were stopped after 40-60% fractional conversions (148). The error will increase significantly at both low and high conversions of reaction. The percent relative standard deviation for a KIE experiment must be less than 0.25%. For a single determination of the counts, the standard deviation approximately equals the square root of the number of counts, $s=cpm^{1/2}$. Therefore, at least 350,000 cpm are needed to get a standard deviation below 0.3% (147).

The Non-competitive Method

Unlike the competitive method, the non-competitive method measures the reaction rate of two isotopomers individually in two separate reaction mixtures. Therefore, they can be used to measure the KIE for the overall reaction, for a single turnover, for V/K and for V. The major disadvantage of this method is the usually higher errors (2-5%) associated (147), although low errors can be achieved with appropriate experimental design and great care (149). The error can arise from the contamination in the substrates and from the non-identical reaction conditions, such as the differences in substrate concentration, enzyme concentration, and reaction temperature. Continuous assay is most appropriate for the quantification of non-competitive method. The time-point assay can have high error (~10%) and therefore is not suitable for this method. Among the continuous assay methods, UV-vis spectroscopy is the common method employed for the non-competitive KIE method.

KIE Methodology for Trans-sialidase

The dual-label competitive method was employed in all KIE measurements carried out on trans-sialidase. Therefore, all KIEs measured on trans-sialidase in this work report on the kinetic parameter V/K (146). The structures presented in figure 2-3 identify the locations of the isotope labels in sialyl-lactose and sialyl-galactose isotopomers used in the KIE experiments. ^{3}H and ^{14}C labels on the aglycon moieties act as remote reporters for the stable deuterium or ^{13}C isotope labels present on the NeuAc residue. The kinetic isotope effect is manifested as a change of the initial $^{3}H/^{14}C$ ratio over the course of the reaction, which is detected by liquid scintillation counting of residual substrate, fractionated from reaction mixtures by chromatography on anion-exchange mini-columns.

Results

KIE Methodology Control Experiment

Control for isotopic fractionation of sialyl glycoside on Dowex-1 (formate) resin. Chromatography of a $^{3}H/^{14}C$ mixture of sialyl-lactose on a Dowex-1 (formate) mini-column eluted with 200 mM ammonium formate gave a $^{3}H/^{14}C$ ratio of 3.387, compared to a value of 3.387 found before chromatography. The total counts applied to and recovered from the column were found to be 20675 and 20431 cpm, indicating that the recovery from the column is >98.8%. A $^{3}H/^{14}C$ mixture of sialyl-galactose gave a ratio of 2.528 after Dowex-1 (formate) mini-column, compared to 2.525 found before chromatography. The recovery

from the column is >99.5%. The results indicate that insignificant isotopic fractionation occurs during chromatography on Dowex-1.

KIE experiment accuracy control. When mixtures of ^{3}H and ^{14}C labeled substrates were prepared to reflect the results anticipated for a KIE of 1.025, chromatography of these mixtures afforded a "mock" KIE of 1.028 ± 0.007.

Acid Solvolysis KIEs on Sialyl-glycosides

Both β-dideuterium and ^{13}C primary KIEs were measured for the acid solvolysis reaction. The ^{13}C primary KIEs for hydrolysis of sialyl-lactose and sialyl-galactose are 1.016 ± 0.011 and 1.015 ± 0.008, respectively. The measured β-dideuterium KIE for sialyl-lactose hydrolysis is 1.13 ± 0.012. The control KIE was measured with a substrate pair of only remote radiolabels. The measured control KIE is 1.002 ± 0.005. The results are listed in table 3-1.

Table 3-1. KIE results of the acid solvolysis reactions

Isotope Positions on SL / SG[a]	Location / type of KIE	Observed KIE
[3,3'-^{2}H] NeuAc, [1-^{14}C] Glc / [6-^{3}H] Glc	β-dideuterio	1.113 ± 0.012 (SL)
[2-^{13}C] NeuAc, [1-^{14}C] Glc / [6-^{3}H] Glc [2-^{13}C] NeuAc, [6-^{3}H] Gal / [1-^{14}C] Gal	[2-^{13}C] primary	1.016 ± 0.008 (SL) 1.015 ± 0.008 (SG)
[6-^{3}H] Gal / [1-^{14}C] Gal	Control KIE	1.002 ± 0.005 (SG)

a: SL, sialyl-lactose; SG, sialyl-galactose.

Control of the Hydrolysis Reaction in the KIE Studies on Trans-sialidase Catalyzed Transfer Reactions

A mixture of carrier-free ([9-^{3}H] NeuAc) sialyl-lactose and ([1-^{14}C] Glc) sialyl-lactose were included in a reaction catalyzed by trans-sialidase in the presence of 0.8 mM lactose. The reaction mixture was analyzed by MonoQ anion-exchange chromatography (figure 3-6). The data showed that 0.8 mM lactose suppressed the hydrolysis reaction to an undetectable level with sialyl-lactose as the donor substrate.

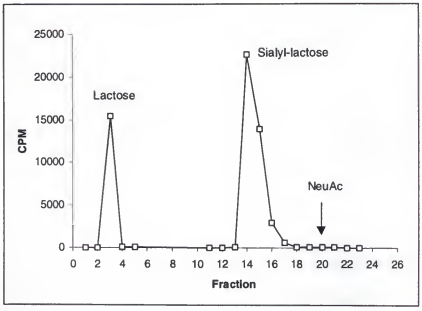

Figure 3-6. Determination of the extent of the hydrolysis reaction of sialyl-lactose under KIE conditions. The anion exchange HPLC chromatogram depicts the elution of lactose, sialyl-lactose and NeuAc.

Carrier-free ([3,3'-^{2}H] NeuAc, [6-^{3}H] Gal) sialyl-galactose and ([1-^{14}C] NeuAc) sialyl-galactose were included in a reaction catalyzed by trans-sialidase in the presence of either 0.8 or 100 mM lactose. The reaction mixture was analyzed by MonoQ anion-exchange chromatography (figure 3-7). The data

showed that 0.8 mM lactose was not sufficient to suppress the hydrolysis reaction when sialyl-galactose is the donor substrate. However, the hydrolytic reaction was suppressed to an undetectable level when 100 mM lactose was used.

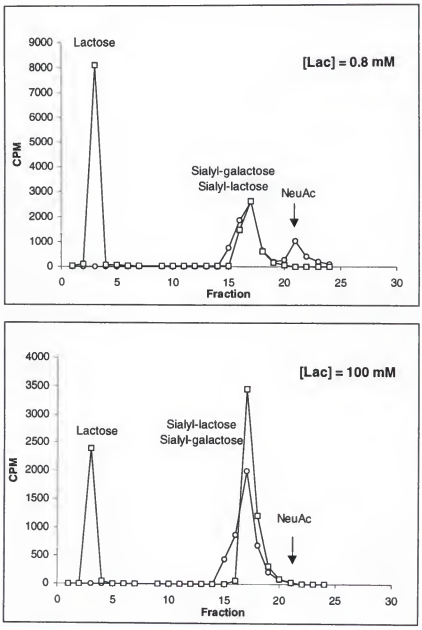

Figure 3-7. Determination of the extent of the hydrolysis reaction of sialyl-galactose under the condition for KIE experiments with sialyl-galactose. Open squares represent ^{3}H counts; open circles represent ^{14}C counts.

Determination of Isotopic Scrambling under the Conditions for the KIE Experiments on Trans-sialidase Catalyzed Transfer Reactions

([6-^{3}H] Gal) sialyl-galactose (0.19 μCi, 60 mCi/mmol) and [1-^{14}C] galactose (0.1 μCi, 52 mCi/mmol) were included in a reaction mixture that contained 100 mM nonradioactive lactose in pH 7.0, 40 mM HEPES buffer. The total reaction volume was 50 μl. The reaction was initiated by the addition of trans-sialidase and carried out at 26 ºC. No ^{14}C radioactivity was found in the chromatographic fractions containing sialyl-glycosides. This result indicates that there is no detectable isotope scrambling under the conditions for KIE experiments.

Initial Velocity Comparison Between Sialyl-lactose and Sialyl-galactose in Enzymatic Transfer Reactions

Initial velocities were compared for the transfer reaction under V/K conditions for sialyl-lactose and sialyl-galactose. The calculated V/K for sialyl-lactose and sialyl-galactose under the experimental conditions are 1.79×10^{-1} and 8.90×10^{-4} μmol/min/mg enzyme, respectively. The V/K of sialyl-lactose is therefore ~ 200 fold greater than that of sialyl-galactose.

KIE Studies on the Enzymatic Transfer Reactions with Sialyl-lactose and Sialyl-galactose

Kinetic isotope effects for trans-sialidase catalyzed transfer of sialyl-lactose and sialyl-galactose to acceptor lactose are presented in table 3-2. The KIE results showed that for sialyl-lactose, there is a small inverse binding isotope effect of 0.993 ± 0.008 for the remote ^{3}H label. For sialyl-galactose, there is a 1.024 ± 0.006 normal binding isotope effect for the remote ^{3}H label. In the

enzymatic transfer reactions, β-^{2}H isotope effects were measured with two lactose concentrations (0.8 and 8 mM) in otherwise identical reaction mixtures with sialyl-lactose as the donor substrate. The measured values were 1.046 ± 0.008 and 1.042 ± 0.01, which gave 1.053 ± 0.010 and 1.049 ± 0.013 after correction for the binding isotope effect and propagation of error. The corrected ^{13}C primary isotope effect of sialyl-lactose with 0.8 mM lactose is 1.021 ± 0.014. For sialyl-galactose reactions, the corrected ^{13}C primary and β-^{2}H isotope effects are 1.032 ± 0.008 and 1.060 ± 0.008, respectively.

Table 3-2. KIE results for the enzymatic transfer reactions.

Isotope Positions on SL / SG[a]	Location / type of KIE	Observed KIE	Corrected KIE
[3,3'-^{2}H] NeuAc, [1-^{14}C] Glc / [6-^{3}H] Glc	β-dideuterio	1.046 ± 0.008[b] (SL) 1.042 ± 0.010[c] (SL)	1.053 ± 0.010 1.049 ± 0.013
[3,3'-^{2}H] NeuAc, [6-^{3}H] Gal / [1-^{14}C] Gal	β-dideuterio	1.085 ± 0.006 (SG)	1.060 ± 0.008
[2-^{13}C] NeuAc, [1-^{14}C] Glc / [6-^{3}H] Glc [2-^{13}C] NeuAc, [6-^{3}H] Gal / [1-^{14}C] Gal	[2-^{13}C] primary	1.014 ± 0.012 (SL) 1.056 ± 0.005 (SG)	1.021 ± 0.014 1.032 ± 0.008
[6-^{3}H] Glc / [1-^{14}C] Glc [6-^{3}H] Gal / [1-^{14}C] Gal	Control KIE	0.993 ± 0.008 (SL) 1.024 ± 0.006 (SG)	

a: SL, sialyl-lactose; SG, sialyl-galactose.
b: [Lac] = 0.8 mM.
c: [Lac] = 8 mM.

Discussion

KIE Methodology

Kinetic isotope effects are usually small effects (although in some type of reactions, such as hydride transfer reactions, large isotope effects can be observed). Therefore the methodology for KIE measurement needs to be rigorously tested for its applicability in the experiments. The following questions should be asked: are there any factors, other than kinetic isotope effect, that contribute to the observed rate difference? Is the separation of product from substrate clean and complete? Does the method in any way introduce isotopic partition other than the one resulting from the rate difference? These questions were addressed in the present study during the establishment of the KIE methodology.

The method for KIE measurement employed in this project is the dual labeled competitive method (67). One major advantage of this method is the elimination of factors, other than kinetic isotope effect, that could affect the ratio of reaction rates. The entire methodology can be divided into three parts: a) the preparation of the reaction mixture and the conduction of the reaction; b) the chromatographic separation of substrates from products; c) the quantification of substrate and product by liquid scintillation counting. All reaction mixtures were made with aliquots taken from a common substrate stock solution and a common buffer solution to ensure identical composition. At least triplicates of each of t_o and $t_{1/2}$ reactions were performed in all KIE measurements. All reactions were conducted under identical conditions. The method chosen for the separation of

product and substrate was anion-exchange chromatography as described in the "experimental" section. This method can cleanly separate the product from the substrate sialylglycosides. This method was tested for any possible isotopic fractionation that may be resulted from chromatography. A $^{3}H/^{14}C$ mixture of sialyl-glycoside (both sialyl-lactose and sialyl-galactose were tested) isotopomers with pre-determined total radioactivity and $^{3}H/^{14}C$ ratio was loaded onto the column which was eluted in the way as described in the "experimental' section. The eluate was then counted and the total radioactivity as well as the $^{3}H/^{14}C$ ratio of the substrate fractions were calculated. An applicable chromatographic procedure should allow all applied radioactivity to be eluted off the column. The complete recovery of the radioactivity can also be an indication of high sample purities. As described in the "results" section, close to 99% recovery of the total radioactivity was achieved by this method. The identical $^{3}H/^{14}C$ ratio before and after column eliminated the possibility of isotopic fractionation due to chromatography. If fractionation occurred, then the column could retain one isotopomer longer than the other, which may give artifactual isotope effects. These two tests are necessary, and in many cases sufficient, for the establishment of the chromatographic methodology for a KIE experiment. To have a more rigorous examination of our KIE methodology, we gave the method a final test on its reliability by performing a "mock" KIE experiment. $^{3}H/^{14}C$ substrate mixtures were made which would give a KIE of 1.025. The mixtures were then treated as if we were running a real KIE experiment. If no artifact exists in the entire process (including chromatography step), then a KIE of 1.025

should be observed. We obtained a KIE of 1.028 ± 0.007 which is in good agreement of the pre-determined KIE of 1.025.

Kinetic Parameters for Sialyl-galactose

We were unable to detect saturation of trans-sialidase by sialyl-galactose even at concentrations up to 100 mM. Therefore the K_m for sialyl-galactose is greater than 100 mM. This K_m is about 100 times greater than the reported K_m for sialyl-lactose (109). Since saturation of trans-sialidase with sialyl-galactose could not be obtained, no estimate of the V_{max} for this substrate is yet available. We were able to estimate that the k_{cat}/K_m for sialyl-galactose is approximately 200 times lower than the k_{cat}/K_m for sialyl-lactose, which identifies sialyl-galactose as a good substrate to probe for commitments to catalysis.

Kinetic Isotope Effect Studies

The acid solvolysis KIE experiments required relatively mild conditions due to the lability of glycosidic bonds to NeuAc (0.1 N HCl, 37 °C, 10 h). The stability of the products lactose and NeuAc were determined by incubating them under reaction conditions for 30 hours and the structures were confirmed unchanged by ^{1}H-NMR. A control KIE was measured to determine any KIE resulting from the remote $^3H/^{14}C$ labels in the acid solvolysis reaction. A unity KIE was observed (1.002 ± 0.005). For the acid solvolysis reaction, this result was expected because there should be no binding isotope effect in a solvolysis reaction.

Trans-sialidase has both transferase and hydrolase activity. In order to study the transferase reaction only, it was necessary to show that no hydrolysis occurs under the conditions used for KIE measurements. Utilizing sialyl-lactose or sialyl-galactose with a radiolabel in the NeuAc sugar, hydrolysis would manifest in the production of free radiolabeled NeuAc, whereas transferase activity would not. Our results indicated that as long as sufficient acceptor lactose was present, hydrolysis was completely suppressed. The small difference in the retention times of the middle peak in the chromatograms presented in figure 3-6 and 3-7 are due to two reasons. First, the middle peak in figure 3-6 is composed by sialyl-lactose only, whereas the peak in figure 3-7 is mainly sialyl-galactose, which has a longer retention time than that of sialyl-lactose. Second, the sample loadings were different. The results are accurate enough to differentiate the NeuAc peak from the sialyl-lactose/sialyl-galactose peaks. Thus, it is clear from the results that for transfer between sialyl-lactose and lactose, 0.8 mM lactose was sufficient to ensure that only transferase activity occurred. Much higher concentrations (100 mM) of lactose were required for the poorer substrate sialyl-galactose to saturate the enzyme and eliminate competing hydrolysis. Due to the reversibility of the trans-sialidase catalyzed transfer reaction, a large excess of unlabeled acceptor substrate lactose was used in all KIE experiments to prevent isotope scrambling which would result if the reverse reaction is allowed to occur. In a control experiment, a mixture of sialyl-[6-^{3}H] galactose, [1-^{14}C] galactose and a large excess of unlabeled lactose was allowed to proceed to 50% completion. The remaining substrate contained no detectable

^{14}C, which excludes any significant isotopic scrambling under the conditions for carrying out the KIE experiments. Control KIEs with only remote labels gave 0.993 ± 0.008 and 1.024 ± 0.006 for sialyl-lactose and sialyl-galactose, respectively. KIEs of enzymatic transfer reactions that use dual-label substrates with the remote labels therefore need to be corrected by these binding isotope effects.

Kinetic complexity of enzymatic reactions can mask the intrinsic KIEs and lead to the misinterpretation of the transition state structures (144). KIE results generated from experiments can be used directly in the transition state analysis only when the isotopic sensitive step is the slowest step in the catalytic sequence and is free of commitment (145). In cases where these requirements are not met, there will be commitment factors involved which mask the intrinsic KIEs and result in the diminished observed KIEs (144). In such cases, in order to correctly interpret the KIE results, one needs to either measure the commitment factors that are present in the system, or to choose an alternate condition under which the chemistry step is slowed down and the commitment factor is eliminated. The former method requires information about the individual rate constants of the binding and the chemistry steps. These can be difficult to measure in some cases. The latter method has been previously applied in the KIE study of α-2,6-sialyltransferases (99) and has been proven to be feasible in generating intrinsic KIEs, which would otherwise be masked under the optimal condition of enzymatic reactions. The common methods employed to slow down the chemistry step is to change reaction pH, or to use an alternate slow substrate. In

the present KIE experiments on trans-sialidase, two substrates were tested and the KIE results were analyzed for the possible existence of the commitment factor. Sialyl-lactose is a good substrate for trans-sialidase whereas sialyl-galactose is a poor substrate. We estimated that V/K for sialyl-galactose is ~200 fold lower than that of sialyl-lactose, indicating very little external commitment that should exist in the system with sialyl-galactose as substrate. Our KIE data suggest that the internal commitment factor is also eliminated in this system. In spite of the 200-fold lowered V/K for sialyl-galactose, KIEs for sialyl-galactose are very similar to KIEs for the fast substrate sialyl-lactose. This result does not agree with the possibility that there is a significant commitment factor involved in this system. The KIE pattern observed provides additional support for the above conclusion. For the enzymatic transfer reactions, small dideuterio KIEs (~1.06) and (relatively) large primary ^{13}C KIEs (~1.03) were obtained. The pattern of a small deuterium and a (relatively) large carbon isotope effect indicates that these are intrinsic isotope effects, free of significant commitment factors. If there were a commitment factor in operation, then the intrinsic values of *both* KIEs would be higher than the observed ones, a pattern which is unknown to us. The observed KIEs in the present study are intrinsic and thus are suitable for the interpretation of the transition state structure of trans-sialidase reaction.

The nature of the transition state and the nature of the reaction intermediate remain the two most controversial subjects in the reactions catalyzed by glycosylhydrolases and glycosyltransferases. These controversies are the direct reflection of the mechanistic subtlety of nucleophilic substitution

reactions. Nucleophilic substitution reactions follow multiple reaction pathways which can be generalized as S_N1 and S_N2 mechanisms. In the following discussion, C, Nu and Lg will be used to represent the center carbon atom, the nucleophile and the leaving group. The limiting S_N1 mechanism involves the dissociation of C-Lg bond to form a stable carbocation intermediate, which is then captured by the incoming Nu. The dissociation of C-Lg is the rate limiting step in this mechanism. This dissociation process involves the formation of a contact or intimate ion pair, a solvent separated ion pair, and finally a carbocation intermediate (150). No nucleophilic assistance is present in the entire dissociation process. In a limiting S_N2 mechanism, the dissociation of C-Lg is facilitated by the incoming Nu, with the sum of bond orders between C-Lg and C-Nu being unity. It is therefore a highly concerted mechanism with no positive charge formation on the reaction center carbon. In reality, many reactions follow mechanisms with mixed S_N1 and S_N2 characters. They differ in the amount and/or the timing of nucleophilic participation in the transition state, which are dictated by the nucleophilicity of Nu, the leaving group ability of Lg, the stability of the carbocation and the ionic property of the environment. These different reaction paths can be illustrated in figure 3-8 which represents the projection of the reaction coordinates onto a two-dimensional plane (140). The limiting S_N2 mechanism is depicted as the line connecting M, T and P. The limiting S_N1 reaction is depicted by the line connecting M, N and P. With increasing amount of nucleophilic participation, the reaction path changes from the limiting S_N1 reaction to one with increasing S_N2 characters as the line connecting M, S and P

in figure 3-8. Therefore, in nucleophilic substitution reactions, the determination of the amount of nucleophilic participation in the transition state provide key information to unravel the reaction mechanism.

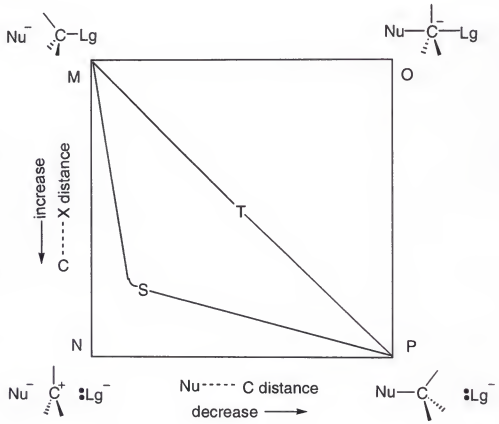

Figure 3-8. Schematic illustration of the two-dimensional projection of the reaction coordinate of nucleophilic substitution reactions (140).

For glycosylhydrolases and glycosyltransferases, it was proposed that both group of enzymes proceed through an oxocarbenium ion-like transition state and many of them are dissociative in nature (151). By dissociative we specifically mean that loss of bonding between the leaving group and anomeric carbon has progressed further than bond formation between the nucleophile and the anomeric carbon has. In one mechanistic extreme, there is no bond

formation between the incoming nucleophile and the anomeric carbon in the transition state. This dissociative transition state is S_N1 like and leads to the formation of an oxocarbenium ion, which can itself act as the reaction intermediate, or can collapse with an active site amino acid residue to form a covalent intermediate. At the other mechanistic extreme, there is a considerable amount of nucleophilic participation in the transition state. This transition state has increasing associative nature and will lead to the direct formation of a covalent intermediate without first forming the oxocarbenium ion intermediate. The nature of the transition state is likely to be dictated by the active site geometry, the nature of the leaving group and the inherent stability of the glycosyl oxocarbenium ion.

Based on crystal structure information, the mechanism of lysozyme was proposed to include an oxocarbenium ion-like transition state, leading to the formation of an oxocarbenium ion intermediate (59). However, for many other retaining glycosidases, there is a large body of experimental evidence supporting the formation of covalent intermediates in the reaction pathways. Such intermediates have been trapped by using fluorinated sugar substrates in a number of glycosidase reactions (70-76). Interestingly, no comparative KIEs have been reported for fluorosugars and their natural analogs. Kinetic isotope effect techniques have been employed in the study of many glycosylhydrolase and glycosyltransferase reactions in order to resolve the transition state structure and the reaction mechanism. KIE studies on α-2,6 and 2,3-sialyltransferases provided strong evidence for a dissociative transition state with little, if any,

nucleophilic participation (85, 100). The small primary ^{14}C isotope effect and large β-dideuterio isotope effect provided convincing evidence for a highly dissociative transition state in sialyltransferase-catalyzed reactions. Formation of such a transition state could be a result of the increased stability of sialyloxocarbenium ions, the nature of the leaving group CMP, and the architecture of the active site.

Our KIE results for the acid solvolysis of sialyl-lactose and sialyl-galactose (1.113 and 1.016 for β-dideuterio and primary ^{13}C isotope effect, respectively) indicate a dissociative S_N1 like transition state with little, if any, nucleophilic participation. This result is in agreement with the dissociative transition state for the acid solvolysis reaction of CMP-NeuAc (98). Identical primary carbon isotope effects were obtained in both systems. The small magnitude of the ^{13}C KIE suggests a highly asymmetric transition state with little nucleophilic participation. The β-dideuterio isotope effect of CMP-NeuAc solvolysis (1.28) (98) is nearly twice as big as the one for the sialyl-lactose solvolysis reaction, indicating a more advanced bond cleavage between the leaving group and the anomeric carbon in the transition state of the CMP-NeuAc acid solvolysis reaction.

Compared to the acid solvolysis reactions of sialyl-lactose and sialyl-galactose, enzymatic transfer reaction of trans-sialidase has a decreased β-dideuterio isotope effect (1.06) and an increased ^{13}C primary isotope effect (1.032). The 1.032 primary ^{13}C isotope effect can be converted to 1.06 of a ^{14}C isotope effect by the following equation 3-7 (152):

$$(^{12}k/^{13}k)^{1.9} = {}^{12}k/^{14}k \qquad (3\text{-}7)$$

This primary isotope effect is too large to allow the mechanism to be classified as the typical dissociative or S_N1-like mechanism often associated with glycosylhydrolases and glycoside hydrolysis reactions. With few exceptions, primary ^{14}C isotope effects of glycosyltransfer reactions fall between 1.01-1.05 (with ^{13}C effects being converted to ^{14}C effects) and dissociative transition states were proposed. The reactions encompass enzymatic hydrolyses, phosphorolysis, and solution hydrolyses of nucleosides, and fluoro- and alkyl-glucosides (107, 142, 143, 153-158). Exceptions to this pattern are found in the large ^{13}C KIEs of 1.032 reported for the aqueous hydrolysis of α-glucosyl fluoride (105) and 1.028 for α-glucosidase catalyzed hydrolysis of α-D-glucopyranosyl pyridinium bromide (159). In both of these cases, transition states with nucleophilic participation were proposed. Indeed, a ^{13}C primary isotope effect of 1.032 is close to the lower limit for a true S_N2 transition state. For example, displacement of 1-phenyl-1-bromoethane with sodium ethoxide affords a ^{13}C KIE of 1.036. This reaction shows a first order dependence on the concentration of ethoxide and is certainly a bimolecular process (160). The 1.032 ^{13}C isotope effect and 1.06 β-dideuterio isotope effect, therefore, strongly argue for a reaction transition state with nucleophilic participation and limited oxocarbenium ion character. Such a transition state will lead to the formation of a covalent intermediate. I suggest that for trans-sialidase catalysis, nucleophilic participation is enforced by the architecture of the active site and may facilitate expulsion of the aglycon.

Trans-sialidase catalysis proceeds with the retention of configuration in both transfer and hydrolysis reactions (108, 161). The KIE results support the idea that trans-sialidase follows a double displacement mechanism with the formation of a covalent intermediate. Two mechanistic possibilities can then be proposed for the trans-sialidase catalyzed glycosyltransfer reaction, as shown in figure 3-9. Suitable candidates for the nucleophile can be an amino acid residue on the enzyme (possibly Tyr342) or the carboxylate group on the anomeric carbon of the NeuAc moiety. The amino acid residues acting as the nucleophiles in a number of retaining glycosidase reactions have been determined. While it is common for an amino acid residue on the enzyme to act as a nucleophile, it is somewhat unusual for the substrate carboxylate group to carry out the same function. However, several lines of evidence do exist in favor of this possibility. G-type lysozymes universally lack the counterpart of HEW lysozyme Asp52. The function of this residue is instead fulfilled by the carboxylate group on the substrates (162). KIE studies on the solvolysis of NeuAc derivatives under different pH conditions also provided evidence for the nucleophilic participation of the carboxylate group in the transition state (88). Nucleophilic participation of the carboxylate group results in the formation of α-lactone, a highly strained intermediate. The strain incurred may, however, provide the reactivity needed in catalysis. The possibility of the C2 carboxylate group acting as the nucleophile was tested and is disfavoured by the trapping experiment described in the next chapter.

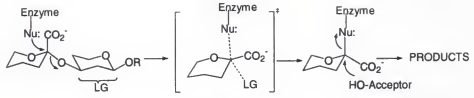

Scheme 1

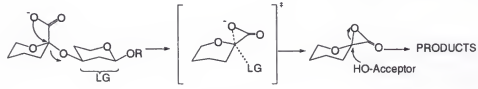

Scheme 2

Figure 3-9. Proposed mechanistic possibilities for trans-sialidase.

The formation of a covalent intermediate in trans-sialidase catalysis could serve more than one purpose. Subsequent attack of the covalent intermediate by an acceptor substrate leads to the overall retention of configuration. Furthermore, a covalent intermediate could serve to chemically sequester the NeuAc residue until it reaches a geometric relationship with the bound acceptor saccharide that is competent for glycosyltransfer. The NeuAc oxocarbenium ion has a very short life time, which makes it less selective regarding capture by water or by an acceptor saccharide hydroxyl group (163). In glycosidase reactions, a NeuAc oxocarbenium ion intermediate can be formed and subsequently trapped by water molecules in aqueous solution. Trans-sialidase, however, favors sugar molecules over water as the acceptor substrate. Therefore, the short life time and the resulting unselective reactivity of the NeuAc oxocarbenium ion must be properly accomodated by trans-sialidase catalysis. The development of a different catalytic scenario than those of sialidases is

necessary. I propose that by forming a covalent intermediate, trans-sialidase increases the selectivity of the reaction intermediate and favors its capture by sugar acceptor molecules.

As mentioned above, a number of covalent intermediates have been trapped and characterized in the glycosidase reactions with fluorinated sugar substrates (70-76). Such intermediates could form by direct nucleophilic participation in the transition state, or by collapse of an oxocarbenium ion/active site side chain ion pair. On the other hand, the presence of fluorine in the substrate could, in principle, perturb the reaction transition state and divert it into the one that leads to the formation of a covalent intermediate. Carbon primary isotope effects can be employed to reveal the formation of covalent intermediates by the transition state signature of nucleophilic participation. This method is advantageous in that the transition state of reactions with natural substrate can be determined. In the case of trans-sialidase, the combination of ^{13}C primary and β-dideuterio isotope effects allow the identification of the transition-state signature of a forming covalent intermediate. This not only indicates the formation of a covalent intermediate, but also rules out that it originates by capture of an oxocarbenium ion.

Mechanistic studies on sialidases, sialyltransferases and trans-sialidase therefore reveal different transition state structures and different reaction paths for group transfer of the same sugar. Despite the sequence similarities, trans-sialidase displays a different transition state than that of *Salmonella* sialidase. Indeed, the potent sialidase inhibitor, 2,3-dehydro-3-deoxy neuraminic acid

(DANA), does not inhibit trans-sialidase (164, 165). This compound is a geometric analog of an oxocarbenium ion-like transition state. The selective inhibition pattern provides additional support for a different transition state character in the trans-sialidase catalyzed glycosyltransfer reactions.

The kinetic mechanism for trans-sialidase has not yet been established. One tool to help rule out possibilities is the substrate concentration dependence of measured KIEs (166). The KIE data presented in Table 3-2 suggest that an ordered sequential mechanism with sialyl-lactose binding first is less probable for trans-sialidase catalysis. Essentially unchanged β-^{2}H KIEs were observed (1.046 and 1.042) at lactose concentrations of 1/10 and 1.5 K_m. If the kinetic mechanism were ordered with the labeled donor sialyl-lactose binding first, increasing acceptor concentration would result in the decrease in measured KIE, which was not observed (166). Trans-sialidase, however, must be able to bind donor substrate to carry out hydrolysis. These results, when combined, suggest that either a random sequential or a ping-pong mechanism is operative for trans-sialidase catalysis. This will be addressed in the next chapter.

Conclusions

The results of the KIEs measured on the acid solvolysis reactions of sialyl-lactose and sialyl-galactose suggest a dissociative, S_N1-like transition state with large positive charge formation on the anomeric carbon and little, if any, nucleophilic participation. This transition state is contrasted by the transition state of the enzymatic transfer reactions. The KIEs measured on the enzymatic transfer reactions indicate an associative transition state with a significant

amount of nucleophilic participation and decreased positive charge formation on the anomeric carbon. This transition state will subsequently lead to the formation of a covalent intermediate. KIE results with different acceptor concentrations suggest that a sequential ordered mechanism is not operative in the enzymatic transfer reaction catalyzed by trans-sialidase.

Experimental

Control for Isotopic Fractionation of Sialyl Glycosides on Dowex-1 (formate) Column

Individual controls were performed to test for isotopic fractionation of sialyl-galactose or sialyl-lactose by Dowex 1x8 (formate) resin anion-exchange chromatography. Master ^{3}H /^{14}C mixtures of ([6-^{3}H] Gal) sialyl-galactose (50,000 cpm, 60 mCi/mmol) and ([1-^{14}C] Gal) sialyl-galactose (50,000 cpm, 52 mCi/mmol), or ([6-^{3}H] Glc) sialyl-lactose (12,000 cpm, 27 Ci/mmol) and ([2-^{13}C] NeuAc, [1-^{14}C] Glc) sialyl-lactose (8,000 cpm, 60 mCi/mmol) were prepared. Each mixture was divided into two equal volume fractions. One fraction was transferred directly into a LSC vial with 4 ml of 200 mM ammonium formate (pH 6.6) added into the vial. The other fraction was loaded onto a 5 cm column of Dowex 1x8 (formate) resin in a Pasteur pipet which was then washed with 200 mM ammonium formate buffer to allow recovery of the substrates. Fractions (4 mL) were collected directly into LSC vials, to which was added 16 mL of liquid scintillation fluid. Care was taken to collect the entire peak of eluted sialyl-lactose. All vials were counted 10 minutes each for 10 cycles.

KIE Experiment Accuracy Control

Mixtures of ([6-^{3}H] Glc) sialyl-lactose (100,000 cpm) and ([2-^{13}C] NeuAc, [1-^{14}C] Glc) sialyl-lactose (100,000 cpm) were made to give $^{3}H/^{14}C$ ratios that would correspond to an actual KIE of 1.025. This was done by first individually measuring the cpm per unit mass of solutions of the ^{3}H and ^{14}C labeled sialyl-lactose isotopomers on an analytical balance. The masses of both isotopomer solutions required to give a KIE of 1.025 were then calculated and measured on the same analytical balance. The "KIE" was measured by the method described below and the prepared solutions were treated as if they were actual KIE reaction mixtures. The measured KIE was compared with the expected KIE to provide a measurement of the accuracy of the KIE method.

Trans-sialidase Kinetic Experiments

Initial velocities were measured at 26 °C, pH 7.0 in a buffer system containing 20 mM HEPES and 2 mg/ml ultrapure BSA. For glycosyltransfer reactions, the concentration of the acceptor substrate lactose was 100 mM. About 60,000 cpm of ([1-^{14}C] Glc) sialyl-lactose (54.3 mCi/mmol) or ([1-^{14}C] Gal) sialyl-galactose (52 mCi/mmol) was added into each reaction mixture (final volume 50 µL). Reactions were initiated by addition of 125 ng of trans-sialidase. Three time point aliquots (15 µL) were withdrawn within the initial velocity range. Aliquots were quenched into 1 ml cold deionized water and 960 µl of the quenched mixture was applied to a Dowex 1x8 (formate) mini-column (4 cm height, Pasteur pipet). Product (radioactive lactose or galactose) was collected in the water fractions and quantified by liquid scintillation counting.

Determination of the Isotopic Scrambling under the Conditions for the KIE Experiments

([6-^{3}H] Gal) sialyl-galactose (0.186 μCi, 60 mCi/mmol) and [1-^{14}C] galactose (0.095 μCi, 52 mCi/mmol) were included in a reaction mixture containing 100 mM nonradioactive lactose in pH 7.0, 40 mM HEPES buffer. The reaction was initiated by the addition of trans-sialidase. The reaction was conducted at 26 °C for 23 hours and analyzed on Dowex 1X8 (formate) anion-exchange mini-column cast in a Pasteur pipet. The column was first washed by water to elute product lactose, followed with 200 mM ammonium formate buffer to elute sialyl-glycosides. The amount of ^{3}H and ^{14}C in each fractions was measured by liquid scintillation counting as described below.

Determination of the Hydrolysis reactions under the Conditions for the KIE Experiments

(a) sialyl-lactose reaction. A mixture of carrier-free ([9-^{3}H] NeuAc) sialyl-lactose and ([1-^{14}C]Glc) sialyl-lactose were included in a reaction mixture with 0.8 mM cold lactose and a buffer system containing pH 7.0, 20 mM HEPES and 2 mg/mL ultrapure BSA. The reaction was initiated by the addition of trans-sialidase. The reaction was allowed to proceed and then quenched in 0.5 mL of ice cold deionized water. The reaction mixture was separated by anion-exchange HPLC on a MonoQ column with a 0-5 mM ammonium bicarbonate gradient. ([1-^{14}]Glc) lactose, ([9-^{3}H] NeuAc) sialyl-lactose, ([1-^{14}C]Glc) sialyl-lactose and [9-^{3}H] NeuAc peaks were collected into the LSC vials (4 mL/vial) which were assayed by liquid-scintillation counting.

(b) sialyl-galactose reaction. Carrier-free ([3,3'-^{2}H] NeuAc, [6-^{3}H] Gal) sialyl-galactose and ([1-^{14}C] NeuAc) sialyl-galactose were mixed in pH 7.0, 20 mM HEPES buffer with 2 mg/mL BSA and either 0.8 mM cold lactose or 100 mM cold lactose. The same procedure (see above) was adopted. [6-^{3}H] Gal, ([3,3'-^{2}H] NeuAc, [6-^{3}H] Gal) sialyl-galactose, ([1-^{14}C] NeuAc) sialyl-galactose and [1-^{14}C] NeuAc peaks were collected and counted in the liquid scintillation counter as described above.

KIE Experiments

The competitive method was used to measure the V/K isotope effects (67). About 100,000 cpm each of ^{3}H and ^{14}C labeled substrates were included in one reaction. Radiolabeled substrates utilized in KIE experiments were greater than 99.9% free of lactose or galactose. A master mixture of ^{3}H/^{14}C labeled substrates was made, from which aliquots were withdrawn and the reference ^{3}H/^{14}C ratio at time zero was determined. Reactions were initiated by addition of trans-sialidase for enzymatic reactions or HCl to a final concentration of 0.1 M for acid solvolysis reactions. Pre-chilled deionized water was added to stop the reaction after 40-60% conversion had been reached (148). The reaction mixture was immediately loaded onto Dowex 1x8 (formate form) mini-columns (5 cm height in a Pasteur pipet) to separate the unreacted substrate from the product. The column was first eluted with deionized water until all of the radioactive lactose or galactose eluted. The unreacted sialyl-glycoside was obtained by elution with 200 mM ammonium formate buffer. Care was taken to collect the entire peak. The eluate (4 mL) was collected into liquid scintillation vials, to

which 16 mL of liquid scintillation fluid was added. The $^{3}H/^{14}C$ ratio of the unreacted substrate was determined by dual-channel liquid scintillation counting (channel A, 0-15 keV; channel B, 15-90 keV) with each tube being counted for 10 minutes, and all tubes cycled through the counter 6-10 times to afford better counting statistics (147). Triplicate samples of ([1-^{14}C] Glc) sialyl-lactose or ([1-^{14}C] Gal) sialyl-galactose were used to determine the ratio of ^{14}C counts in channels A and B ($A:B_{14}$). Since ^{3}H is only detected in channel A, the $^{3}H/^{14}C$ ratio in a given tube was calculated with the following equation 3-8 (147):

$$^{3}H/^{14}C = (\text{cpm A} - \text{cpm B} \times A:B_{14})/(\text{cpm B} + \text{cpm B} \times A:B_{14}). \qquad (3\text{-}8)$$

The reported value and error of a KIE represents the mean and standard deviation of the mean of at least three individual KIE experiments taken over 6-10 cycles through the liquid scintillation counter. The observed KIE was calculated according to equations 3-9, 3-10 and 3-11. Equations 3-9 or 3-10 are used when the heavy isotope-labeled substrate has a ^{3}H or ^{14}C remote label, respectively. Equation 3-11 is used to correct the observed isotope effect for fractional conversion (f) (167). At least three independent experiments were conducted for measurement of all KIEs.

$$KIE_{observed} = (^{14}C/^{3}H)_0 / (^{14}C/^{3}H)_t \qquad (3\text{-}9)$$

$$KIE_{observed} = (^{3}H/^{14}C)_0 / (^{3}H/^{14}C)_t \qquad (3\text{-}10)$$

$$KIE_{observed} = \ln (1 - f) / \ln [(1 - f) * KIE_{observed})] \qquad (3\text{-}11)$$

The enzymatic KIE reactions were performed at 26 °C in 20 mM HEPES containing 2 mg/ml BSA at pH 7.0. The typical sialyl-galactose KIE reaction

mixture was 50 μL in volume, contained 100 mM lactose, and was initiated by addition of 500 ng of trans-sialidase in a 10 μL volume. The fractional conversion was determined by taking aliquots from the reaction mixture and analyzing the amount of product and remaining substrate on a Dowex 1X8 anion-exchange (formate) column. Approximately 5 h was required to reach 50% conversion. The typical sialyl-lactose KIE reaction mixture was 50 μL in volume, contained 0.8 mM lactose, and was initiated by addition of 50 ng of trans-sialidase in a 1 μL volume. Approximately 30-60 minutes were required to reach 50% conversion. For the acid solvolysis KIEs, 0.2 M HCl solution was added into an equal volume of ^{3}H /^{14}C labeled substrate mixture (final volume = 50 μL) to initiate the reactions which were conducted at 37 °C.

CHAPTER 4
MECHANISTIC STUDIES ON TRANS-SIALIDASE

Introduction

Chemical Trapping Experiments

Formation of an enzyme bound covalent intermediate is a common scheme employed in enzymatic reactions. A covalent intermediate may serve more than one purpose. First, it can affect the stereochemical outcome of a reaction, as evidenced in the double displacement mechanism for retaining glycosidases. Second, it can also increase the life time of an otherwise unstable intermediate by sequestering it, rendering its selectivity higher.

There are a number of methods available for the detection of a covalent intermediate. Burst kinetics, stereochemical analysis and chemical trapping are among the most common methods employed in this area. Knowledge about the reaction kinetic mechanism can also provide information regarding the presence of a covalent intermediate. A ping-pong mechanism, for example, often implies that such an intermediate is formed in the reaction. On the other hand, the demonstration of a covalent intermediate also provides insight into the reaction kinetic mechanism.

KIE results on the trans-sialidase catalyzed transfer reaction suggest the occurance of nucleophilic participation in the transition state, which will

subsequently lead to the formation of a covalent intermediate. Chemical trapping experiments have been conducted in order to detect the formation of such an intermediate.

Initial Velocity Studies

At the first glimpse, it may seem formidable to study enzyme mechanisms, due to their complexity. The establishment of Michaelis-Menten kinetics provides a powerful tool for enzymologists to study the enzyme mechanism through initial velocity studies. Enzyme kinetic mechanisms have been found to fall into several common schemes with characteristic initial velocity patterns. Thus, the pattern generated in the initial velocity studies can be used to differentiate among different types of kinetic mechanisms.

Kinetic mechanisms for bisubstrate enzymatic reactions fall into two major groups: sequential and ping-pong mechanisms (figure 4-1). In a sequential mechanism, both substrates must combine with the enzyme before chemistry can take place and any product be released. For a classic ping-pong mechanism, chemistry occurs after the binding of the first product and leads to the formation of a modified enzyme form, which then combines with the second substrate and completes the reaction. Thus, a reaction with a classic ping-pong mechanism can be considered as a combination of two half reactions. One product is released in each half reaction. The initial velocity patterns for these two types of mechanisms are different. For a sequential mechanism, the double reciprocal initial velocity plot gives a set of lines that converge at a common point. For the ping-pong mechanism, the same plot yields a set of parallel lines

(168). The intersect and the slope in a double-reciprocal plot (1/V vs. 1/[A]) represent $1/V_{max}$ and K_m/V_{max}, respectively. The intercept may be altered if the reaction rate at the saturating concentration of the varied substrate (A) is altered by the change of the concentration of the changing fixed substrate (B). The slope is affected by the changing fixed substrate (B) when the point of combination of E and A and that of E and B are connected by reversible steps (168). In a classic ping-pong mechanism, no reversible step exists between these two points of combination in the absence of products. Therefore, a parallel double-reciprocal plot is characteristic for such a mechanism. However, such reversible step does exist in a sequential mechanism which results in convergent lines in the double-reciprocal plot. Therefore, in mechanistic studies, initial velocity kinetics usually provides the first indication of whether a sequential or a ping-pong mechanism is in effect for a given enzymatic reaction.

Substrate bindings in a sequential mechanism can be either random or ordered (figure 4-1). For a random sequential mechanism, either substrate can combine with the enzyme first. For an ordered mechanism, however, the combination of the first substrate (A) with enzyme must take place before the combination of the second substrate (B) with enzyme. Both random and sequential mechanisms have the same initial velocity pattern. Other methods, such as product inhibition studies, may be used to distinguish between them. Kinetic isotope effects are also able to distinguish between random and sequential mechanisms (166). In a random mechanism, change in concentration of B does not affect the kinetic isotope effect on A. In an ordered mechanism,

increasing B concentration drives more EA complex through the catalytic step. As a result, the forward commitment factor is increased and the KIE is decreased. When [B] reaches infinity, no KIE on A can be observed. Therefore, by measuring the KIE on A at different B concentrations, random and ordered mechanism can be distinguished (166).

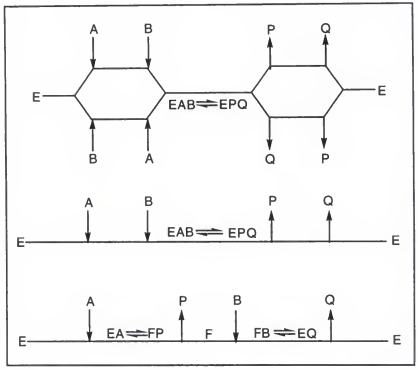

Figure 4-1. Random sequential (top), ordered sequential (middle) and ping-pong (bottom) mechanisms. A/B and P/Q refer to substrates and products, respectively. F is the modified enzyme form in a ping-pong mechanism.

Although distinct initial velocity patterns can be obtained for classic sequential and ping-pong mechanisms, these patterns may change if there are modifications in the reaction mechanism. For example, when a branch reaction is added into the classic ping-pong mechanistic scheme, the initial velocity patterns change correspondingly. In this branched ping-pong mechanism (figure

4-2), intersecting lines are generated when the second product formation is monitored (169). The change in B concentration affects the partition between the branching path and the path leading to the second product formation. This alters the apparent second order rate constant for the second product formation, resulting in the slope effect in the double-reciprocal plot. When the first product is monitored, parallel double-reciprocal lines are generated. Since the first product is formed prior to the point of divergence, varying B concentration does not give a slope effect in a double-reciprocal plot when the first product is monitored. For the random sequential mechanism with a branch, however, convergent lines are observed when either product formation is monitored (170). Therefore, by measuring the initial velocities for the first and the second product formation, one can obtain information for the differentiation between a ping-pong mechanism and a random sequential mechanism.

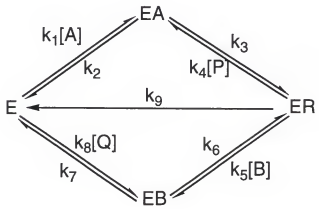

Figure 4-2. Branched ping-pong mechanism. A/B and P/Q represent the substrates and products, respectively. R is the portion of substrate A that is transferred in the reaction.

Here we report the initial velocity experiments on trans-sialidase. The results of our experiments led to the proposal of a ping-pong mechanism with a hydrolytic branch for trans-sialidase catalysis.

Site-directed Mutagenesis and Chemical Rescue Studies

Kinetic isotope effect studies and chemical trapping experiments provided strong evidence for the formation of a covalent intermediate in the trans-sialidase catalyzed reaction and for the involvement of an active site amino acid residue in the nucleophilic attack. The primary sequence alignment among TCTS, *Salmonella* sialidase and *T. rangeli* sialidase have revealed a conserved Tyr residue (Tyr342 in recombinant trans-sialidase). This residue is close (~ 3 Å) to the DANA C-2 atom in the crystal structures of both *Salmonella* and *T. rangeli* sialidases (92, 110). It was proposed to stabilize the oxocarbenium ion intermediate formed in the active site of *Salmonella* sialidase (93). Tyr342 in trans-sialidase is crucial for enzymatic activity. Y342F mutation inactivates trans-sialidase (113). Therefore, we seek to investigate the role of this amino acid residue in trans-sialidase catalysis by site-directed mutagenesis and chemical rescue experiments. The rationale behind this experimental design is the following: if Tyr342 is the critical nucleophile, the abolished trans-sialidase activity by Y342A and/or Y342G mutations may be rescued by small organic nucleophiles, such as phenol, which can diffuse into the active site and fill in the cavity created by the mutations. The observation of such rescue, and particularly the observation of the rescued product, such as phenol-β-D-NeuAc, can provide

strong evidence for the nucleophilic function of Tyr342 in trans-sialidase catalysis.

The work presented in this section includes the cloning, overexpression and purification of Y342A and Y342G mutated enzymes and the preliminary results of the chemical rescue experiments performed on these two mutants.

Inhibition Tests of Sialidase Transition State Analogs on Trans-sialidase

Enzyme inhibitors have both practical and theoretical applications. Theoretically, enzyme inhibitors can be used to study the transition state and mechanism of enzyme catalyzed reactions. Rational inhibitor design takes advantage of the transition state and mechanistic information on enzymatic reactions in the design of specific enzyme inhibitors. The inhibitors thus synthesized can also be used as a tool in mechanistic enzymology to further probe the transition state and mechanism of enzymatic reactions.

A number of transition state analogs for sialidases have been synthesized in this lab. These compounds are electronic analogs of the oxocarbenium ion-like transition state proposed for a number of sialidases as described in Chapter 1. In this section, the inhibition studies of these compounds on trans-sialidase are described. The compounds tested (figure 4-3) include *trans,trans*-5-N-(1'-Carboxyethyl)-3,5-dihydroxy-4-acetamidopiperidine (**1**) and *trans,trans*-5-N-(1'-Carboxybenzylethyl)-3,5-dihydroxy-4-acetamidopiperidine (**2**) synthesized by Dr. Ian Parr (171); *trans,trans*-N-(1'-carboxyethyl)-4-acetamido-5-acetoxy-3-hydroxypiperidine (**3**) synthesized by Kim Millar (172) and *trans,trans*-(3,4-dihydroxy-5-propyl-piperidin-1-yl)-acetic acid (**4**) and *trans,cis*-(3,4-dihydroxy-5-

propyl-piperidin-1-yl)-acetic acid (**5**) synthesized by Dr. Hongbin Sun (173). This work has been conducted in order to provide information regarding the differences between the transition state for trans-sialidase and those for sialidases.

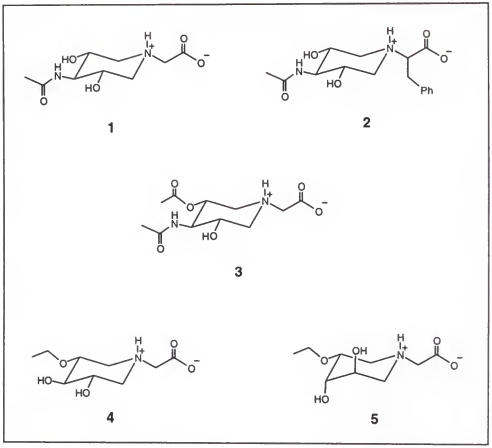

Figure 4-3. Sialidase transition state analogs tested in trans-sialidase inhibition experiments.

Results

Chemical Trapping Experiment

Quenching of trans-sialidase activity by 4 M urea/1% SDS. Trans-sialidase activities with and without the presence of 4 M urea/1% SDS are

presented in table 4-1. The activity is represented as the radioactive product (lactose) formed versus time. No product formation was observed for the reaction with 4 M urea/1% SDS, indicating the complete quenching of trans-sialidase activity under this condition.

Table 4-1. The quenching of trans-sialidase activity by 4M urea/1% SDS.

Min	With urea/SDS (cpm)	Without urea/SDS (cpm)
1	46	1764
2	47	2881
3	45	3772

Control of chromatographic method. The Sephadex G-50 size exclusion chromatography technique was employed in the trapping experiment. A sample identical to the reaction mixture in the trapping experiment was separated by this method and the elution pattern was observed. The consistency of column elution was tested by performing triplicate runs of the above experiment. The data was shown in figure 4-4.

The trapping experiment. The reaction of trans-sialidase with the substrate ([9-^{3}H] NeuAc) sialyl-lactose was quenched in 4 M urea/1% SDS. The reaction mixture was dialyzed against 4 M urea and separated on Sephadex G-50 column. A control experiment was also carried out, in which trans-sialidase was quenched before the addition of substrate. Radioactivity and protein concentration (Bradford assay) in each fraction were measured in both

experiments. The results are shown in figure 4-5. The appearance of radioactivity under the protein peak was observed in the trapping experiment, but not in the control experiment.

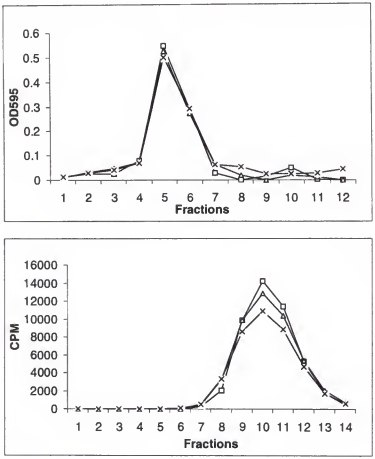

Figure 4-4. Elution pattern of Sephadex G-50 chromatography in the trapping experiment. Top panel: protein concentration in each fraction; bottom panel: radioactivity in each fraction. Data from triplicate runs were plotted in each graph.

Initial Velocity Studies

Initial steady-state kinetic experiments were performed on the total reaction and the transfer reaction catalyzed by trans-sialidase in order to investigate the kinetic mechanism. For the study of the total reaction, radioactive

([1-^{14}C] Glc) sialyl-lactose was employed as the donor substrate and the formation of ([1-^{14}C] Glc) lactose was monitored. For the study of the transfer reaction, [(1-^{14}C) Glc] lactose was employed as the acceptor substrate and the formation of [(1-^{14}C) Glc] sialyl-lactose was monitored.

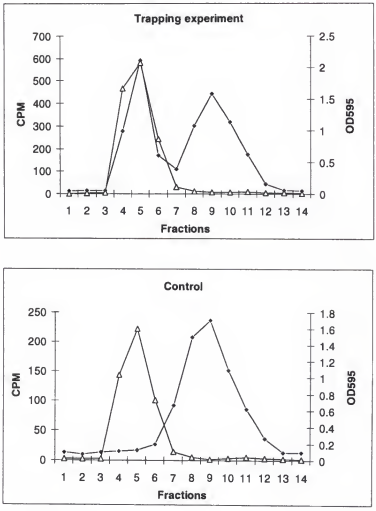

Figure 4-5. Intermediate trapping. Top panel: the trapping experiment; bottom panel: the control experiment. In both panels, open triangle and solid diamond represent protein concentration and radioactivity, respectively.

Rate equations (174) for both the total and the transfer reactions (refer to figure 4-2 for the mechanistic scheme) are presented in figure 4-6. The double-

reciprocal plot of the total reaction is shown in figure 4-7. Apparent parallel lines were observed. The intercepts were fitted into the rate equation for the total reaction. The result of data fitting is shown in figure 4-8 and the fitted values are listed in table 4-2.

$$V_{total} = \frac{V_a A}{K_{ah} + \frac{(1 + B/K_{bt})A}{(1+B/K_{ibb})}}$$

$$V_{transfer} = \frac{V_{ab} AB}{K_{ah}K_{bt} + K_{at}B + K_{bt}A + AB}$$

$$K_{ah} = \frac{(k_2 + k_3)k_9}{k_1(k_3 + k_9)} \qquad K_{bt} = \frac{(k_6 + k_7)(k_3 + k_9)}{k_5(k_3 + k_7)}$$

$$K_{at} = \frac{k_7(k_2 + k_3)}{k_1(k_3 + k_7)} \qquad K_{ibb} = \frac{k_9(k_6 + k_7)}{k_5 k_7}$$

$$V_{ab} = \frac{k_3 k_7 E_0}{k_3 + k_7} \qquad V_a = \frac{k_3 k_9 E_0}{k_3 + k_9}$$

Figure 4-6. Rate equations for the branched ping-pong mechanism.

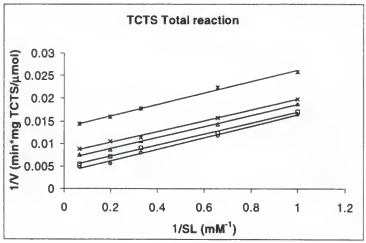

Figure 4-7. The double-reciprocal plot of the total reaction.

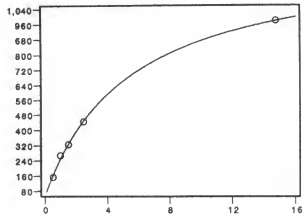

Figure 4-8. Data fitting of the total reaction. The X-axis is the lactose concentrations (mM); the Y-axis is the reciprocal of intercepts (cpm/min) derived from figure 4-7 by linear regression analysis.

Table 4-2. Kinetic parameters derived from the initial kinetic study of the total reaction.

Kinetic parameters	Fitted values
V_a	0.026 ± 0.009 μmol/min/μg enzyme
K_{bt}	5.4 ± 0.8 mM
K_{ah}	0.35 ± 0.14 mM
K_{ibb}	0.25 ± 0.12 mM

The transfer reactions were studied at two different substrate concentration ranges. The data obtained with high substrate concentrations are

shown in figure 4-9. Substrate inhibition was observed in this concentration range. The data obtained with low substrate concentrations are shown in figure 4-10. Convergent lines were observed in this plot.

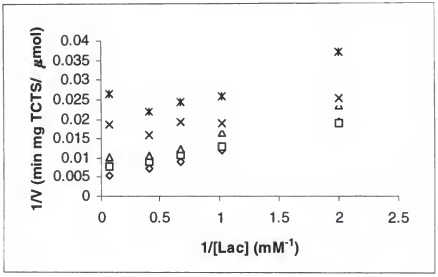

Figure 4-9. The double-reciprocal plot of the TCTS transfer reaction at high substrate concentrations.

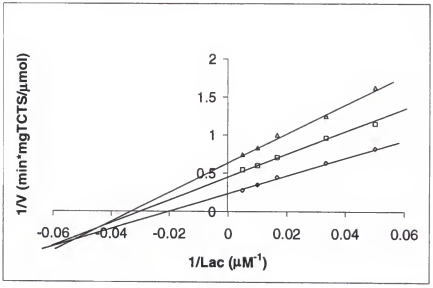

Figure 4-10. The double-reciprocal plot of the TCTS transfer reaction at low substrate concentrations.

Site-directed Mutagenesis and Chemical Rescue Studies

Tyr342 in trans-sialidase was mutated to either Gly or Ala and the mutated enzymes were used in chemical rescue experiments. The presence of both mutations were confirmed by sequencing and by restriction analysis (figure 4-11). Both mutated enzymes were purified to homogeneity as analyzed by SDS-PAGE gel electrophoresis (figure 4-12). From 1 liter culture, about 5 and 34 mg of Y342A and Y342G were obtained, respectively.

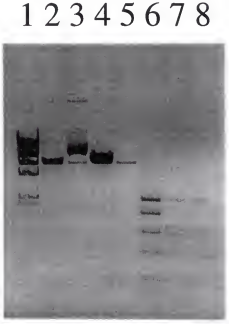

Figure 4-11. Restriction analysis of Y342A and Y342G plasmids. Plasmids were extracted from two Y342A colonies (Y342A1 and Y342A2) and two Y342G colonies (Y342G1 and Y342G2). Lane 1 to 8: λ standard; (TCTS/pET14b)/Apa I; TCTS/pET14b; Y342A1/Sac I; Y342A2/SacI; (TCTS/pET14b)/BsrF I; Y342G1/BsrF I; and Y342G2/BsrF I.

Phenol, *p*-nitro-phenol, azide, imidazole, acetate, trifluoroethanol and 4-fluoro-phenol were tested in the chemical rescue experiments on Y342A and Y342G at pH 7.3. The results indicate that enzymatic activities of both Y342A

and Y342G mutants were totally abolished. And no activity was observed in the presence of the above-mentioned nucleophiles.

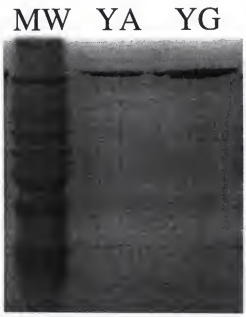

Figure 4-12. SDS-PAGE of purified Y342A and Y342G enzymes.

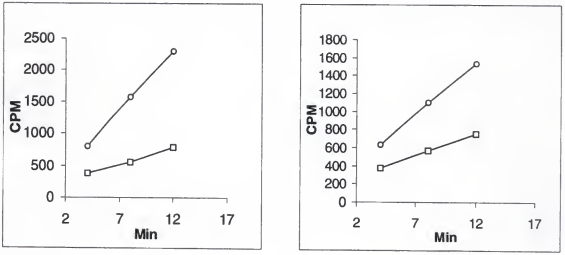

Figure 4-13. Inhibition of compound **3** on trans-sialidase. Left panel: inhibition on the transfer reaction; right panel: inhibition on the hydrolysis reaction. In both panels, open circles represent the reaction without compound **3**; open squares represent the reaction with compound **3**.

Inhibition Tests of Sialidase Transition State Analogs on Trans-sialidase

Five compounds that were designed and synthesized as transition state analogs of sialidases were tested on trans-sialidase. Initial velocities of trans-sialidase were measured with and without the presence of inhibitors. No inhibition was observed with compounds **1**, **2**, **4** and **5**. Compound 3 inhibits both transfer and hydrolysis reactions catalyzed by trans-sialidase (figure 4-13), with an estimated K_i of 460 μM on the hydrolysis reaction.

Discussion

Chemical Trapping Experiments

Kinetic isotope effect studies on the glycosyltransfer reactions catalyzed by trans-sialidase gave an increased ^{13}C primary isotope effect (1.032) and a decreased β-dideuterio isotope effect (1.06), compared to those of the acid solvolysis reaction (1.016 and 1.13 for ^{13}C and β-^{2}H isotope effect, respectively). This KIE pattern suggests the involvement of nucleophilic participation in the transition state, which will lead to the formation of a covalent intermediate. However, two possibilities exist that fit in this scenario. An amino acid residue in the enzyme active site could serve as the nucleophile and lead to the formation of an enzyme-bound covalent intermediate. The NeuAc C-2 carboxylate group could also nucleophilically participate in the transition state, leading to the formation of an α-lactone intermediate (88). The difference between these two schemes is whether or not the intermediate is covalently attached to the enzyme active site. In this experiment, we seek to answer two questions: is there a covalent intermediate? And if so, is it covalently bound in the enzyme active

site? The answer to the second question serves to distinguish between the participation of an active site nucleophilic amino acid residue and of the NeuAc C-2 carboxylate group. A method was developed to address these two questions.

To perform a trapping experiment, It is generally desirable that the rate of the formation of the intermediate is faster than the rate of its breakdown, which would lead to its accumulation. However, the step leading to the formation of the covalent intermediate in the trans-sialidase catalyzed reaction is at least partially rate-limiting because intrinsic KIEs were observed that report on this step. Therefore, the intermediate, once formed, probably does not accumulate. Hence, large amount of enzyme and radioactive substrate with high specific activity were used in this experiment in order to detect the low steady-state level of the intermediate. Recombinant trans-sialidase employed in this experiment was expressed from the plasmid TCTS/pET14b, which gave a high expression level at ~10 mg trans-sialidase/liter culture. The radioactive substrate employed was ([9-^{3}H] NeuAc) sialyl-lactose with a specific activity of 15 Ci/mmol. The formation of an enzyme-bound covalent intermediate results in the transfer of [9-^{3}H] NeuAc from the substrate to the enzyme, generating radiolabeled enzyme molecules. Urea (4 M) with 1% SDS was employed to quench the enzyme reaction. This condition was chosen because of the following reasons. First, a control experiment showed that trans-sialidase was quenched rapidly and no turnover was observed. Second, urea and SDS are mild reagents and allow the characterization of the covalent nature of the intermediate. Non-covalent

combination of the intermediate with enzyme should dissociate once the secondary structures of the enzyme are destroyed. Third, the most probable candidate for the active site nucleophile is Tyr342. The bond thus formed is acid labile, but is relatively stable in 4 M urea solution. The presence of 1% SDS also helped solubilize the denatured protein. The reaction thus quenched was dialyzed against 4M urea extensively to allow the dissociation of any non-covalent combination of the low molecular weight species with enzyme. This step also removed most of the radioactivity in the reaction mixture, rendering the next chromatographic step more feasible. After dialysis, trans-sialidase and low molecular weight molecules in the reaction mixture were separated by size-exclusion chromatography. Consistent elution patterns were achieved by this method, as shown by the proper control experiments. The clean separation of the enzyme peak and the substrate peak on this column was also demonstrated. Fractions were analyzed for both protein concentration and the amount of radioactivity. Trans-sialidase was quenched before addition of the substrate in a control experiment under otherwise identical conditions. This experiment was carried out in order to measure the amount of background association between low molecular weight species and the enzyme. No radioactivity was found under the protein peak in this control experiment. The result of the control experiment suggested that non-specific binding did not take place under the experimental conditions. However, we can not rule out the possibility that the binding of the substrate to enzyme stabilizes the enzyme secondary structure so that quenching may not result in the complete dissociation of enzyme and substrate.

In this case, identification of the covalent adduct by mass spectrometry would provide further support.

The successful trapping of the enzyme-bound covalent intermediate not only provides supporting evidence for the conclusion drawn from the previous KIE experiments, but also argues against the possibility that the NeuAc C-2 carboxylate group nucleophilically participates in the transition state. This leaves only one mechanistic possibility in which an active site amino acid residue acts as the nucleophile to form the covalent intermediate. Trans-sialidase shares 30% and 70% sequence similarity with *Salmonella* sialidase (47, 90) and *T. rangeli* sialidase (111, 112), respectively. The crystal structures of these two sialidases reveal a conserved Tyr342 in the active sites that is in close proximity to NeuAc C-2 atom (~ 3 Å) (92, 110). This residue is also conserved at the same position in the primary sequence of trans-sialidase (90). Our hypothesis is that Tyr342 of trans-sialidase serves as the nucleophile and leads to the formation of a phenolic glycoside intermediate in the active site. One such example is found in type IB topoisomerase family in which an active site tyrosine acts as the nucleophile and leads to the formation of a DNA-(3'-phosphotyrosyl)-protein covalent intermediate (175). A phenolic anion is a much stronger nucleophile than an acetate ion (176). However, at physiological pH, tyrosine is nearly completely protonated. A glutamate was found to be near the active site tyrosine in both influenza and *Salmonella* sialidases (91, 93). This residue is also conserved in TCTS active site (113). This residue could serve as the general base catalyst and facilitate the deprotonation of the tyrosine. Theoretical

calculations showed that in doing so, a covalent intermediate could form at a relatively low energetic cost (177). Unfortunately, the amount of trapped intermediate in this experiment was not enough for the characterization of the nature of the chemical bond and of the active site nucleophile. Later in this chapter, site-directed mutagenesis and chemical rescue experiments are described in which this hypothesis is tested further.

Initial Velocity Studies

KIE experiments on the trans-sialidase catalyzed glycosyltransfer reaction revealed a transition state with nucleophilic participation which will result in the subsequent formation of a covalent intermediate. The chemical trapping experiment provided evidence for the existence of such an intermediate. These results, along with the retention stereochemistry of both the transfer and the hydrolysis reactions catalyzed by trans-sialidase (108, 161), suggest a double displacement mechanism for trans-sialidase catalysis. Previous steady-state kinetics on the transfer reaction of trans-sialidase yielded a set of intersecting lines in the double-reciprocal plot. This result was interpreted as implying that the reaction follows a sequential, rather than a ping-pong, kinetic mechanism (108, 109). However, the existence of the hydrolytic branch reaction was not addressed in the derivation of the rate equations in the previous kinetic studies. As described in the "introduction" section of this chapter, when this branch reaction is included, a ping-pong mechanism also gives intersecting pattern in the double-reciprocal plot when the second substrate formation (the transfer reaction) is monitored. Therefore, steady-state kinetic experiments were

performed on trans-sialidase to further investigate its mechanism. Previous KIE results argue against an ordered sequential mechanism. The discussion presented below will thus be focused on the differentiation of a random sequential and a ping-pong kinetic mechanisms.

Initial velocity experiments for the formation of both the first and the second product were conducted. The double reciprocal plot of the total reaction (monitoring the first product formation) gave a set of apparent parallel lines. The intercepts of lines were fitted into the rate equation for the total reaction of the branched ping-pong mechanism by MacCurveFit data fitting program (version 1. 5. 2, Kevin Ranger Software). As shown in the figure 4-9, the data fitting is reasonably good. The kinetic parameters generated are listed in table 4-1. V_a is the maximum velocity of the hydrolysis reaction. K_{ah} and K_{bt} are the K_m of sialyl-lactose in the hydrolysis reaction and the K_m of lactose in the transfer reaction, respectively. K_{ibb} reflects the partition between the hydrolytic and transfer paths.

The initial kinetics of the transfer reaction (monitoring the second product formation) were conducted in two substrate concentration ranges. The hydrolysis reaction was significant at low substrate concentrations, resulting in an apparent convergent pattern of the double-reciprocal plot. No data fitting was performed with this plot because the substrate concentrations employed were much lower than their K_m values. Nevertheless, the apparent parallel pattern of the total reaction and the convergent pattern of the transfer reaction, when taken together, provide supporting evidence for the branched ping-pong mechanism.

At this time it is proposed that this mechanism is operative in trans-sialidase catalysis.

When the transfer reaction was studied at higher substrate concentrations, the convergence of lines was obscured by two factors: the diminished hydrolysis reaction and the substrate inhibition. A clear pattern of substrate inhibition by lactose was observed, which was eliminated by the presence of high sialyl-lactose concentrations. At this point, there is not enough experimental result for an unambiguous interpretation of this phenomenon. One possible explanation is that lactose can bind to a regulatory site on the enzyme and the binding suppresses the transfer, but not the hydrolysis reaction. This binding can be abolished by the presence of high sialyl-lactose concentrations. In this scenario, the transfer rate would be reduced by high lactose concentrations. The total reaction, however, is less affected because the reduction of the transfer reaction is partially compensated by the increased flux of reaction through the hydrolysis pathway.

In conclusion, the initial velocity studies on the total and the transfer reactions catalyzed by trans-sialidase led to the proposal of a branched ping-pong mechanism for this enzyme. The same mechanism has been found in a number of other enzymes, including glucose-6-phosphatase, transglutaminase, γ-glutamyltransferase, alkaline phosphatase, etc. (169, 178-180). We propose that trans-sialidase is a new member of this kinetic family.

At this point, it is not known if trans-sialidase contains a distinct binding site for the acceptor substrate. Although the existence of only one binding site is

a common pattern for enzymes that follow a ping-pong mechanism, a multiple-site ping-pong mechanism is known and a number of enzymes are found to follow this mechanism (181-184). In the absence of products, the initial velocity kinetic equation for the two-site ping-pong mechanism is identical to the one for the classic ping-pong mechanism (181). Therefore, the present initial kinetic results are also compatible with a two-site ping-pong mechanism. Some evidence does exist in favor of such a mechanism. A distinct acceptor binding site was suggested by crystallographic study on *T. rangeli* sialidase as well as by mutagenesis studies on both *T. rangeli* sialidase and TCTS (110). Other evidence includes the finding that some inactive trans-sialidases expressed in *Trypanosoma cruzi* can bind galactose (185, 186). Our previous data also suggest the presence of such an acceptor binding site. Compared with sialyl-lactose, higher lactose concentration was required to suppress the hydrolysis reaction of sialyl-galactose. Although this experiment was not conducted under initial velocity conditions, it did show that the partition between transfer and hydrolysis is related to the donor substrate. This result is better explained by the presence of a distinct acceptor binding site on trans-sialidase. In this scenario, lactose can bind before, during and after the glycosidic bond cleavage of the donor substrate. Different donor substrates can therefore affect the binding affinity of enzyme for the acceptor substrate, resulting in different partition between transfer and hydrolysis. More experiments need to be carried out in order to address this possibility.

Site-directed Mutagenesis and Chemical Rescue Studies on Trans-sialidase

Both Y342A and Y342G mutations were made on plasmid TCTS/pET14b. The trans-sialidase gene (1944 bp) is inserted in the Nde I and BamH I sites of pET14b. Six primers were designed in order to carry out the mutagenesis by PCR. The locations of the trans-sialidase gene and primers are shown in figure 4-14. The designed primers include two outer primers P1 and P2, and four inner primers YAL, YAR, YGL, and YGR. The sequences and annealing positions of all primers are listed in table 4-3. Mutations were designed in the four inner primers. YA mutation created a Sac I site (G/AGCTC), while YG mutation created a Bsrf I site (Pu/CCGGPy). Overlap extension PCR was performed to amplify the segment of TCTS gene flanked by primers P1 and P2 (187). This gene segment contains two unique restriction sites: Apa I and BssH II near the 5' and 3' ends, respectively. The PCR products were cloned into TOPO pCR 2.1 vector by Invitrogen. The desired mutations in the plasmids were confirmed by restriction analysis and by sequencing. The gene segment in the TOPO vector was then subcloned into TCTS/pET14b plasmid. The restriction analysis was carried out on two mutated plasmids to confirm the presence of the mutation. The Sac I site is not present in the wild type plasmid. Sac I digestion linearized the Y342A plasmid and verified the presence of YA mutation. BsrF I yields ten digested fragments of the wild type plasmid. With the presence of a YG mutation, the BsrF I digestion pattern is altered. Among the four largest fragments, three remain the same for both WT and Y342G plasmid. Fragment 2, however, changes its size from 1582 bp for the WT plasmid to 1211 bp for the

YG plasmid. This result was observed which confirmed the presence of the YG mutation.

The transformation procedure and the overexpression and purification of mutant enzymes follow essentially the procedure described in Chapter 2 for the wild type trans-sialidase. Care was taken to prevent the contamination of wild type trans-sialidase in the entire overexpression and purification process.

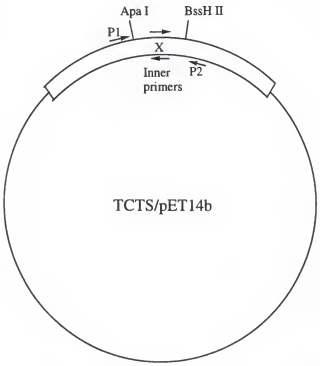

Figure 4-14. Schematic illustration of TCTS/pET14b plasmid. The primers designed for the mutagenesis experiment are shown at their annealing positions. Important restriction sites are also shown in the figure.

The enzymatic activities of both Y342A and Y342G were measured by trans-sialidase activity assay. Approximately 10^6 fold rate decreases were observed for both mutants. This result confirms that Tyr342 is crucial for enzymatic activity (113). Rescue experiments were carried out with the following

seven nucleophiles at neutral pH: Phenol, *p*-nitro-phenol, azide, imidazole, acetate, trifluoroethanol and 4-fluoro-phenol. The amount of mutant enzyme used in each reaction was about a thousand fold higher than that of the wild type enzyme. The preliminary results show that no rescued enzymatic activity was observed with these nucleophiles under the experimental conditions. There are a couple of possibilities that could explain the experimental results. One explanation is that Tyr342 is not functioning as the nucleophile, but rather performs other essential roles. Other possibilities include the low accessibility of the active sites of Y342A and Y342G for the organic nucleophilies, as well as the possible alteration of enzyme conformation by the mutations. Further experiments are required to address these possibilities.

Table 4-3. Sequences and annealing positions of designed primers.

Primers	Sequences	Annealing positions (bp)
P1	5'-GTGGGTGGAGGCTGTCGGCACGC-3'	4934 to 4957
P2	5'-GCACTGATTTAATGATCCGTAGCTCGCC-3'	5265 to 5293
YAL[a]	5'-ACGGAGCTCGCGGCGGAATTTTCATC-3'	5157 to 5183
YAR	5'-ATTCCGCCGCGAGCTCCGTCCTGTA-3'	5164 to 5189
YGL	5'-ACGGAGCTGCCGGCGGAATTTTCATC-3'	5157 to 5183
YGR	5'-ATTCCGCCGGCAGCTCCGTCCTGTA-3'	5164 to 5189

a. Sites of mutations are underlined.

Inhibition Tests of Sialidase Transition State Analogs on Trans-sialidase

Transition state analogs were designed and synthesized in this lab to mimic the oxocarbenium ion-like transition state of sialidases. This transition

state has two features: the positive charge formation on the anomeric carbon and the flattening of the pyranosyl ring of NeuAc about C-6, O-6, C-2 and C-3. The compounds tested mimic the charge formation in the transition state of sialidase reactions. Among all the compounds tested, only compound **3** showed moderate inhibition of trans-sialidase. At this point, it is not clear what structural features are required for the design of potent trans-sialidase inhibitors. Based on our findings of the nucleophilic participation in the transition state of trans-sialidase catalyzed reactions, it could be a useful strategy to incorporate an electrophile on the proper position of the inhibitors. The reaction between the electrophile and the active site nucleophile could provide an efficient way to inactivate trans-sialidase.

Conclusions

An enzyme-bound covalent intermediate has been detected by the chemical trapping experiments. This not only provides supporting evidence for nucleophilic participation in the transition state of trans-sialidase catalyzed reactions, as revealed by KIE studies, but also suggests that an active site amino acid residue is acting as the nucleophile in the reaction. Initial kinetic studies on both the total and the transfer reactions catalyzed by trans-sialidase support a branched ping-pong mechanism. This mechanism agrees with the results of our initial kinetic studies on trans-sialidase and with the conclusion drawn from the KIE and chemical trapping experiments. The nature of the nucleophile was tested by site-directed mutagenesis studies. Both Y342A and Y342G mutants are inactive, indicating the crucial role of Tyr342 in catalysis. However, the

rescue experiments were inconclusive. Therefore, the exact role of Tyr342 and the nature of the nucleophile remain unknown. The inhibition tests on trans-sialidase suggest that the transition state analogs of sialidase are not efficient in the inhibition of trans-sialidase. A new strategy is proposed to incorporate an electrophile on the inhibitor to capture the active site nucleophile.

Experimental

Chemical Trapping Experiment

Quenching of trans-sialidase activity by 4 M urea/1% SDS. The reaction mixture contained 72,000 cpm ([1-^{14}C] Glc) sialyl-lactose (54.3 mCi/mmol), 4 M urea and 1% SDS in pH 7.3, 60 mM HEPES buffer. Trans-sialidase (300 ng in a volumn of 5 µl) was added to initiate the reaction. The total reaction volume was 50 µl. The reaction was run at room temperature and 16 µl aliquots were withdrawn at 1, 2, and 3 minutes. The aliquot was immediately diluted in 1 ml ice-cold deionized water and loaded onto a Dowex 1X8-200 (formate) mini-column in a glass Pasteur pipet. The column was washed with 4 ml of deionized water to elute the product ([1-^{14}C] Glc) lactose, which was quantified by liquid scintillation counting. The same volume of deionized water was added instead of urea and SDS in a control reaction conducted under otherwise identical conditions. The progress of the control reaction was monitored in the same way as described above.

Control of chromatographic method. A mixture containing 4.8 mg BSA and 50,000 cpm ([1-^{14}C] Glc) sialyl-lactose (54.3 mCi/mmol) in pH 7.3, 60 mM HEPES buffer with 4 M urea in a volume of 100 µl was loaded onto a Sephadex

G-50 column (in a 1 ml Tuberculin syringe). The column was washed with 4 M urea and 100 µl fractions were collected. Aliquots from each fraction were withdrawn for the quantification of radioactivity and protein concentration (Bradford assay). In a separate experiment, three identical mixtures containing 3 µg BSA and 50,000 cpm ([1-^{14}C] Glc) sialyl-lactose (54.3 mCi/mmol) in pH 7.3, 60 mM HEPES buffer with 4 M urea in a volume of 100 µl was loaded onto Sephadex G-50 columns. Elution and quantification procedures were the same as described above.

Trapping experiment. The reaction mixture contained 37 µl TCTS (3.66 mg, 0.052 µmol, taken from an enzyme stock in pH 8.0, 20 mM Tris-HCl buffer) and 3 µl ([9-^{3}H] NeuAc) sialyl-lactose (~10 million cpm, 0.467 nmol, 15 Ci/mmol) in pH 7.3, 60 mM HEPES buffer. The total reaction volume was 50 µl. TCTS was added last to initiate the reaction which was carried out at room temperature. The reaction was immediately quenched by addition of 1 ml of 4 M urea/1% SDS at room temperature. The time between the addition of enzyme and the addition of urea was less than 10 seconds. The quenched reaction mixture was transferred into a dialysis tube and dialyzed against 200 ml of 4 M urea at room temperature. The dialysis solution was changed every 12 hours. The dialysis was stopped when there was no detectable radioactivity in the dialyzing solution. The reaction mixture inside the dialysis tube was then concentrated by microcon (YM 10). Precipitate of urea was observed during the concentration. This precipitate was removed by centrifugation and the supernatant (~50 µl) was loaded onto a Sephadex G-50 mini column cast in a 1ml Tuberculin syringe

which was pre-equilibrated with 4 M urea. The urea precipitate from the last step was rinsed with another 50 µl of 4 M urea solution and the rinse was also applied onto the column. The column was then washed with 4 M urea. A total of 14 fractions were collected with 100 µl per fraction. Aliquots (75 µl) from each fraction were transferred into LSC vials and quantified by liquid scintillation counting for the amount of radioactivity. The second aliquots (20 µl) from each fraction were mixed with 1 ml Biorad Bradford protein assay reagent. OD595 was measured for the quantification of the protein concentration in each fraction. For the control experiment, the same conditions were used except that the substrate was added after the quenching of the enzyme by 4 M urea/1% SDS. The reaction mixture was then treated exactly the same as described above. The data were compared with those from the trapping experiment.

Initial Velocity Studies

The total reaction. The total (transfer and hydrolysis) reaction of trans-sialidase was studied by using ([1-^{14}C] Glc) sialyl-lactose and nonradioactive lactose as substrates, and the formation of ([1-^{14}C] Glc) lactose was monitored. Five sialyl-lactose concentrations: 15.21, 5.07, 3.04, 1.52 and 1 mM, and five lactose concentrations: 14.76, 2.16, 1.48, 0.98 and 0.5 mM were used. A total of 25 different combinations of sialyl-lactose and lactose concentrations were studied. All reactions were carried out at 26 °C in pH 7.2, 60 mM HEPES buffer with 2 mg/ml BSA. The reaction volumes varied from 25 to 100 µl. TCTS (from plasmid TCTS/pQE60 expression) concentrations were 2.38 nM in all reactions. The percent conversions of all reactions were kept under 10% to allow the

observation of the initial rate of product formation. Three aliquots were withdrawn from each reaction mixture. Aliquots were quenched immediately in 1 ml ice-cold deionized water and then applied onto Dowex 1X8 (formate form) anion-exchange mini columns cast in glass Pasteur pipets. ([1-^{14}C] Glc) lactose was eluted off the column with 4 ml deionized water. The eluate was collected directly into LSC vials and quantified by liquid scintillation counting. The linearity of the data were confirmed in a control experiment under the same conditions where an aliquot was withdrawn at a time point earlier than the three time points taken in the above experiment. The results showed that this point colinerizes with the time points taken in the initial velocity experiments. The data obtained in the initial kinetic experiment for the total reaction was plotted in a double-reciprocal plot. The slopes and intercepts of data series were obtained by MicroSoft Excel linear regression analysis. The intercepts were fitted into the rate equation for the total reaction in a branched ping-pong mechanism by computer program MacCurveFit (version 1. 5. 2, Kevin Ranger Software).

The transfer reaction. The transfer reactions were studied by using nonradioactive sialyl-lactose and [(1-^{14}C) Glc] lactose as substrates and monitoring the formation of [(1-^{14}C) Glc] sialyl-lactose. Two different substrate concentration ranges were used. In the first experiment, the concentrations of both sialyl-lactose and of [(1-^{14}C) Glc] lactose were the same as those used in the total reactions described above. In the second experiment, three sialyl-lactose concentrations: 100, 50, 30 μM and five lactose (carrier-free) concentrations: 200, 100, 60, 30, 20 μM were used. The combinations of sialyl-

lactose and lactose concentrations gave a total of 15 reactions. The reaction conditions were the same as those for the total reaction. Product and substrate were separated on Dowex mini-columns as described above. The columns were first washed with 4 ml of deionized water to elute the substrate, then washed with 200 ml ammonium formate buffer to elute the product, [(1-^{14}C) Glc] sialyl-lactose, which was quantified by liquid scintillation counting.

Site-directed Mutagenesis and Chemical Rescue Studies on Trans-sialidase

The mini-prep of plasmid TCTS/pET14b from *E. coli* BL21 (DE3) cells was carried out by standard methods. The trans-sialidase gene (1944 bp) is inserted in the Nde I and BamH I site of pET14b. Six primers were designed. Two outer primers, P1 and P2, base pair with sequences from 4934 bp to 4957 bp and from 5265 bp to 5293 bp, respectively. P1 and P2 primers flank two unique restriction sites: Apa I at 4970 bp and BssH II at 5253 bp. Mutations were designed in four inner primers (YAL, YAR, YGL, and YGR) with the sequences listed in table 4-3. The YA mutation created a Sac I site (G/AGCTC), while the YG mutation created a Bsrf I site (Pu/CCGGPy). PCR experiments were performed with the following pairs of primers: P1/YAL, P1/YGL, P2/YAR, and P2/YGR. PCR reaction mixtures contained 0.1 ng TCTS/pET14b, 1 μM outer primer, 1 μM inner primer, 0.2 mM dNTPs in 1X PCR buffer (from Invitrogen TOPO TA cloning kit) with 5 U Taq polymerase. PCR reactions were carried out in Perkin Elmer GeneAmp PCR System 2400 with the following conditions: the reaction mixture was heated at 94 °C for 1 minute. Thirty PCR cycles (94 °C for 1 min, 57 °C for 1 min, 72 °C for 1 min) were then performed followed with a 10 min extension at 72 °C. PCR

products were gel purified by Qiagen Qiaquick gel extraction kit. The overlapping extension PCR was carried out with the following conditions: The two PCR products (the left piece and the right piece synthesized above) were first diluted and 0.1 ng of each was mixed in a reaction mixture with 1 μM each of primers P1 and P2. Other components in the reaction mixture were the same as those used in the above PCR reactions. The PCR reaction was performed the same way as described above. The PCR product was gel purified and characterized by restriction analysis with Sac I and Bsfr I for YA and YG mutation, respectively. The PCR products containing the mutations was cloned into the Topo pCR 2.1 cloning vector with Invitrogen TOPO TA cloning kit following the standard procedures. Plasmid midi-prep was carried out with Qiagen Hispeed plasmid midi-prep kit. The desired mutations in the prepared plasmids were confirmed by restriction analysis with Sac I or Bsrf I and by DNA sequencing performed by the DNA Sequencing Core at the University of Florida. Apa I/BssH II digestion of the plasmid released the insert, which was gel purified by the method described above. The same enzyme digestion and gel purification procedures were applied to plasmid TCTS/pET14b. The ligation was then performed between the digested fragment of TCTS/pET14b and the insert from the Topo vector. The ligation mixture contained 20 ng insert and 200 ng digested TCTS/pET14b. The ligation reaction was carried out at 16 °C overnight. The ligated DNA was transformed into BL21 (DE3) competent cells following Novagen procedures. Plasmid mini-prep was conducted with Qiagen Qiaprep spin mini-prep kit. Restriction analyses were performed to confirm the presence of mutations in the

new constructs. The procedure of the overexpression and purification for mutant enzymes was essentially the same as the one for the wild type trans-sialidase described in Chapter 2.

Inhibition Tests of Sialidase Transition State Analogs on Trans-sialidase

Trans,trans-5-N-(1'-Carboxyethyl)-3,5-dihydroxy-4-acetamidopiperidine (**1**) and *trans,trans*-5-N-(1'-Carboxybenzylethyl)-3,5-dihydroxy-4-acetamidopiperidine (**2**). Reaction mixture contained 0.8 mM lactose, 91.5 μM ([1-^{14}C] Glc) sialyl-lactose (30,000 cpm), 515 μM of either compound **1** or compound **2** in pH 7.3, 20 mM HEPES buffer. Trans-sialidase (60 ng) was added to initiate the reaction. The total reaction volume was 50 μl. Three aliquots were taken at 3, 6 and 9 minutes. Aliquots were immediately quenched in 1 ml ice-cold deionized water and loaded onto Dowex 1X8-200 (formate) anion-exchange column. The column was washed with 4 ml water to elute the product ([1-^{14}C] Glc) lactose, which was quantified by liquid scintillation counting. The control reactions were conducted with the same procedure in the absence of compounds **1** and **2**.

trans,trans-N-(1'-carboxyethyl)-4-acetamido-5-acetoxy-3-hydroxypiperidin (**3**). Both transfer and hydrolysis reactions were tested. Reaction mixture for the transfer reaction contained 0.8 mM lactose, 0.18 mM ([1-^{14}C] Glc) sialyl-lactose (58,000 cpm) and 0.96 mM **3** in pH 7.3, 20 mM HEPES buffer. Trans-sialidase (90 ng) was added to initiate the reaction. The total reaction volume was 50 μl. The reaction mixture for the hydrolysis reaction was the same as above except that lactose was not included. The reactions were run at 37 °C and three

aliquots were withdrawn at 4, 8 and 12 minutes. The chromatography procedure and product quantification were the same as described above.

trans,trans-(3,4-dihydroxy-5-propyl-piperidin-1-yl)-acetic acid (**4**) and *trans,cis*-(3,4-dihydroxy-5-propyl-piperidin-1-yl)-acetic acid (**5**) These compounds were tested on the hydrolysis reaction catalyzed by trans-sialidase. Reaction mixture contained 0.18 mM ([1-^{14}C] Glc) sialyl-lactose (58,000 cpm) and 1.15 mM either **4** or **5** in pH 7.3, 20 mM HEPES buffer. Trans-sialidase (90 ng) was added to initiate the reaction. The total reaction volume was 50 µl. The reactions were carried out at 37 °C and three aliquots were withdrawn at 5, 10 and 15 minute. The chromatography procedure and product quantification were the same as described above.

CHAPTER 5
CONCLUSIONS AND FUTURE WORK

Conclusions

This work has resulted in a better understanding of the transition state structure and the mechanism of reactions catalyzed by *Trypanosoma cruzi* trans-sialidase. The transition state structures of both the solvolysis and the enzymatic transfer reactions of sialyl-glycosides were investigated through the kinetic isotope effect studies. A dissociative transition state with substantial oxocarbenium ion character was determined for the acid solvolysis reactions. This transition state is contrasted by the one for the enzymatic transfer reactions in which a significant amount of nucleophilic participation is involved with a simultaneous decrease in the positive charge formation on the anomeric carbon. This work therefore provides an example of an altered transition state character by enzyme catalysis. The associative nature of the transition state of enzymatic transfer reactions suggests the direct formation of a covalent reaction intermediate. This was confirmed by the successful trapping of this intermediate. The intermediate was shown to be covalently attached to the enzyme. This result argues against the possible nucleophilic role of NeuAc C-2 carboxylate group in catalysis and suggests that an active site amino acid residue is nucleophilically involved in the transition state. A Tyr342 residue in the active

site was proposed to be the nucleophile. Site-directed mutagenesis studies indicated the essential catalytic function of this residue. However, its exact role in catalysis remains unclear. Initial steady-state kinetic studies led to the proposal of a branched ping-pong mechanism for trans-sialidase catalysis, which agrees with the presence of an associative transition state and the formation of an enzyme-bound covalent intermediate, as revealed by kinetic isotope effect studies and by intermediate trapping experiments.

The results generated from this work have implications in the design of inhibitors of trans-sialidase. It may be important to include an electrophile on the appropriate position of inhibitors. The capture of the active site nucleophile by this electrophile could provide an efficient way for the inactivation of trans-sialidase.

Future Work

Preliminary evidence for a branched ping-pong mechanism was obtained through this work. Further kinetic studies are required to provide detailed information on the reaction mechanism. These include: 1) a full range of inhibition studies to test the hypothesis of a branched ping-pong mechanism as well as the possibility of a two-site ping-pong mechanism; 2) pH-rate study to reveal possible general acid/base catalysis in the reaction; and 3) pre-steady-state kinetics to measure the rate constants of individual steps.

Due to the lack of structural information on trans-sialidase, it is necessary to carry out in the further site-directed mutagenesis study on this enzyme. Possible active site residues based on sequence alignment can be tested

through mutagenesis study for their possible functions. Chemical rescue and kinetic study, in conjunction with the mutagenesis study, may provide detailed information about the nature of the reaction nucleophile as well as general acid/base catalysts.

Methods need to be developed to study the transition state of the hydrolysis reaction and of the deglycosylation portion of the transfer reaction. Results from these studies can not only verify the conclusions drawn from the previous work, but also provides a more complete picture of trans-sialidase catalysis.

APPENDIX A
^{1}H NMR OF SIALYL-LACTOSE SYNTHESIZED ENZYMATICALLY

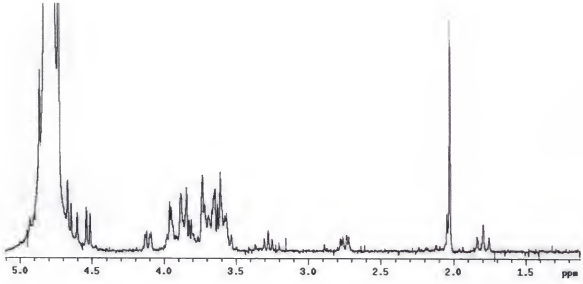

APPENDIX B
^{1}H NMR OF SIALYL-GALACTOSE SYNTHESIZED ENZYMATICALLY

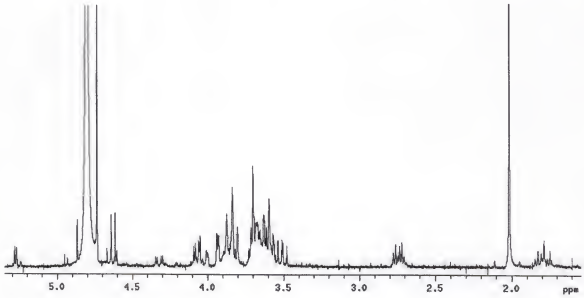

APPENDIX C
^{1}H NMR OF 4,6-BENZYLIDENE-A-D-METHYL GALACTOSIDE

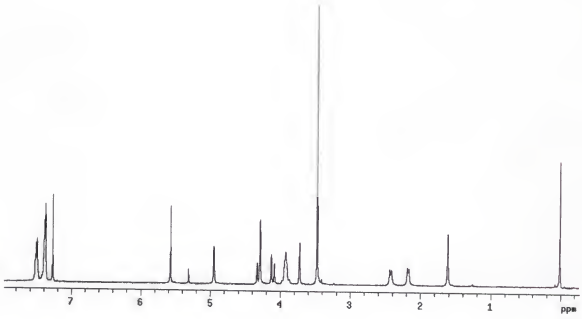

APPENDIX D

^{1}H NMR OF 2-BENZOYL-4,6-BENZYLIDENE-A-D-METHYL GALACTOSIDE

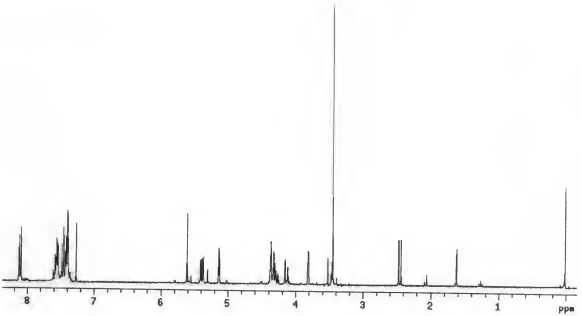

APPENDIX E
^{1}H NMR OF 2-BENZOYL-3-KETP-4,6-BENZYLIDENE-A-D-METHYL GALACTOSIDE

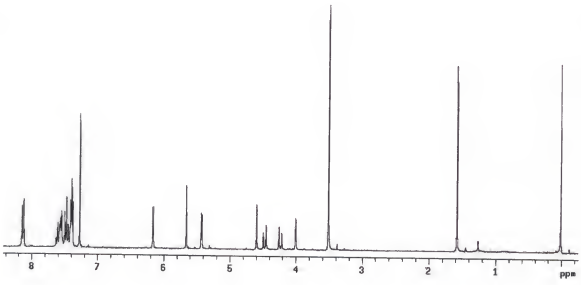

LIST OF REFERENCES

(1) Rosenberg, R., *Biology of sialic acids.* Plenum Press, New York and London. (1995)

(2) Schauer, R., *Sialic Acids--Chemistry, Metabolism and Function.* Springer-Verlag Wien New York. (1982)

(3) Klenk, E., *Hoppe-Seylers Z.* (1935) 235, 24-36

(4) DucDodon, M., Quash, G. A., *Immunology* (1981) 42, 401-408.

(5) Reutter, W., Bauer, C., *Morris Hepatomas: Mechanisms of Regulation.* Morris, H. P., Criss, W. E., eds.. Plenum Press (1978), 405-437.

(6) Litt, M., Wolf, D. P., Khan, M. A., *Adv. Exp. Med. Biol.* (1977) 89, 191-201.

(7) Rogers, G. N., Paulson, J. C., *Virology* (1983) 127, 361-373.

(8) Evans, D. G., Evans, D. J., Moulds, J. J., Graham, D. Y., *Infect. Immun.* (1988) 56, 2896-2906.

(9) Perkins, M. E., Rocco, L. J., *J. Immunol.* (1988) 141, 3190-3196.

(10) Zeng, F. Y., Gabius, H. J., *Z. Naturforsch.* (1992) 47c, 641-653.

(11) Lawrence, M. B., Springer, T. A., *Cell* (1991) 65, 859-873.

(12) Biancone, L., Araki, M., Araki, K., Vassalli, P., Stamenkovic, I., *J Exp Med* (1996)183, 581-7.

(13) Crocker, P. R., Gordon, S., *J. Exp. Med.* (1986) 164, 1862-1875.

(14) Crocker, P. R., Kelm, S., Dubois, C., Martin, B., McWilliam, B. S., Shotten, D. M., Paulson, J. C., Gordon, S., *EMBO J* (1991) 10, 1661-1669.

(15) Stamenkovic, I., Seed, B., *Nature* (1990) 345, 74-77.

(16) Stamenkovic, I., Sgroi, D., Aruffo, A., *Cell* (1992) 68, 1003-1004.

(17) Leprince, C., Draves, K. E., Geahlen, R. L., Ledbetter, J. A., Clark, E. A., *Proc. Natl. Acad. Sci. USA* (1993) 90, 3236-3240.

(18) Jancik, J. M., Schauer, R., Andres, K. H., von Düing, M., *Cell Tissure Res.* (1978) 186, 209-226.

(19) Halbhuber, K. -J., Helmke, U., Geyer, G., *Folia Haematol.* (1972) 97, 196-203.

(20) Greenberg, J. P., Packham, M. A., Guccione, M. A., Rand, M. L., Reimers, H. -J., Mustard, J. F., *Blood* (1979) 53, 916-927.

(21) Woodruff, J. J., Gesner, B. M., *J. Exp. Med.* (1969) 129, 551-567.

(22) Ashwell, G., Morell, A. G., *Adv Enzymol Relat Areas Mol Biol.* (1974) 41, 99-128.

(23) Kolb-Bachofen, V., *Biochem. Biophys. Res. Commun.* (1978) 85, 678-683.

(24) Kawasaki, T., Ashwell, G. *J. Biol. Chem.* (1976) 251, 1296-1302.

(25) Roelcke, D., Pruzanski, W., Ebert, W., Römer, W., Fischer, E., Lenhard, V., Rauterberg, E., *Blood* (1980) 55, 677-681.

(26) Bergman, L. W., Harris, E., Kuehl, M., *J. Biol. Chem.* (1981) 256, 701-706.

(27) Winkelhake, J. L., Kunicki, T. J., Elcombe, B. M., Aster, R. H., *J. Biol. Chem.* (1980) 255, 2822-2828.

(28) Roitt, I., *Essential Immunology.* Blackwell Science Ltd., (1997) 11-14.

(29) Austen, K. F., Fearon, D. T., *Adv. Exp. Med. Biol.* (1979) 120 B, 3-17.

(30) Docampo, R., Schmuñis, G. A., *Parasitol. Today* (1997) 13, 129-130.

(31) Brener, Z., *Ann. Rev. Microbiol.* (1973), 27, 347-382.

(32) Dias, J. C. P., *Rev. Soc. Bras. Med. Trop.* (1989) 22, 147-156.

(33) Brener, Z., *Rev Inst Med Trop Sao Paulo* (1971)13, 171-8.

(34) Rimoldi, M. T., Sher, A., Heiny, S., Lituchy, A., Hammer, C. H., Joiner, K., *Proc. Natl. Acad. Sci.* (1988) 85, 193-197.

(35) Andrews, N. W., Hong, K. -S., Robbins, E. S., Nussenzweig, V., *Exp. Parasitol.* (1987) 64, 474-484.

(36) Schenkman, S., Ponts de Carvalho, L., Nussenzweig, V., *J. Exp. Med.* (1992)*175*, 567-575.

(37) Ferrero-Gracia, M. A., Trombetta, S.E., Sanchez, D. O., Reglero, A., Frasch, A. C. C., Parodi, A. J., *Eur. J. Biochem.* (1993) 213, 765-771.

(38) Piras, M. M., Henriquez, D., Piras, R., *Mol. Biochem. Parasitol.* (1987) 22, 135-143.

(39) Villalta, F, Zhang, Y, Bibb, K. E., Burns, J. M. Jr., Lima, M. F., *Biochem. Biophy. Res. Comm.* (1998) 249, 247-252.

(40) Franchin, G., Pereira-Chioccola, V. L., Schenkman, S., Rodrigues, M.M., *Infect. Immun.* (1997) 65, 2548-2554.

(41) Schenkman, S., Diaz, C., Nussenzweig, V., *Exp. Parasitol.* (1991) 72, 76-86.

(42) Kazatchkine, M. D., Fearon, D. T., Austen, K. F., *J. Immunol.* (1979)122, 75-81.

(43) Norris, K. A., Schrimpf, J. E., *Infect. Immun.* (1994) *62*, 236-243.

(44) Tardieux, I., Webster, P., Ravesloot, J., Boron, W., Lumm, J. A., *Cell* (1992) 71, 1117-1130.

(45) Andrews, N. W., Abrams. C. K., Slatin, S. L., Griffiths, G., *Cell* (1990) *61*, 1277-1287.

(46) Hall, B. F., Webster, P., Ma, A. K., Joiner, K. A., Andrews, N. W., *J. Exp. Med* (1992) 176, 313-325.

(47) Pereira, M. E. A., Mejia, J. S., Ortega-Barria, E., Matzilevich, D., Prioli, R. P., *J. Exp. Med.* (1991) 174, 179-191.

(48) Campetella, O. E., Uttaro, A. D., Parodi, A. J., Frasch, A. C., *Mol. Biochem. Parasitol.* (1994) 64, 337-340.

(49) Schenkman, S., Chaves, L. B., Pontes de Carvalho, L., Eichinger, D., *J. Biol. Chem* (1994) *269*, 7970-7975.

(50) Buscaglia, C. A., Campetella, O., Leguizamon, M. S., Frasch, A. C., *J. Infect. Diseases* (1998)*177*, 431-436.

(51) Buscaglia, C. A., Alfonso, J., Campetella, O., Frasch, A. C., *Blood* (1999) 93, 2025-2032.

(52) Andrews, N. W., Robbins, E. S., Ley, V., Hong, K. S., Nussenzweig, V., *J. Exp. Med.* (1988) 167, 300-314.

(53) Egima, C. M., Briones, M. R. S., Junior, L. H. G. F., Schenkman, R. P. F., Uemura, H., Schenkman, S., *Mol. Biochem. Parasitol.* (1996) 77, 115-125.

(54) Pereira, M. E. A., *Science* (1983) 219, 1444-1446.

(55) Botelho-Chaves, L., Briones, M. R. S., Schenkman, S. *Mol. Biochem. Parasitol.* (1993) 61, 97-106.

(56) Harth, G., Haidaris, C. G., So, M., *Proc. Natl. Acad. Sci. USA* (1987) 84, 8320-8324.

(57) Pereira-Chioccola, V. L., Costa, F., Ribeirao, M., Soares, I.S., Arena, F., Schenkman, S., Rodrigues, M. M., *Parasite Immunol.* (1999) 21, 103-110.

(58) Blake, C. C. F., Koenig, D. F., Mair, G. A., North, A. C. T., Phillips, D. C., Sarma V. R., *Nature* (1965) 22, 757-761.

(59) Phillips, D. C., *Proc. Natl. Acad. Sci.* (1967) 57, 484-495.

(60) Henrissat, B., *Biochem. J.* (1991) 280, 309-316.

(61) Henrissat, B., Bairoch, A., *Biochem. J.* (1993) 293, 781-788.

(62) Baird, S. D., Hefford, M. A., Johnson, D. A., Sung, W. L., Yaguchi, M. Seligy, V. L., *Biochem. Biophys. Res. Commun.* (1990)169, 1035-1039.

(63) Koshland, D. E., *Biol. Rev. Cambridge Phil. Soc.* (1953) 28, 416-436.

(64) Salton, M. R. J., Ghuysen, J. M., *Biochim. Biophys. Acta* (1959) 36, 552-554.

(65) Salton, M. R. J., Ghuysen, J. M., *Biochim. Biophys. Acta* (1960) 45, 355-363.

(66) Malcolm, B. A., Rosenberg, S., Corey, M. J., Allen, J. S., de Baetselier, A., Kirsch, J. F., *Proc. Natl. Acad. Sci. USA.* (1989) 86, 133-137.

(67) Dahlquist, F.W., Rand-Meir, T., Raftery, M.A., *Biochemistry* (1969) 8, 4214-4221.

(68) Rosenberg, S., Kirsch, J. F., *Biochemistry* (1981) 20, 3196-3204.

(69) Gebler, J. C., Aebersold, R., Withers, S. G., *J. Biol. Chem.* (1992) 267, 11126-30.

(70) Kuroki, R., Weaver, L. H., Matthews, B. W., *Science* (1993) 262, 2030-2033.

(71) He, S. and Withers, S. G., *J. Biol. Chem.* (1997) 272, 24864-24867.

(72) Withers, S. G., Antony, R., Warren, J., Street, I. P., Rupitz, K., Kempton, J. B., Aebersold, R., *J. Am. Chem. Soc.* (1990) 112, 5887-5889.

(73) Sidhu, G., Withers, S.G., Nguyen, N.T., McIntosh, L.P., Ziser, L., Brayer, G.D., *Biochemistry*, (1999) 38, 5346-5354.

(74) Vocaldo, D. J., Mayer, C., He, S., Withers, S. G., *Biochemistry* (2000) 39, 117-126.

(75) Wong, A. W., He, S., Grubb, J. H., Sly, W. S., Withers, S. G., *J. Biol. Chem.* (1998) 273, 34057-34062.

(76) Hart, D. O., He, S., Chany, II, C. J., Withers, S. G., Sims, P. F. G., Sinnott, M. L., Brumer, III, H., *Biochemistry* (2000) 39, 9826-9836.

(77) Cupples, C. G., Miller, J. H., Huber, R. E., *J. Biol. Chem.* (1990) 265, 5512-5518.

(78) Jacobson, R. H., Zhang, X. J., Dubose, R. F., Matthews, B. W., *Nature* (1994) 369, 761-766.

(79) Richards, J. P., Huber, R. E., Lin, S., Heo, C., Amyes, T. L., *Biochemistry* (1996) 35, 12377-12386.

(80) Richards, J. P., Huber, R. E., Heo, C., Amyes, T. L., Lin, S., *Biochemistry* (1996) 35, 12387-12401.

(81) Corfield, A. P., *Glycobiology* (1992) 2, 509-521.

(82) Palese, P., Tobita, K., Ueda, M., Compans, R. W., *Virology* (1974) 61, 397-410.

(83) Griffin, J. A., Compans, R. W., *J. Exp. Med.* (1979) 150, 379-391.

(84) Chong, A. K., Pegg, M. S., Taylor, N. R., von Itzstein, M., *Eur. J. Biochem.* (1992) 207, 335-343.

(85) Varghese, J. N., Colman, P. M., *J. Mol. Biol.* (1991) 221, 473-486.

(86) Lentz, M. R., Webster, R. G., Air, G. M., *Biochemistry* (1987) 26, 5351-5358.

(87) Guo, X., Laver, G., Vimr, E., Sinnott, M. L., *J. Am. Chem. Soc.* (1994) 116, 5572-5578.

(88) Ashwell, M., Guo, X., Sinnott, M. L., *J. Am. Chem. Soc.* (1992) 114, 10158-10166.

(89) Tiralongo, J., Pegg, M. S., von Itzstein, M., *FEBS Letters* (1995) 372, 148-150.

(90) Cremona, M. L., Sanchez, D. O., Frasch, A. C., Campetella, O., *Gene* (1995)160, 123-128.

(91) Crennell, S.J., Garman, E.F., Philippon, C., Vasella, A., Laver, W.G., Vimr, E.R., Taylor, G.L., *J. Mol. Biol.* (1996) 259, 264-280.

(92) Crennell, S.J., Garman, E.F., Laver, W.G., Vimr, E.R., Taylor, G.L., *Proc. Natl. Acad. Sci. USA* (1993) 90, 9852-9856.

(93) Burmeister, W. P., Henrissat, B., Cusack, B. C., Ruigrok, R. W. H., *Structure* (1993) 1, 19-26.

(94) Barnes, J. A., Williams, I. H., *Biochem. Soc. Trans.* (1996), 24, 263-268.

(95) Comb, D. G., Waston, D. R., Roseman, S. J., *J. Boiol. Chem.* (1966) 241, 5637-5642.

(96) Schauer, R., *Adv. Carbohydr. Chem. Biochem.* (1982) 40, 131-234.

(97) Paulson, J. C., Rearick, J. I., Hill, R. L., *J. Biol. Chem.* (1977) 252, 2363-2371.

(98) Horenstein, B. A., Bruner, M., *J. Am. Chem. Soc.*, (1996) 118, 10371-10379.

(99) Bruner, M., Horenstein, B. A. *Biochemistry* (2000) 39, 2261-2268.

(100) Bruner, M., *Characterization of the Reaction Catalyzed by Alpha (2• 6) Sialyltransferase,* Doctoral Dissertation, University of Florida (1999).

(101) Hardy, L. W., Poteete, A. R., *Biochemistry* (1991) 30, 9457-9463.

(102) Amyes, T. L., Jencks, W. P. *J. Am. Chem. Soc.* (1989) 111, 7888-7900.

(103) Horenstein, B. A., Bruner, M., *J. Am. Chem. Soc.* (1998) 120, 1357-1362.

(104) Banait, N. S., Jencks, W. P., *J. Am. Chem. Soc.* (1991) 113, 7958-7963.

(105) Zhang, Y., Bommuswamy, J., Sinnott, M. L., *J. Am. Chem. Soc.* (1994) 116, 7557-7563.

(106) Knier, B. L., Jencks, W. P., *J. Am. Chem. Soc.* (1980) 102, 6789-6798.

(107) Tanaka, Y., Tao, W., Blanchard, J. S., Hehre, E. J., *J. Biol. Chem.* (1994) 269, 32306-32312.

(108) Scudder, P., Doom, J. P., Chuenkova, M., Manger, I. D., Pereira, M. E. A., *J. Biol. Chem.* (1993) 268, 9886-9891.

(109) Ribeirao, M., Pereira-Chioccola, V. L., Eichinger, D., Rodrigues, M., Schenkman, S., *Glycobiology* (1997) 7, 1237-1246.

(110) Buschiazzo, A., Tavares, G. A., Campetella, O., Spinelli, S., Cremona, M. L., Paris, G., Amaya, M. F., Frasch, A. C. C., Alzari, P. M., *EMBO J.* (2000) 19, 16-24.

(111) Buschiazzo, A., Campetella, O., Frasch, A. C. C., *Glycobiology* (1997) 7, 1167-1173.

(112) Buschiazzo, A., Cremona, M. L., Campetella, O., Frasch, A. C. C., Sanchez, D. O., *Mol. Biochem. Parasitol.* (1993) 62, 115-116.

(113) Cremona, M.L., Pollevick, G.D., Frasch, A.C., Campetella, O., *Cell. Mol. Biol.* (1996) 42, 697-702.

(114) Veh, R. W., Michalski, J.,-C., Corfield, A. P., Sander-Wewer, M., Gies, D., Schauer, R., *J. of Chromatography* (1981) 212, 313-322.

(115) Kim, M.-J., Hennen, W. J., Sweers, H. M., Wong, C.-H., *J. Am. Chem. Soc.* (1988) 110, 6481-6486.

(116) Friebolin, H., Dabrowski, U., Supp, M., Brossmer, R., *Tet. Letters* (1979) 48, 4637-4640.

(117) Aminoff, D., *Biochem. J.* (1961) 81, 384-391.

(118) Schmidt, H., Friebolin, H., *J. Carbohyd. Chem.* (1983) 2, 405-413.

(119) Dorland, L., HaverKamp, J., Schauer, R., Veldink, G. A., Vliegenthart, J. F.G., *Biochem. Biophys. Res. Comm.* (1982)104, 1114-1119.

(120) Shames, S. L., Simon, E. S., Christopher, C. W., Schmid, W., Whitesides, G. M., Yang, L.-L., *Glycobiology* (1991)1, 187-191.

(121) Simon, E. S., Bednarski, M. D., Whitesides, G. M., *J. Am. Chem. Soc.* (1988)110, 7159-7163.

(122) Sadler, J. E., Beyer, T. A., Oppenheimer, C. L., Paulson, J. C., Prieels, J. P., Rearick, J. I., Hill, R. L., *Methods Enzymol.* (1982) 83, 458-515.

(123) Kleineidam, R. G., Schmelter, T., Schwarz, R. T., Schauer, R., *Glycoconjugate J.* (1997) 14, 57-66.

(124) Fernley, H.N., *The Enzymes*, 3rd Ed. Academic Press, Boyer, P.D., ed. (1971) Vol IV, 417-447.

(125) Wlasichuk, K. B., Kashem, M. A., Nikrad, P. V., Bird, P., Jiang, C., Venot, A. P., *J. Biol. Chem.* (1993) 268, 13971-13977.

(126) Ogawa, T., Sugimoto, M., *Carbohyd. Res.* (1985) 135, C5-C9.

(127) Haverkamp, J., Van Halbeek, H., Dorland, L., Vliegenthart, J. F. G., Pfeil, R., Schauer, R., *Eur. J. Biochem.* (1982) 122, 305-311.

(128) Ferro, V., Mocerino, M., Stick, R. V., Tilbrook, D. M. G., *Aust. J. Chem.* (1988) 41, 813-815.

(129) Szeja, W., *Synthesis* (1979) 10, 821-822.

(130) Follmann, H., Hogenkamp, H. P. C., *J. Am. Chem. Soc.* (1970) 92, 671-677.

(131) Sambrook, J., Fritsch, E. F., Maniatis, T., *Molecular Cloning - A Laboratory Manual*, 2nd Ed., Cold Spring Harbor Laboratory Press. (1989).

(132) *pET System Manual*, Novagen Inc. (http://www.novagen.com/html/vectfram.html). Accessed date January, 2000.

(133) Bradford, M., *Anal. Biochem.* (1976) 72, 248-254.

(134) Zapata, G., Vann, W. F., Aaronson, W., Lewis, M. S., Moos, M. J., *J. Biol. Chem.* (1989) 264, 14769-14774.

(135) Liu, J. L., Shen, G., Ichikama, Y., Rutan, J. F., Zapata, G., Vann, W. F., Wong, C. H., *J. Am. Chem. Soc.* (1992) 114, 3901-3910.

(136) Dygert, S., Li, L. H., Florida, D., Thoma, J. A., *Anal. Biochem.* (1965) 13, 367-374.

(137) Bigeleisen, J., Mayer, M. G., *J. Chem. Phys.* (1947) 15, 261-267.

(138) Wolfsberg, M., Stern, M. J., *Pure Appl. Chem.* (1964) 8, 225-242.

(139) Cleland, W. W., O'Leary, M., Northrop, D. B., *Isotope Effects on Enzyme Catalyzed Reactions,* University Park Press, New York, (1976), 235-238.

(140) Lowry, T. H., Richardson, K. S., *Mechanism and Theory in Organic Chemistry*, 3rd ed., Harper Collins Publishers, New York, 1987, 233-240.

(141) Melander, L. and Saunders, W.H., *Reaction Rates of Isotopic Molecules,* Kreiger, Malabar, FL., (1980), chapter 8.

(142) Goitein, R. K., Chelsky, D., Parsons, S. M., *J. Biol. Chem.* (1978) 253, 2963-2971.

(143) Bennett, A. J., Sinnott, M. L., *J. Am. Chem. Soc.* (1986) 108, 7287-7294.

(144) Northrop, D.B., *Ann. Rev. Biochem.* (1981) 50, 103-131.

(145) Cleland, W.W., *Methods Enzymol.* (1982) 87, 625-641.

(146) Simon, H. and Palm, D., *Angew. Chem. Int. Ed. Eng.* (1966) 5, 920-933.

(147) Parkin, D. W., *Enzyme Mechanisms from Isotope Effects,* CRC press, Boca Raton, FL., Cook, P. F. ed. (1991), 269-290.

(148) Duggleby, R. G. and Northrop, D. B., *Bioorg. Chem.* (1989) 17, 177-193.

(149) Rosenberg, S., Kirsch, J. F., *Anal. Chem.* (1979) 51, 1379-1383.

(150) Winstein, S., Robinson, G. C., *J. Am. Chem. Soc.* (1958) 80, 169-181.

(151) Schramm, V.L., *Methods Enzymol.* (1999) 308, 301-355.

(152) Melander, L. and Saunders, W.H., *Reaction Rates of Isotopic Molecules*, Kreiger, Malabar, FL., (1980), chapter 2.

(153) Parkin, D. W., Schramm, V. L., *Biochemistry* (1987) 26, 913-920.

(154) Parkin, D. W., Leung, H. B., Schramm, V. L., *J. Biol. Chem.* (1984) 259, 9411-9417.

(155) Kline, P. C., Schramm, V. L., *Biochemistry* (1993) 32, 13212-13219.

(156) Horenstein, B. A., Parkin, D. W., Estupinan, B., Schramm, V. L., *Biochemistry* (1991) 30, 10788-10795.

(157) Rising, K. A., Schramm, V. L., *J. Am. Chem. Soc.* (1997) 119, 27-37.

(158) Scheuring, J., Schramm, V. L., *Biochemistry* (1997) 36, 8215-8223.

(159) Huang, X.C., Tanaka, K.S.E., Bennet, A.J., *J. Am. Chem. Soc.* (1997) 119, 11147-11154.

(160) Bron, J., Stothers, J. B., *Can. J. Chem.* (1968) 46, 1825-1829.

(161) Todeschini, A. R., Mendonca-Previato, L., Previato, J. O., Varki, A., van Halbeek, H., *Glycobiology* (2000) 10, 213-21.

(162) Matsumura, I. Kirsch, J. F., *Biochemistry* (1996) 35, 1881-1889.

(163) Richard, J.P., *Tetrahedron* (1995) 51, 1535-1573.

(164) Meindl, P., Bodo, G., Palese, P., Schulman, J., Tuppy, H., *Virology* (1974) 58, 457-463.

(165) Vandekerckhove, F., Schenkman, S., Ponts de Carvalho, L., Tomlinson, S., Kiso, M., Yoshida, M., Hasegawa, A., Nussenzweig, V., *Glycobiology* (1992) 2, 541-548.

(166) Cook, P.F., *Enzyme Mechanisms from Isotope Effects.*, CRC press, Boca Raton, FL., Cook, P. F. ed. (1991), 203-230.

(167) Bigeleisen, J., Wolfsburg, M., *Adv. Chem. Phys.* (1958) 1, 15-76.

(168) Cleland, W. W., *The Enzymes*, 3rd ed., Academic Press, Boyer, P. D. ed. (1970) Vol II, 1-65.

(169) Nordlie, R. C., *Methods Enzymol.* (1982) 87, 319-352.

(170) Casazza, J. P., Fromm, H. J., *Biochemistry* (1977) 16, 3091-3097.

(171) Parr, I. B., Horenstein, B. A., *J. Org. Chem.* (1997) 62, 7489-7494.

(172) Kim, M. M., *Synthesis and Sialidase Inhibition Studies of 3,4,5,-Trisubstituted Piperidines,* Master's Dissertation, University of Florida (2000).

(173) Sun, H., Millar, K., Yang, J., Horenstein, B. A., *Tetrahedron Letters* (2000), 41, 2801-2804.

(174) Folk, J. E., *J. Biol. Chem.* (1969) 244, 3707-3713.

(175) Shuman, S., *Biochim. Biophys. Acta.* (1998) 1400, 321-337.

(176) Pearson, R. G., Sobel, H., Songstad, I. J., *J. Am. Chem. Soc.* (1968) 90, 319-326.

(177) Thomas, A., Jourand, D., Bret, C., Amara, P., Field, M. J., *J. Am. Chem. Soc.* (1999) 121, 9693-9702.

(178) Gross, M., Folk, J. E., *J. Biol. Chem.* (1973) 248, 1301-1306.

(179) Karkowsky, A. M., Bergamini, M. V. W., Orlowski, M., *J. Biol. Chem.* (1976) 251, 4736-4743.

(180) Anderson, W. B., Nordlie, R. C., *J. Biol. Chem.* (1967) 242, 114-119.

(181) Northrop, D. B., *J. Biol. Chem.* (1969) 244, 5808-5819.

(182) Chang, C. H., Cha, S., Brockman, R. W., Bennett, L. L., *Biochemistry* (1983) 22, 600-611.

(183) Milner, Y., Wood, H. G., *J. Biol. Chem.* (1976) 251, 7920-7928.

(184) Tsai, C. S. Burgett, M. W., Reed, L. J., *J. Biol.Chem.* (1973) 248, 8348-8352.

(185) Chuenkova, M., Pereira, M., Taylor, G., *Biochem. Biophys. Res. Comm.* (1999) 262, 549-556.

(186) Cremona, M. L., Campetella, O., Sanchez, D. O., Frasch, A. C. C., *Glycobiology* (1999) 9, 581-587.

(187) Ho, S. N., Hunt, H. D., Horton, R. M., Pullen, J. K., Pease, L. R., *GENE* (1989) 77, 51-59.

BIOGRAPHICAL SKETCH

Jingsong Yang, son of Chuan Yang and Yumei Ni, was born in Siyang, Jiangsu Province, People's Republic of China, on April 17, 1968. He completed his early education in Siyang and graduated from Siyang High School in 1985. He entered the Nanjing University in the same year and graduated with a Bachelor of Science degree in biochemistry in 1989. From 1989 to 1996, he worked as a research scientist in the Chinese Academy of Agricultural Sciences in Beijing, China. He married his wife, Nianying Wang, in 1992 and had his daughter, Xinyue (Sherry) Yang, in 1995. He entered the Graduate School in the Chemistry Department of the University of Florida in 1996 and started working on the project of mechanistic enzymology of trans-sialidase under the guidance of Dr. Benjamin A. Horenstein. He will finish his Doctor of Philosophy degree in May, 2001.

I certify that I have read this study and that in my opinion it conforms to acceptable standards of scholarly presentation and is fully adequate, in scope and quality, as a dissertation for the degree of Doctor of Philosophy.

Benjamin A. Horenstein, Chair
Associate Professor of Chemistry

I certify that I have read this study and that in my opinion it conforms to acceptable standards of scholarly presentation and is fully adequate, in scope and quality, as a dissertation for the degree of Doctor of Philosophy.

Nigel G. Richards
Associate Professor of Chemistry

I certify that I have read this study and that in my opinion it conforms to acceptable standards of scholarly presentation and is fully adequate, in scope and quality, as a dissertation for the degree of Doctor of Philosophy.

Jon D. Stewart
Associate Professor of Chemistry

I certify that I have read this study and that in my opinion it conforms to acceptable standards of scholarly presentation and is fully adequate, in scope and quality, as a dissertation for the degree of Doctor of Philosophy.

Weihong Tan
Assistant Professor of Chemistry

I certify that I have read this study and that in my opinion it conforms to acceptable standards of scholarly presentation and is fully adequate, in scope and quality, as a dissertation for the degree of Doctor of Philosophy.

David N. Silverman
Distinguished Professor of
Physiology and Pharmacology

This dissertation was submitted to the Graduate Faculty of the Department of Chemistry in the College of Liberal Arts and Sciences and to the Graduate School and was accepted as partial fulfillment of the requirements for the degree of Doctor of Philosophy.

May, 2001

Dean, Graduate School

LD
1780
20 01
.422

UNIVERSITY OF FLORIDA
3 1262 08555 3583